# THE ENVIRONMENT CANADA HANDBOOK ON FOG AND FOG FORECASTING

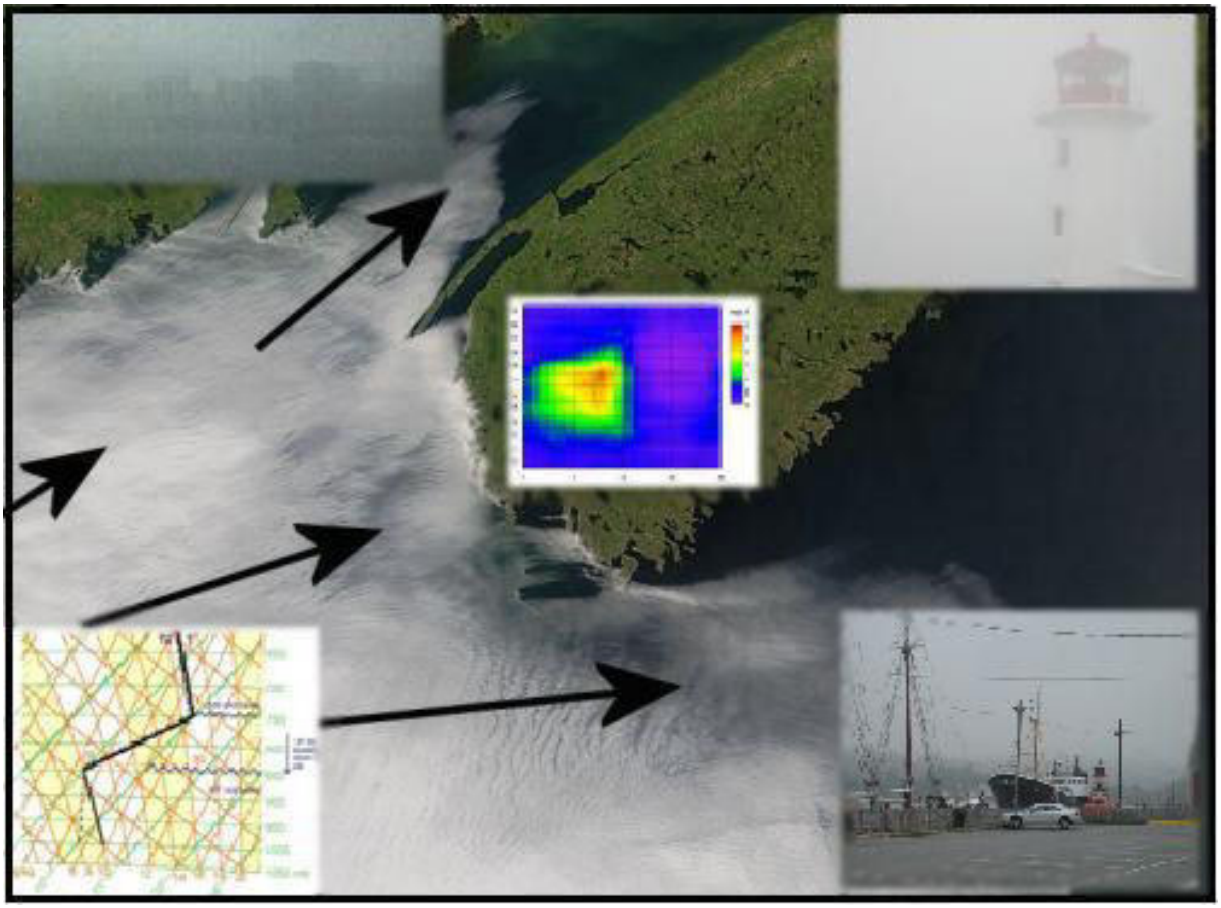

***Garry Toth, Ismail Gultepe, Jason Milbrandt, Bjarne Hansen, Garry Pearson, Chris Fogarty, and William Burrows***

## Table of Contents

# Preface

The authors of this document are Garry Toth, Ismail Gultepe (project lead, FRAM), Bjarne Hansen, Jason Milbrandt, Garry Pearson, Chris Fogarty and William Burrows.

The funding for this technical manual came from SAR Office of Canada during June 1 2005 - April 1 2009. Scientific and operational forecasting knowledge were developed while observational studies were carried out at three locations: 1) Toronto, Ontario 2) Lunenburg, Nova Scotia, and 3) Barrow, Alaska.

Contributions for this work came from various individuals. G. Toth integrated all the work done in the early versions of this Handbook and, together with Dr. W. Burrows, contributed rules-based methods for automated forecasting of areas of fog (and also low stratus ceilings) that utilize GEM-regional model output. Dr. I. Gultepe contributed information on microphysics and parameterizations of fog visibility, FRAM field projects, and providing scientific results to numerical model applications and rules-based techniques. B. Hansen described the climatology of fog. Dr. J. Milbrandt developed a new microphysical scheme applicable to fog forecasting that utilized visibility parameterizations developed by Gultepe. G. Pearson and Dr. C. Fogarty provided validation of forecast techniques.

# 1 Background

Gultepe et al. (2007a) studied fog related works and provided an extensive overview on fog forecasting and observations. This chapter summarizes their work based on various studies given in their article.

The effect of fog on human life was recognized in the early ages of mankind but impact has significantly increased during the last few decades due to increasing air, marine, and road traffic. In fact, the financial and human losses related to fog and low visibility became comparable to the losses from other weather events such as tornadoes or even hurricanes. This section presents a brief history of fog studies and research.

The earliest works on fog can be traced back to Aristotle's Meteorologica (284-322 B.C.). These were extensively referenced by Neumann (1989) in his study of early works on fog and weather. This paragraph is mainly based on his detailed work. In the English translation (Aristotle, translated by Lee 1952), a statement is given on the relationship between fog and good weather. Also, Neumann (1989) relates a poem by Aratus (315-240 B.C.), which was

referred to as Prognostication Through Weather Signs, in an English translation by G.R. Mair (Aratus 1921). The poem reads "If a misty cloud be stretched along the base of a high hill, while the upper peaks shine clear, very bright will be the sky. Fair weather, too, shall thou have, when by sea-verge is seen a cloud low (fog) on the ground, never reaching a height, but penned there like a flat reef of rock." In this regard, Pliny the Elder (A.D. 23-79, Pliny 1971), a Roman historian, admiral, scientist and author, states in his work of Natural History "……. Mist (fog) coming down from the mountains or falling from the sky or settling in the valleys will promise fine weather." These works suggested that fog was recognized for use as a fair weather predictor.

The influence of fog was also felt on historical events. Lindgrén and Neumann (1980) describe one such event during the Crimean war, when the Russian empire faced the alliance of Britain, France, and Turkey. The allied forces landed in Crimea in September 1854. Dense fog developed early on the morning of the 5th, just when the Russian forces were launching their first major offensive. The allied forces could not realize what was occurring on the other side. It was stated that "…for the vapours, fog, and drizzling mist obscured the ground to such an extent as to render it impossible to see what was going on at a distance of a few yards." This suggests that fog was a major player in this historical event.

The formation of fog and its extent at the surface are not easy to predict. The fog formation does not always occur in calm windless conditions. In fact, the formation of fog associated with turbulent windy conditions was studied at the end of 18th century. Scott (1896) related that fogs with strong winds occurred in the British Isles, and sometimes lasted a month. He also mentioned that the strong wind fogs were accompanied by rain which was frequently heavy. Scott (1894) showed that fog occurrence was correlated to strong winds (Beaufort scale of 6), and that there was no clear relationship between weather patterns (e.g. cyclonic or anticyclonic) and fog formation. Scott also stated that the total number of fog cases with strong wind was estimated to be about 135 over 15 years. The role of aerosols in fog formation was recognized by Mensbrugghe (1892) who stated that "aqueous vapour condenses in the air only in the presence of solid particles around which the invisible vapour becomes a liquid." The heavy London fog on 10-11 January 1925 followed the great fog of December 1924 (Bonancina 1925). During this episode, two types of fog occurred: 1) unsaturated haze without condensation and 2) fog with liquid characteristics. These fog episodes paralyzed the entire city with very low visibility values. This discussion shows that fog formation and its relation to environmental conditions were known early on but detailed field and modeling works were limited.

The importance of fog and low ceiling in weather forecasting was studied by Willett (1928). In his detailed work, he emphasized the importance of condensation nuclei for fog formation. He stated that dust particles with some degree of surface curvature, particles having an electric charge or ions, and hygroscopic particles were facilitating agents to droplet formation. He also proposed a classification for fog and haze based on causes and favourable

synoptic conditions. Overall fogs were classified into two groups: 1) airmass fogs and 2) frontal fogs. Subsequently, he emphasized the importance of all meteorological parameters affecting fog formation. For each group, he then sub-classified them e.g. advection type, radiation fog, and marine fog, etc. He also summarized the works done by others such as Köppen (1916, 1917), Taylor (1917), and Georgii (1920).

Numerous field studies with a focus on fog and other boundary layer clouds were performed over the last few decades. Among the regions where these experiments took place are the coastal regions off the California coast. Review articles on West Coast marine fog, stratus and stratocumulus were presented by Leipper (1994) and Kloesel (1992). Among the noteworthy experiments was the CEWCOM project (Cooperative Experiment in West Coast Oceanography and Meteorology) (Noonkester, 1977) which consisted of a major set of experiments off the California coast conducted during 1972-1982 time period under the US Navy Naval Air Systems Command. These meso- and micro-meteorological experiments involved a land and sea network of radiosonde observations, ships, aircraft, balloons, and kites. Studies based on observations were complemented by modeling studies. An investigation of low level stratus/fog was performed by Koracin et al. (2001) using a one-dimensional (1D) model and observations. His results suggested that radiative cooling and large-scale subsidence were important factors for fog formation. The interactions between radiative and turbulence processes studied in detail by Oliver et al. (1977-78) suggested that radiative cooling at fog top was an important process in the fog life cycle. Similarly, it was shown by Welch and Wielicki (1986) that ~5°C/hour cooling occurred during a simulation of a warm fog layer in which the liquid water content (LWC) reached 0.3 g $m^{-3}$. These results were found to be comparable with observations. Radiation fog studies using detailed surface observations were made by Meyer and Lala (1986), Roach et al. (1976), and Choularton et al. (1981). Those authors also focused on various aspects of fog formation and its evolution by using numerical models. Fuzzi et al. (1992) carried out the Po Valley Fog Experiment which was a joint effort by several European research groups from five countries. The physical and chemical behaviour of the multiphase fog system was studied experimentally by following the temporal evolution of the relevant chemical species in the different phases (gas, droplet, interstitial aerosol) and the evolution of micrometeorological and microphysical conditions, from the pre-fog situation through the whole fog life cycle, to the post-fog period. Fuzzi et al. (1998) also conducted a second field project called Chemdrop (CHEMical composition of DROPlets) that took place in the Po Valley region. Their project focused mostly on fog microphysics and chemistry as in the previous field experiment. Ice fog studies (Bowling et al. 1968; Girard and Blanchet, 2001; Gotaas and Benson 1965) were limited due to the difficulties of measurement ice particles at sizes less than 100 μm (Gultepe et al. 2001). However, Gotaas and Benson (1965) showed that 10°C/day cooling was due to ice fog occurrence in January 1962. More recently, Gultepe et al. (2009)

conducted a field project over eastern Canada for marine fog studies, and at a site in the Ontario region for winter warm fog studies, with a focus on nowcasting/forecasting issues. These projects contributed to the better understanding of fog physics, and the development of parameterizations for numerical models and remote sensing studies.

In addition to fog formation, development and decay, the artificial dissipation of fog was also studied in the early 1970s. The main objective of these works was to study how fog can be eliminated from a specific area such as over an airport or a shipping port. Fog droplets are found in a narrow drop size range, e.g. 4-10 μm. If somehow this range could be changed to include larger droplets, then fog dissipation could occur through coalescence. The work by Houghton and Radford (1938) was the first to use hygroscopic particle seeding to dissipate fog droplets. Jiusto et al. (1968) studied the possibility of fog dissipation by giant hygroscopic nuclei seeding and stated that the use of carefully controlled sizes and amounts of hygroscopic nuclei (e.g. NaCl) can produce significant improvements in visibility. Kornfeld and Silverman (1970) and Weinstein and Silverman (1973) also indicated similar results and stated that if the fog droplet size distribution is known the seeding nuclei are to be chosen carefully. These works suggested that fog dissipation seems possible but depends on the detailed microphysics. Another method used helicopters to dissipate fog on the basis of turbulent mixing of dry air into the fog layer by the helicopter's downwash (Plank et al., 1971).

The increased fog water content as dripping water, opposite to the fog dissipating idea, was used as a resource for the ecosystem hydrology and water resources. The Standard Fog Collector (SFC) was developed by Schemenauer and Cereceda (1994). It is a 1- meter square frame with a double layer of 40% shade cloth mesh. It is set up perpendicular to the prevailing wind direction. The collected fog (and rain) water is routed from the collection trough to a large-capacity tipping bucket gage with data logger to measure amount and frequency of precipitation. Polypropylene nets similar to the original SFC over coastal cliffs and desert areas transform windborne fog and mists into water. Fog catchers use a simple idea in which a fine-mesh netting is placed against the wind that carries fog droplets, so that water condenses on the filaments. In the arid stretches of coastal Chile, Peru, Ecuador, and several other countries around the world, this method is used to get water from fog droplets. Trees also serve as natural fog catchers (Azevedo and Morgan, 1974); a forest growing in an arid area can provide as much water as rain into the dry soil. They suggest that fog drifting inland is caught by plant leaves so that the nutrients contained in the fog as nuclei and dissolved gases become available to the plants. Some nutrients may be absorbed directly by the leaves while the rest becomes available to the plants via the soil as water drips to the ground.

The number of articles that include the word "fog" in American Meteorological Society (AMS) published journals was found to be about 4700. Clearly there is an abundance of works on this subject. In spite of this extensive body of work, concerns related to fog

forecasting/nowcasting still remain because of fog's considerable time and space variability related to interactions among various physical processes.

Among the reasons behind the challenges in accurately forecasting/nowcasting fog are the difficulties in detecting fog and representing the physical processes involved. Remote sensing of fog using satellites is useful but more spectral channels than are typically available are needed to improve detection algorithms (Ellrod and Gultepe 2007). Lately, MODIS-based fog algorithms (Bendix et al., 2006) have been developed that include more channels in the near IR and better resolution (of about 100 m). Although various methods were developed for forecasting and nowcasting applications, the accuracy of these algorithms needs to be assessed further, especially over snow and ice surfaces. From the numerical modeling point of view, important issues are related to the horizontal (Pagowski et al. 2004) and vertical (Tardif 2007) resolutions, and physical parameterizations (Gultepe and Milbrandt 2007). For instance, if the total droplet number concentration (Nd) is not obtained prognostically, it is obtained diagnostically as a function of supersaturation, or is simply fixed. It is a well known fact that visibility in fog is directly related to Nd. In the large scale models, Nd is either not considered or is simply fixed. In most models, visibility is obtained from extinction versus LWC relationships (Kunkel 1984), while the LWC is obtained using either a simple LWC-T relationship (Gultepe and Isaac 1997) or a prognostic equation (Teixeira 1999; Bergot and Guédalia 1994; Bott and Trautmann 2002; Pagowski et al. 2004). Therefore, detailed three-dimensional cloud/fog models are needed to better understand issues related to fog, but they are not used extensively because of the computational cost involved in producing operational forecasts (Müller et al., 2007, Gultepe et al. 2006a). One-dimensional (1D) models are cheaper to run and can prove to be useful in certain situations (Bergot and Guédalia 1994; Bergot et al. 2005; Bott 1991). However their applicability becomes limited in regions of complex and heterogeneous terrain (Müller et al. 2007). The applicability of the different modeling strategies for fog forecasting and various parameterizations need to be extensively researched.

In order to better evaluate forecasts of fog formation, development, and decay, field observations should be used for verification purposes. This can be done: 1) using carefully analysed climatological surface data (Tardif and Rasmussen 2007), 2) in-situ observations (Gultepe et al. 2006b; Gultepe et al. 2007b), and 3) remote sensing data (Cermak and Bendix 2007). Detailed studies by Tardif and Rasmussen (2007), and Hansen et al. (2007), and Hyvarinen et al. (2007) suggest that the climatological data can help in developing better understanding of fog formation, forecasting methods, and organize better field programs (Gultepe et al. 2009).

For more introductory articles on fog, see Croft (2003), Lewis et al. (2003), and Roach (1994, 1995a, and 1995b). For operationally oriented instruction on fog prediction, visit the COMET Met Ed website, http://www.meted.ucar.edu.

# 2 Importance of fog

In general, fog is important for the safety of individuals and the economic loss that can follow from fog events. Fog has a significant impact on Canadian society, primarily as a hazard to road, aviation and marine transportation activities.

For the general public, probably the largest impact of fog is associated with road transportation (Whiffen 2004). In Canada, 90% of all passenger travel is by road, and fog on the road can abruptly change the visibility over a very short distance. Given that fog is not a rare phenomenon (for example, on average there are 17 days with fog per year in Winnipeg and Montréal, 34 days in Toronto and Vancouver, and 121 days in Halifax and St John's), drivers are almost certain to encounter fog at some time during the year. In fact there is an average of 53 fatal road accidents in Canada per year in which fog was a major contributing factor (Figure 2-1, Transport Canada 2001).

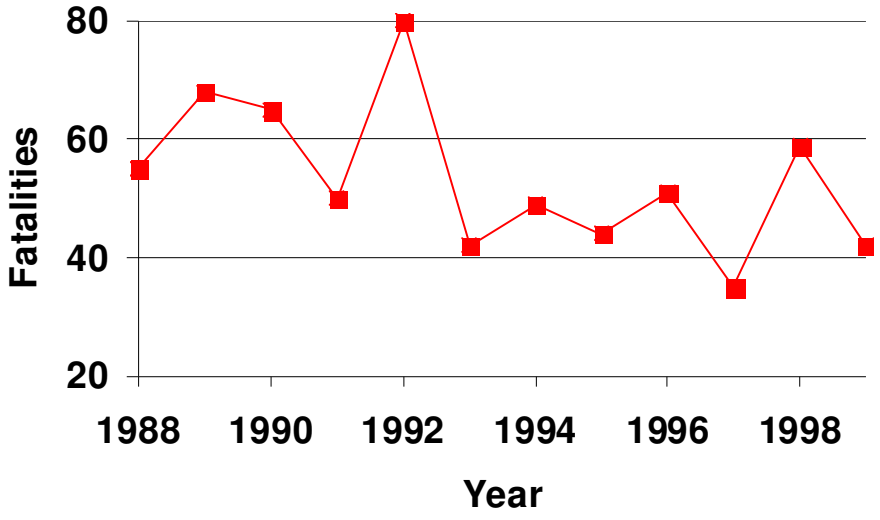


**Figure 2-1:** Yearly fatalities in Canada in vehicle accidents in which fog was a factor.

Fog-related fatal vehicle accidents include single car accidents as well as multi-vehicle accidents such as the ones that occurred near Windsor, Ontario in September 1999 (145 vehicles were involved, with 8 fatalities) and Chambly, Québec in September 2002 (49 vehicles were involved, with one fatality). A technical summary of the Windsor incident was given by Pagowski et al. (2004).

These statistics indicate that fog presents one of the most significant weather hazards to the Canadian public: on average, fog causes seven times more deaths than lightning (Etkin and Maarouf 1995), and 20 times as many fatalities per year as tornadoes (that cause on average two deaths per year; Environment Canada, 2007).

The aviation community can be adversely affected by low ceiling and visibility conditions. Such conditions have been identified as contributing factors in 35% of weather-related aviation accidents in the US civil aviation sector. According to aviation incident occurrence reports compiled by Transport Canada (personal communication), there were 235 aircraft incidents in Canada in the 10 year period 1995 – 2003 in which fog was present (Figure 2-2). These incidents resulted in 47 fatalities and 35 injuries (Transportation Safety Board of Canada, http://www.tsb.gc.ca/en/reports/air, see Figure 2-2 below). While fog may not have been the final cause of all those incidents, clearly it can be one factor in a web of multiple factors that contribute to aviation accidents. Both fixed-wing aircraft and helicopters can be significantly affected by fog, particularly if it contains supercooled water droplets that can cause serious icing.

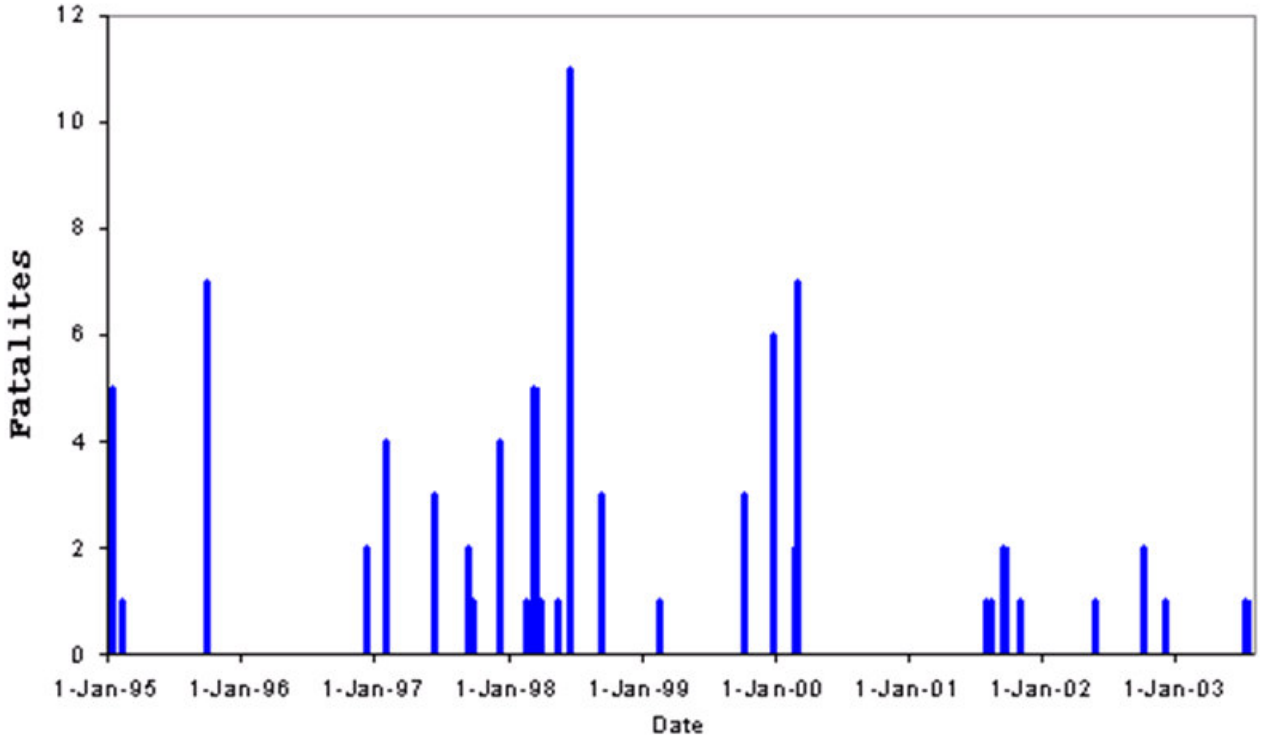


**Figure 2-2** Fatalities and injuries in Canada resulting from aircraft incidents in which fog was a factor for 1995 – 2003.

Fog also affects the marine community. The risk of accidents involving transport ships, ferries and fishing boats increases with decreasing visibility. For this reason, the Canadian

FRAM field project was performed over the Lunenburg, NS, and St. Johns', NFL During FRAM projects, various parameterizations for model application is developed and currently used for nowcasting applications.

Fog can cause significant delays and disruptions in the transportation system, and particularly to air traffic. Not only can flights be delayed or cancelled at a fogged-in airport, but also connecting flights from other airports can in turn be delayed or cancelled, even if those airports have no weather problems. There are both direct and indirect economic consequences to such delays or cancellations. For example, freezing fog at London's Heathrow Airport just prior to the Christmas holiday period of 2006 resulted in almost three days of all flights being grounded, resulting in an estimated £25 million in losses for British Airways alone (Gadher and Baird 2007; Gultepe et al., 2009).

Another possible impact of fog comes to us from biometeorological studies. One statistical study (Villeneuve et al. 2005) has shown that the occurrence of fog or liquid precipitation was associated with an increased number of hospital admissions for children with asthma in Ottawa. Fog may affect air quality, which in turn is related to respiratory problems related to asthma.

In the past, weather has had a significant effect on events such as military battles. For example, as described in section 1 of this document, fog was a major factor in one battle of the Crimean War on September 5, 1854.

Finally, any Canadian sports enthusiast will remember the "Fog Bowl" of 1962. The Grey Cup game of that year took place in Toronto on *both* December 1 and December 2, with the Winnipeg Blue Bombers facing the Hamilton Tiger-Cats. During the game on Dec 1, dense fog rolled in from Lake Ontario, so that the fans in the stands were unable to see what was happening on the field. The fog then thickened even more so that the players on the field could barely see their teammates. The referees finally suspended the game about half way through the fourth quarter, and the remainder was played in the following day (the Bomber won by a score of 28 to 27).

Visibility can be reduced because of various hydrometeors, aerosols, and moisture in the path of visible light. In the following sections, various factors reducing visibility are discussed.

## 2.1 Definitions of Fog, Mist, Haze and Smog

Petterssen (1956) presents traditional descriptions of liquid fog, mist and haze as follows:

> *a) Liquid fog* "consists of almost microscopically small water drops suspended in the air, or a mixture of such droplets and smoke or fine dust, that reduce the horizontal range of visibility to less than 1 km. In fog, the air usually feels clammy and humid; and, on closer examination, one may even see the droplets floating past the eye. Fog is generally

whitish in colour, except in the vicinity of local sources of pollution where it may be of a dirty yellowish or grayish colour."

b) Mist "consists of microscopically small water drops or of highly hygroscopic particles suspended in the air. The droplets in a mist are smaller and more scattered than in a fog; and, as a result, the horizontal range of visibility is greater than in a fog. At temperatures above 0°C, the relative humidity in a mist may be below 97 per cent, and the air, therefore, does not feel as humid or as clammy as in fog. Mist is of a greyish white colour."

c) *Haze* "consists of finely divided dust particles (from arid regions) or of salt particles which are dry and so extremely small that they cannot be felt or distinguished individually by the eye, but which diminished the visibility and give a characteristic smoky (hazy and opalescent) appearance to the air. Haze produces a uniform veil over the landscape and subdues its colours. The veil has a bluish tinge when viewed against a dark background ('blue mountains') but a yellowish or orange tinge when viewed against a white background (e.g. clouds at the horizon, snow-covered mountains, the sun, etc). This distinguishes it from the greyish mist, the density of which it may sometimes attain."

Presently, the above definitions are modified and presented as follows:

*a) Fog and Mist:* According to the internationally-accepted definition of fog, it consists of a collection of suspended water droplets or ice crystals near the Earth's surface that lead to a reduction of horizontal visibility below 1 km (5/8 of a statute mile) (NOAA 1995). If the visibility is greater than 1 km, then it is called mist (WMO 1966). Prevailing visibility is the maximum visibility value common to sectors comprising one-half or more of the horizon circle (ManObs 2006). Water droplets, typically 2 to 50 μm in diameter (Pruppacher and Klett 1997), form as a result of supersaturation generated by cooling, moistening and/or mixing of near surface air parcels of contrasting temperatures. Sufficient suspended droplets and/or crystals can render an object indistinguishable to a distant observer and thus cause poor visibility. This occurs through a reduction in the brightness contrast between an object and its background by particle concentration and size-dependent scattering losses of the light propagating between the object and the observer (Gazzi et al. 1997; Gazzi et al. 2001) and through the blurring effect of forward-scattering of light due to the presence of the droplets/crystals (Bissonette 1992).

Fog (visibility less than 1 km) may be referred to as 'dense fog' in some of the literature, while 'mist' according to the WMO definition may be referred to as 'fog'. For the purposes of this documentation, we may be interested in either 'fog' or 'mist'. For example, at a visibility of three miles (5 km) flight rules change from VFR to IFR, which is significant for aircraft

operations. This visibility falls in the range termed ‘mist’. Also, fog can be related to low stratus, and at times it will be necessary to refer to both F and ST.

*b) Haze*: “Fine dust or salt particles dispersed through a portion of the atmosphere; a type of lithometeor. The particles are so small that they cannot be felt or individually seen with the naked eye, but they diminish the horizontal visibility and give the atmosphere a characteristic opalescent appearance that subdues all colours” (http://nsidc.org/arcticmet/glossary/fog.html).

c) *Smog*: “As originally coined in 1905 by des Voeux: a natural fog contaminated by industrial pollutants, a mixture of smoke and fog. Today, it is the common term applied to problematical, largely urban air pollution, with or without the natural fog; however, some visible manifestation is almost always implied) (Glickman 2000). In extreme cases, photochemical reactions can produce photochemical smog (“air contaminated with ozone, nitrogen oxides and hydrocarbons, with or without natural fog being present” according to the AMS Glossary of Meteorology). However, the Glossary also notes in its definition of fog that “fog droplets are usually absent in photochemical smog, which contains only unactivated haze droplets.”

In this Handbook we will not be concerned with haze or smog, but only with mist and fog as defined above (and low stratus will also be considered).

# 3 Climatology

The AMS Glossary (Glickman 2000) defines descriptive climatology as dealing “with the observed geographic or temporal distribution of meteorological observations over a specified period of time.” Knowledge of climatology (local and regional) is useful in forecasting. There are large amounts of data available, and forecasters familiarize themselves with those data when starting to forecast for a new region.

## 3.1 General Fog Climatology

Phillips (1990) shows the average annual number of days with some fog (including fog and mist) over Canada for the 30 year period 1951 – 1980 (Figure 3-1). The highest values are found along the Nova Scotia and Newfoundland coasts of Atlantic Canada, the southeastern coast of Baffin Island, the central Arctic area, and the BC coast. The Avalon Peninsula and the Hall Peninsula appear to be the foggiest places in Canada from this graphic. An updated chart, Figure 3-2, with data from the years 1971 – 1999, shows similar patterns, but somewhat less fog over the east and the north (e.g. the 150 day contours over the Hall Peninsula and the Avalon Peninsula are approximately replaced by 120 day contours). A similar analysis and pattern is provided by Muraca et al. (2001) based on observations taken from 1971 to 1999.

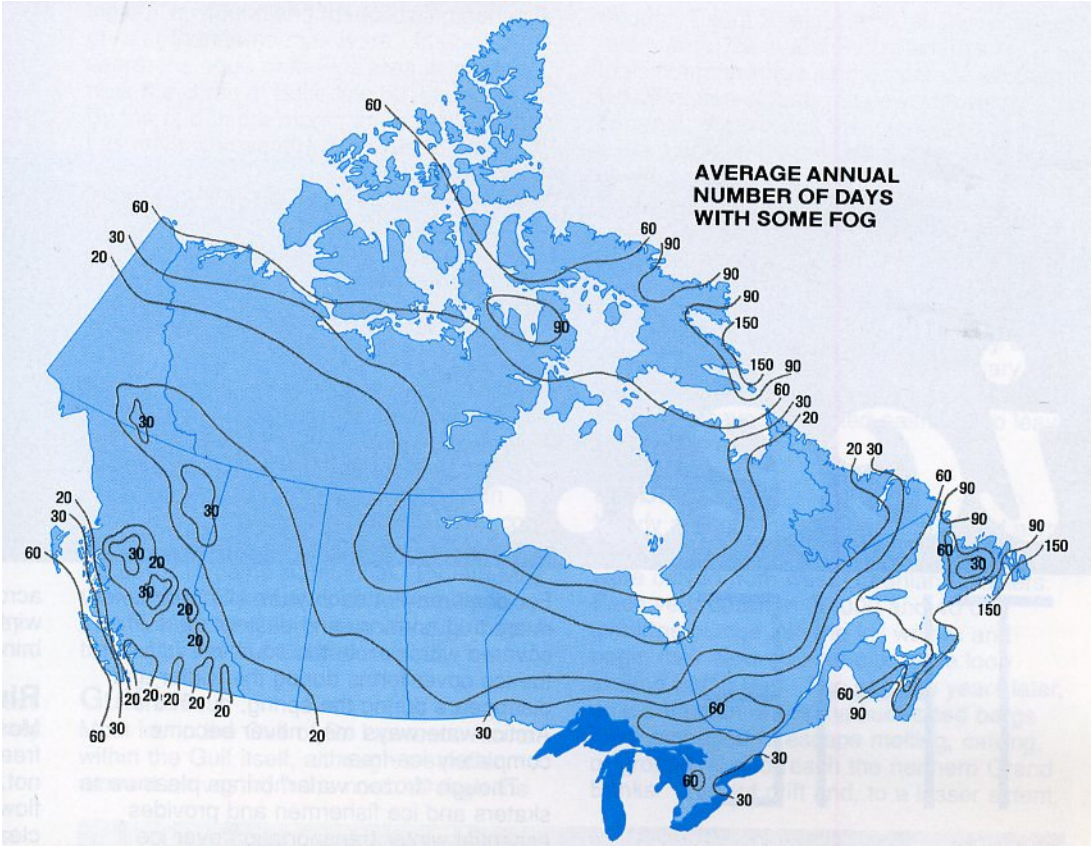


**Figure 3-1 Annual days with some fog (1951-1980) from Phillips (1990).**

A problem with focusing on "days with fog" is that it tends to give an exaggerated impression of fog frequency: if a day has only one hour of fog, it is counted as a day with fog. The percent of hours with fog is always lower than the percent of days with fog, as shown in Figure 3-2 (Hansen and Richards 2006, private communication).

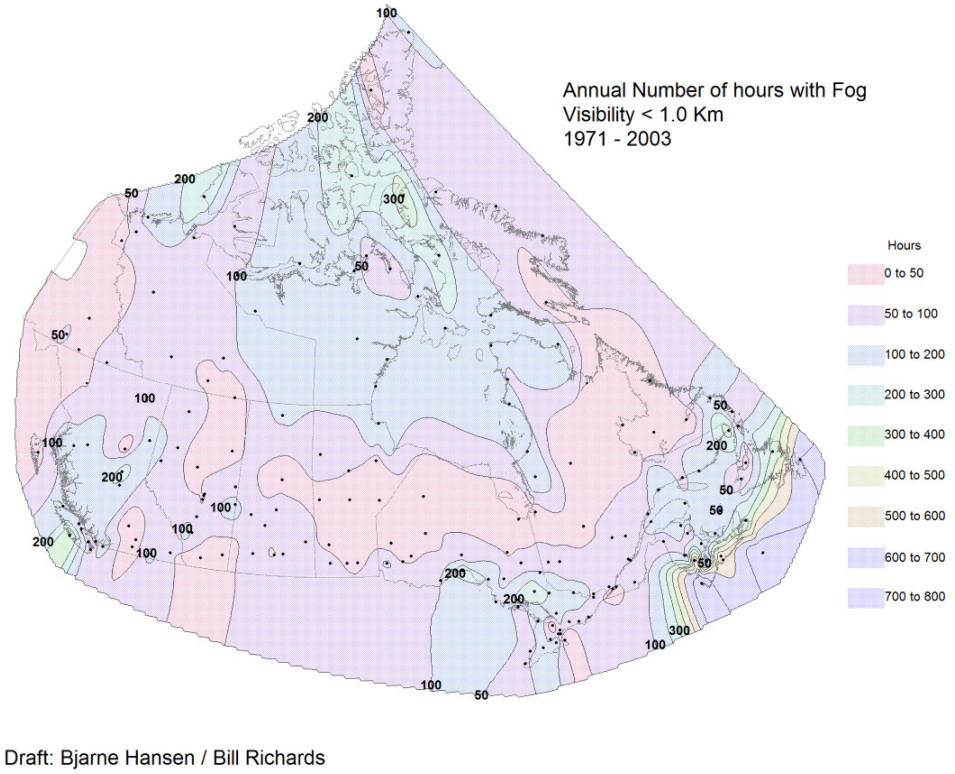


**Figure 3-2** Average annual number of hours with fog based on hourly observations from 1971-2003.

## 3.2 Detailed Fog Climatology

Due to the large variability in climate across Canada owing to its large territory and complex mix of land, sea, mountains and coastline, and also due to the large seasonal variations in Canada's climate, it is not practical to try to present a detailed fog climatology here. Rather, the forecaster must get to know the fog climatology of his or her forecast areas using various sources and through day-to-day experience with the weather. Some of these sources are listed and discussed in the following section *Fog Climatologies at Canadian Observing Sites*. Another interesting descriptive source that does include local details is the Nav Canada Local Area Weather Manual (2002). It presents climatological information for the various regions of Canada in a friendly format that emphasizes the needs of the aviation community but is also useful for the weather community at large.

### 3.2.1 Fog climatologies at Canadian observing sites

A collection of detailed climatological information for most Canadian airports is available at http://pnrinternal.pnr.ec.gc.ca/CMAC-West/site_reference, Prairie and Arctic Storm Prediction Centre/Canadian Meteorological Aviation Centre. Information includes diurnal fog trend, wind rose climatologies, topographic maps for the areas surrounding each airport, and forecasting tips when available (as gleaned from old "Airport Weather Handbooks").

#### 3.2.1.1 Seasonal-diurnal fog climatology

As part of the Fog Remote Sensing and Modeling (FRAM) project (Gultepe et al., 2006b), a set of graphs has been created which displays the seasonal-diurnal climatology of fog, visibility and related weather variables at 198 Canadian airports (Hansen et al. 2007) based on records of hourly observations made during the period from 1971 to 2005. For an example, see Figure 3-3.

Conditional frequencies of observed variables are graphed as fields along two axes: time of day horizontally (hour UTC) and time of year vertically (month), with corresponding gridlines. For additional gridlines, local sunrise and sunset times are plotted (curved lines). Frequencies are also plotted for additional conditions such as wind direction, precipitation, cloud, and persistence (Martin 1972). Field values refer to probabilities of discrete weather events and to statistics of continuous weather variables. Additional weather variables described include: cloud ceiling, blowing snow, snow, ice pellets, freezing rain, freezing drizzle, rain, drizzle, temperature, relative humidity, wind speed, and clouds. The results revealed interesting patterns in diurnal and seasonal variation of visibility.

In the marine environment around Atlantic Canada, the maximum probability of fog is about 35% and is likely mostly due to warm air advection (sea fog). Inland, over Ontario, the maximum probability of fog is about 10% and its occurrence is likely due to a combination of advection and precipitation effects related to frontal systems and radiative cooling. Farther inland, on the Prairies, the maximum probability of fog is about 5% and is most likely due to radiative cooling. It is concluded that the patterns found were both site-specific and regionally coherent.

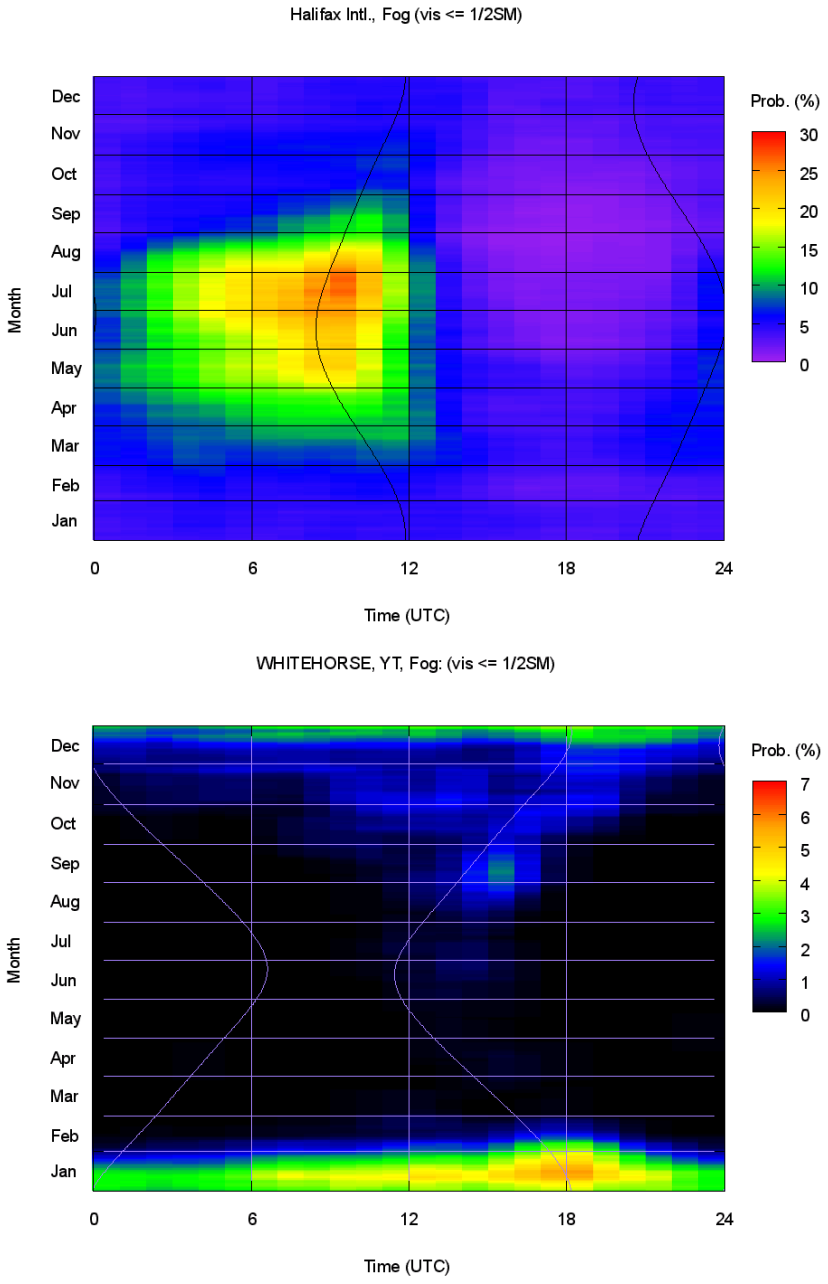


**Figure 3-3** Seasonal-diurnal climatology of fog at Halifax Intl. Airport and at Whitehorse, Yukon Territory. Conditional frequency of fog is graphed along two axes: time of day horizontally (hour UTC) and time of year vertically (month). Local sunrise and sunset times are plotted with curved lines. For Halifax, a peak in fog frequency is apparent in July shortly after sunrise. For Whitehorse, the peak in January is due to ice fog.

# 4 Fog formation and types

This chapter focuses on fog formation and its types related to a synoptic-scale perspective. It is based mainly on the information found in the MOIP (2006) training notes, and Tardif and Rasmussen (2007).

## 4.1 Thermodynamical basis for fog classification

A detailed fog classification based on various thermodynamical processes can be found in Willet (1928), Byers (1944), George (1951), and Byers (1959). Petterssen (1956; his Figure 24.12.3) suggested a simple classification using temperature: 1) water fog (T>-10°C), 2) mixed phase fog (-10°C>T>-30°C), and 3) ice fog (T<-30°C). These three fog types can occur under the various scenarios related moisture and environmental conditions. Figure 4-1 reproduces his results defining fog probability and type.

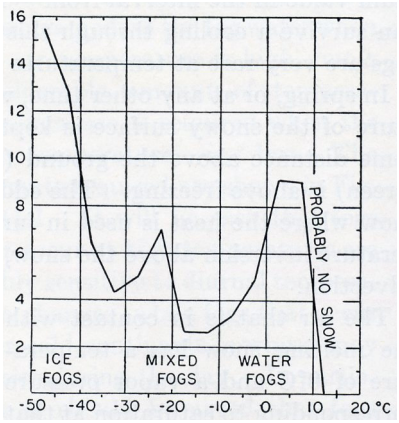


**Figure 4-1** A simple classification of fog based on temperature. "Percentage probability of fog (vertical axis) as a function of temperature at 10 stations in the Ob-Enesei region, October to March. Total number of observations, 4389." (from Petterssen, 1956. p. 124)

## 4.2 Physical and Dynamical Mechanisms leading to fog formation

*1. Mixing of air parcels*

The mixing process involves the mixing of air parcels with different characteristics. It is described briefly by Roach (1994) and by Petterssen (1956 – section 21.11). The mixing process referred to here may operate horizontally, or in a relatively thin layer vertically. Such mixing of two parcels at constant pressure can result in a supersaturation, even if each of the individual parcels was initially unsaturated. The key to fog formation in this case is that the initial temperature difference between the two parcels has to be 'large'. Roach (1994) states that "the

maximum initial supersaturation that can be attained by mixing is roughly proportional to the square of the initial temperature difference between the air parcels which, in the atmosphere, has to be about 10°C to generate a respectable fog."

It is important to distinguish between the large scale mixing and the small scale turbulent mixing processes that play an important role in the formation of radiation fog (see the radiation fog section below). Roach (1995a) discussed the difference: small scale turbulent mixing "is very different from a larger scale event when a nocturnal temperature inversion of 5-10°C over 50-100 m deep layer is overturned by an increasing wind above. It is possible that such an overturning could generate some fogs which are occasionally observed to form suddenly in the early morning after a cloud free night. Once fog has been formed in this way, however, it will require some other mechanism (e.g. radiative cooling) to maintain it." Saunders (1997) mentioned the possibility of formation of mixing fog near sunrise after clear nights due to vertical mixing: "sudden fog formation may result if turbulence mixes cold surface air and warmer air aloft."

George (1951) discussed the case of horizontal mixing in the vicinity of weakening fronts under the heading of 'Mixing-Radiation Fog': "This is not at all a usual type, but it is important to recognize the significant role played by dissolving fronts at many locations. Particularly in late spring and summer, there are many areas which have little or no fog *not* associated with a weak frontal condition. Whether the formation of this kind of fog involves actual mixing of two dissimilar air masses is open to considerable question, but nocturnal radiation is certainly a requirement. Furthermore, there are many occasions when fog does form in a narrow band along a dissolving front even when no daytime clouds are associated with it."

Overall, the consensus in the literature is that fogs formed by mixing process are rare compared to those formed by the evaporation and cooling processes described in the following sections. Therefore, no further discussion will be given related to fog formed by mixing processes.

*2. Evaporation from falling rain: precipitation fog*

Warmer rain can fall through colder air below, where it saturates in the colder air, producing fog. Such fog is called precipitation fog in general or frontal fog if the rain falls through a frontal inversion layer into the cooler airmass below. Often frontal fog will be related to a warm frontal inversion, but it can also occur under a cold frontal inversion. If the temperature difference between the two airmasses is great enough and if the rain continues long enough and if the winds in the cold airmass are light enough, then the evaporation of the rain can cause the cloud base to build downward and to eventually reach the surface as fog, especially over higher terrain.

Precipitation fog in which rain falls through cold air below a non-frontal inversion can occur "along the west coasts of northern continents in winter when cold air from land streams over warmer water and is sprinkled by rain from warm air aloft" (Petterssen 1956). This type of fog also occurs in cold air trapped in mountain valleys, or in air cooled near the shores of large lakes, such as the Great Lakes, at the beginning of the warm season (Petterssen 1956).

*3. Evaporation from water at the surface: Sea smoke, steam fog*

This type of fog is caused by evaporation from a relatively warm water surface into cold dry air flowing over it. "The cold air rapidly absorbs heat and moisture from the ocean by radiative and turbulent transfer of heat. Some of the moisture then condenses as the air in contact with the ocean is mixed with the colder air above" (Roach, 1995b). The greater the temperature difference, the greater the amount of sea smoke that will be formed. Roach (1995b) also notes that this type of fog is "also seen inland as 'steam' fog rising from ice-free streams or lakes in intense cold spells, or sunlit wet ground after a summer shower." George (1951) states that Arctic sea smoke is always shallow and usually does not restrict the visibility to very low values. Roach (1995b) notes that it can be thick and quite extensive but it is rarely a problem in temperate latitudes. Perhaps the most likely situation in which it would become dense would be if it was limited to a small area by terrain (e.g. in a narrow fjord) or in the presence of radiative cooling.

*4. Evaporation from dew at the surface: Morning evaporation fog*

This type of fog was identified by Tardif and Rasmussen (2007). It is due to the evaporation of surface water and mixing in the surface layer. It can occur in situations which are close to those for radiation fog, but in which dew was deposited without the formation of radiation fog. In such cases, within one hour or so following sunrise, it can happen that the temperature increases, but the dew point increases even faster due to evaporation of the dew. The mixing can then lead to fog.

Saunders (1997) also hints at this type of fog: "turbulence and added moisture due to the evaporation from the surface often give a sudden deepening soon after sunrise. Sudden fog formation may occur if turbulence mixes cold surface air with warmer air aloft."

*5. Radiation fog (ground fog)*

This common fog forms in conditions of clear skies and light winds in which the ground loses heat due to outgoing long wave radiation during the night. This cools the air near the ground. If the cooling is great enough, radiation fog can form. The process - deceptively simple

when the details are ignored - actually depends on a complex interplay of surface and atmospheric lower boundary layer characteristics in this radiative cooling situation. Since radiation fog is such a common type of fog, we will examine its formation here in more detail. The discussion and figures are taken with only minor modifications from Saunders (1997).

*Stage 1*: Setup

Physical processes involved in radiation fog formation are illustrated in Figure 4-2 and summarized by Saunders 1997 as follows:

a. Under favourable conditions, the absence of cloud permits strong IR radiative nocturnal cooling at the ground. This cooling is initially rapid, as the net radiative cooling exceeds the upward heat flux from the soil. With the 10m winds < ~7 kt, a temperature inversion forms in the lowest levels near the ground.

b. Once the ground is at the dew (frost) point of the air, dew (frost) deposition onto the surface begins. This dries the air in contact with the ground and slows down surface cooling by the addition of latent heat.

c. Continuation of this process depends on the degree and effectiveness of the vertical mixing in the lowest layers; if sufficient mixing turbulence is present, fresh supplies of moisture will be brought into contact with the ground and deposition of dew (frost) will continue. Hence the amount of water vapour in the atmosphere decreases (as shown by the falling dew or frost points) and air temperatures must fall further before fog can begin to form.

Dew or frost deposition decrease the likelihood of fog formation (except possibly just after sunrise for morning evaporation fog, see the section on morning evaporation fog).

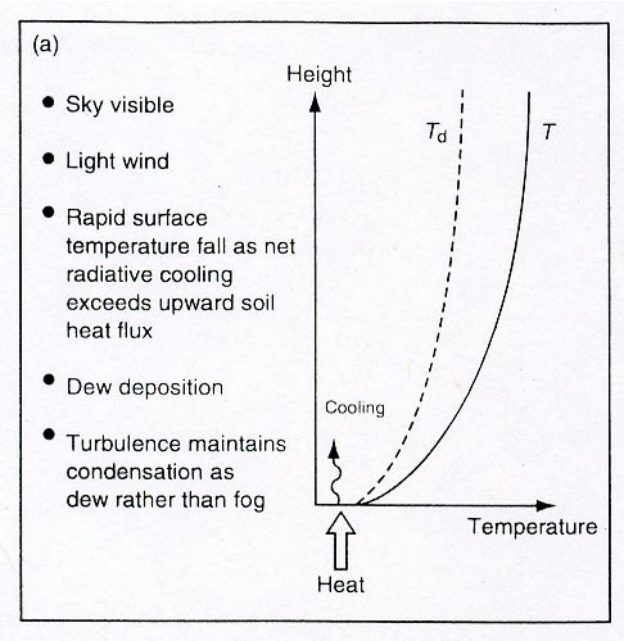


**Figure 4-2** Stage 1 in radiation fog formation (from Saunders 1997).

*Stage 2*: Initial formation

1. Fog formation now depends on a delicate balance of several factors: principally the spreading upward of radiative cooling by turbulence, and the drying and warming of near-surface layers by dew deposition (Figure 4-3).

2. Initial formation often occurs when there is a lull in the 2 m surface wind to around 1 kt or less. This causes turbulence to cease and markedly reduces the rate of dew deposition; with no significant air motion, any further radiative cooling in the lowest layers leads to supersaturation of those layers and hence condensation in the form of thin, shallow wisps of fog at a height of some 20 cm above the ground. (Note that there may not be a 2 m anemometer; under fog formation conditions it will not be possible to deduce the 2 m wind from a 10 m reading.)

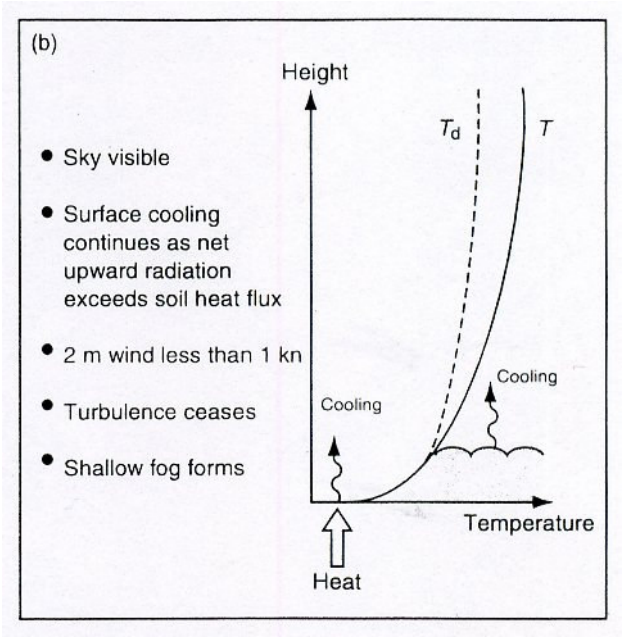


**Figure 4-3** Stage 2 in radiation fog formation (from Saunders 1997).

*Stage 3a*: Mature stage, with sky still visible

1. Radiative cooling continues from the ground and the inversion base remains close to the surface (Figure 4-4).

2. As the screen temperature falls, the fog gradually deepens. The upward heat flux from the soil decreases with time but may still be sufficient to halt the fall in the surface temperature.

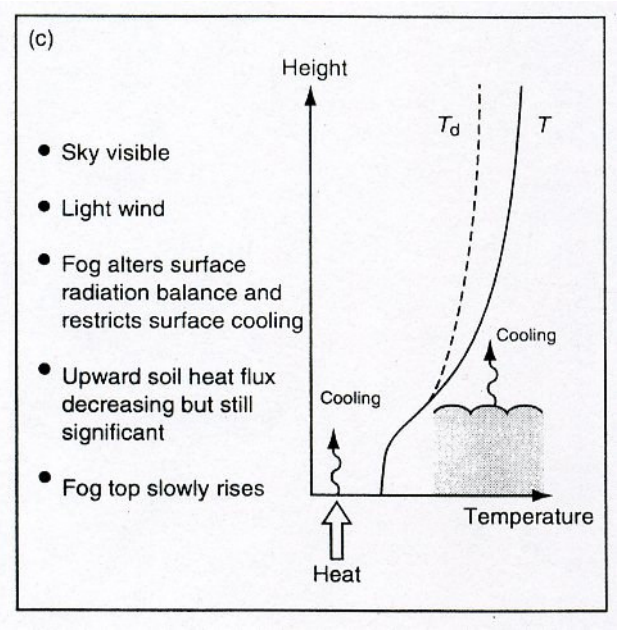


**Figure 4-4** Stage 3a in radiation fog formation (from Saunders 1997).

*Stage 4a:* Mature stage, with sky obscured

1. After a few hours the fog may be deep enough (20 – 50 m) to obscure the sky. The fog top now becomes the radiation surface, radiative cooling at the ground ceases and the surface temperature may start to rise, if the upward soil heat flux is large enough. The resulting heating at the ground and cooling aloft give rise to convective overturning. In fact if the fog is deep enough to have an effective emissivity of ~1, then cooling from the fog top alone can be sufficient to cause overturning (Figure 4-5).

2. This raises the inversion away from the surface as a saturated adiabatic lapse rate profile develops. Continued radiative cooling from the fog top causes the inversion to rise further and fog to continue to deepen.

3. The maximum inversion height of 70 – 230 m is generally reached in 2 – 3 hours after lifting from the surface, with the fog top about 25 m above the base of the inversion; there is a marked wind shear at the fog top.

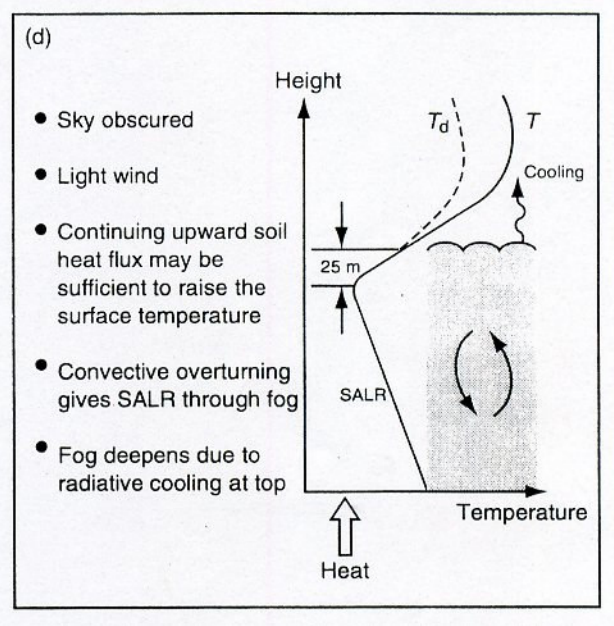


**Figure 4-5** Stage 3b in radiation fog formation (from Saunders 1997).

"The development of the mature radiation fog is dominated by IR radiative cooling from the fog top, whilst the formation process depends upon a subtle balance between turbulent transport and radiative cooling" (Turton and Brown 1987). More specifically, the initial development of radiation fog is primarily controlled by a balance between radiative cooling, which encourages fog, and turbulence, which inhibits it (Capon et al. 2007).

*6. Stratus Build-Down Fog (Cloud-Base Lowering Fog, Inversion Fog)*

This type of fog was not recognized by the researchers of the early 20th century, but modern synoptic experience has shown that it is clearly a type of fog to be reckoned with. Tardif and Rasmussen (2007) include it as one of their five distinct fog types, calling it fog resulting from the lowering of the cloud base. This lowering of the cloud base occurs in the absence of precipitation, so is fundamentally different from precipitation fog. Tardif found that a clear majority of stratus build-down fogs began during the nighttime hours, which implies a relationship to IR radiative cooling.

Petterssen (1956) states that such fogs "are often observed to occur as the result of a downward extension of a layer of stratus situated under the base of a temperature inversion, and such fogs are commonly called inversion fogs."

Baker et al. (2002) describe the formation of these fogs as follows: "While it is true that in the presence of stratus clouds surface radiative cooling is *reduced*, it is generally *not* eliminated, especially when the cloud layer is thin. Furthermore, the top of the stratus itself becomes a radiatively cooling surface in the absence of clouds aloft. Mixing redistributes this heat loss downward, cooling the air below the cloud layer and lowering the condensation level. Cloud top cooling also promotes droplet growth and settling, which further promotes cloud base lowering. Since any upward transfer of heat from the ground counteracts this 'build-down' process, the most rapid 'build-downs' are associated with a cold underlying surface." From this explanation it is clear that radiative cooling of the stratus top is the original cause of such fogs, but turbulent mixing also plays a central role. For such radiative cooling to exist, the atmosphere above the stratus tops must be essentially cloud free, so that the outgoing long wave radiation has a free path to space.

Peak and Tag (1989) have discussed the formation of these fogs as follows: "There first must be a stratus deck at the top of the marine layer. The vertical temperature structure must be conducive to stratus-lowering. That is, the inversion classification (Rogers 1988) must be 'Type 2' (a nonlapsed [i.e. temperature constant or increasing with height] marine layer capped by an inversion aloft) or 'Type 3' (a lapsed [i.e. temperature decreasing with height] capped marine layer). As long as the inversion is at or below 400 m, the marine layer is shallow enough for stratus to lower all the way to the surface". Peak and Tag (1989) note that "the mechanism for lowering the stratus base is radiative cooling of the stratus top with subsequent mixing downward (Pilie et al. 1979)". These researchers all emphasize that a low level inversion is necessary for this type of fog to occur.

The model of Pilie et al. (1979) states that "net radiation from the stratus top caused rapid cooling, which created instability beneath the inversion, causing turbulent transport of cool air and cloud droplets downward. Evaporation of droplets beneath the cloud base caused the increase in humidity. This, coupled with the cooling, lowered the level at which saturation occurred and the base propagated downward." In their observational work, Pilie et al. (1979) found that the stratus lowering process could produce fog at the surface only when the inversion base is below 400 m. The analysis of Oliver et al. (1978) found a similar value of 350 m.

*7. Cooling due to advection: Advection fog*

In situations in which warm air flows over a cold surface, the air near the surface can be cooled to the point where fog forms. Such fog is referred to as advection fog. It frequently forms over the ocean, in areas where the cold sea surface cools the warmer air with which it is in contact. This is common, for example, over the ocean off the Canadian east coast, in which warm moist air flowing from the south eventually encounters cold ocean waters to the north of the Gulf Stream. Petterssen (1956) also notes that "fogs which are predominantly of the advection type occur frequently over land along coasts. Most of these fogs form at night and are caused by advection of moist air from water bodies which later becomes exposed to nocturnal cooling over land."

Advection fog can also form over land without a marine influence. One such common scenario of formation, warm air flowing over cold ground, is very efficient in cooling the air near the surface. Saunders (1997) mentions that "for advection fog over land to be at all widespread or persistent, it is generally necessary for the ground to be very cold – either frozen or snow covered. Particularly widespread and persistent fog may occur when warm air starts snow cover thawing." However, snow-covered ground in certain temperature ranges can act *against* fog formation for other reasons, as described in the section below on fog and surface characteristics.

*8. Cooling due to adiabatic lift: Upslope fog*

In cases of upslope flow, the air moving to higher levels is forced to undergo adiabatic cooling. If the cooling is strong enough, stratus or fog can form. Such fogs are common on the windward side of mountain slopes, or in cases of sustained upslope flow over a more gently rising surface. For such a fog to exist, the saturated air must be stably stratified; otherwise, convection will develop when saturation of the air flowing up the slope is reached, or else vertical mixing will bring drier air down from aloft so that fog will not form at the surface. George (1951) states that upslope conditions by themselves are rarely the primary cause of fog formation (except along the higher and steeper portions of mountain ranges) since the source

areas of the upslope flow are often quite dry. According to him, in areas of more gentle and widespread upslope flow, the upslope cooling most commonly combines with pre-warm frontal precipitation areas to produce widespread areas of fog. However, if the source area is fairly moist, then the upslope flow by itself may provide enough cooling to form fog.

*9. Mixed-phased fog: Microphysical processes and thermodynamics*

Mixed phase fog is composed of both supercooled droplets and ice crystals. Supercooled droplets can exist in temperatures down to -40$^{o}$C (but this is not very common). Below -40°C, droplets freeze and ice crystals form directly from diffusion of vapour over ice nuclei (IN). Fog that contains liquid droplets at temperatures below zero is often referred to as 'freezing fog' because supercooled water droplets will freeze on contact with a surface such as an airplane wing or objects on the ground.

A classification of fog based on T, RHw (relative humidity with respect to water), and RHi (relative humidity with respect to ice) is shown in Table 1, which is based on the fog studies of Gultepe et al. (2008 and 2009), and on fog climatology.

| | | |
|---|---|---|
| T > 0°C | RHw>99% (saturated wrt water) | Warm fog |
| -10 < T < =0°C | RHw>99% (saturated wrt water) | Freezing fog (freezing droplets) |
| -10>T>-40°C | RHw>99% (makes RHi>99%) (saturated wrt water and ice) | Mixed phase fog that includes droplets and ice particles |
| T<=-10°C | RHi>99% but RHw<100% (saturated wrt ice) | Ice fog (heterogeneous nucleation) |
| T<-40°C | RHi>99% | Ice fog (homogeneous nucleation) |

**Table 1** Fog classification based on temperature (T) and relative humidity (RH). Ice fog usually occurs when T < -10°C, but if IN exist at warmer temperatures, e.g., T = -5°C and RHi > 100%, then ice fog may occur (Gultepe et al. 2008). Note that T=-10°C threshold should not be considered a fixed value. Also, note that fog formation and type cannot be directly compared with in-cloud microphysical parameters.

In situ studies of the cloud physics by Cober et al. (2001) found that mixed phase clouds occur about 30% of the time for the T range of 0 to -40°C, but these studies did not represent cloud equilibrium conditions. Predominantly liquid droplets in mixed phase clouds have been seen at temperatures as low as -32°C (Witte 1968). In lower boundary layer clouds, Curry et al. (1996) observed mixed phased clouds over the Beaufort Sea in the temperature range of -8 to -18°C.

*10. Ice fog: Microphysics and thermodynamics*

Ice fog occurs when supersaturation with respect to ice exists over cold regions (T < -10°C). Ice nuclei are required when T > -40°C. They usually become active at T < -10°C but ice fog happens more often when T < -20°C because of high supersaturation regions at cold T. Ice fog occurs at T < -40°C by direct deposition from vapour to IN at RHi > 99%. Homogeneous nucleation occurs at T < -40°C where any liquid particles freeze. The "intensity" of ice fog depends on the number of IN and the available moisture that is used for particle growth. Intensity of fog is measured with how much visible light is scattered around and absorbed by fog particles. The sum of scattering and absorption represents extinction of visible light. This extinction value is then converted to visibility (Gultepe et al., 2006a)

At very cold temperatures, existence of IN over cities is enhanced by man-made pollution sources and transportation from remote pollution sources (e.g. combustion from cars, airplanes, factories, homes, forest fires, and industrial areas). It should be noted that there is still debate about the role of ice nucleation in cloud and fog formation, and in turn about its effect on climate. One of the main conclusions obtained from the ICNAA (International Conference on Nucleation and Atmospheric Aerosols) meeting in Prague, Czech Republic, that took place in August of 2009 suggests that the biogenic origin of IN can also play an important role in ice fog formation.

Concerning ice nuclei, Petterssen (1956, pg. 124) refers to his Fig 24.12.3 (reproduced as Fig 4-1 of this handbook) for the probability of fog formation over various temperature ranges and concluded that "in the interval from -20 to -25°C, there is a secondary maximum which is apparently due to certain sublimation nuclei that become active in that temperature range". No further explanation is offered. The strong maximum in probability of ice fog at temperatures below about -35°C is clear from this graphic. Petterssen specifies that the data in the graphic "refer to stations in the Ob-Enesei region (of the USSR), 1930 to 1936, and are largely unaffected by human activities". It seems that different natural ice nuclei may be activated at different temperatures, and that there are some that are activated in the -20 to -25°C range. Some others could be activated at even warmer temperatures but this needs to be further verified.

Figure 4-6 shows fog occurrence based on temperature. This figure shows that the results of Gultepe et al. (2007a) were similar to Petterssen's (1956) work and suggests that temperature plays an important role in defining fog and should be considered for forecasting applications. One should recognize that these temperature thresholds generally do not separate fogs with different physical characteristics. At best, such a procedure can draw our attention very generally to three different types of fogs: those composed of liquid droplets only (whether warmer than

0°C or supercooled), those of mixed phase, and those composed of ice crystals only (see Table 1).

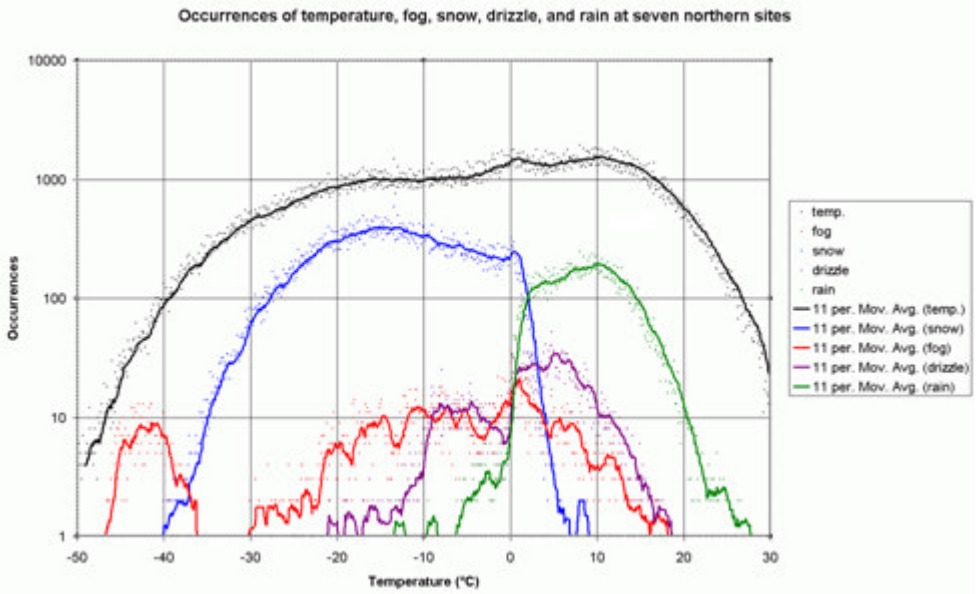


**Figure 4-6** Frequencies of occurrence of fog, snow, drizzle, rain and temperature for seven northern Canadian observing sites (CYQH, Watson Lake; CWDL, Dease Lake; CYXY, Whitehorse; CYVQ, Norman Wells; CYCO, Kugluktuk; CYZF, Yellowknife; CYHY, Hay River). About 600,000 hourly observations in total were used in the preparation of this image, for the period 1996-2005 inclusive.

Figure 4-7 illustrates fog occurrence at Whitehorse, YT as a function of temperature. (Graphics like this for observing stations across Canada are given at http://arxt39.cmc.ec.gc.ca/~armabha/clim/temp_dirn). The number of observations (not the percentage probability) is plotted on the y axis. The main ice fog zone is clearly identified by the spike at temperatures colder than -35°C. Interestingly, there are almost no observations in the -25 to -35°C temperature range. It must be noted that these graphics are site specific, and different observing sites can show different characteristics. For example, Old Crow results show high numbers of fog observations in the -40 to -45°C range. On the other hand, Dawson and Burwash have only a few observations in that temperature range. A division between the cold ice fog mode and the other modes often exists, but this is not the case at some locations. For example, some of the central Arctic stations (e.g. Baker Lake, Cambridge Bay, Arviat) show no clear break between ice fog and other fog types.

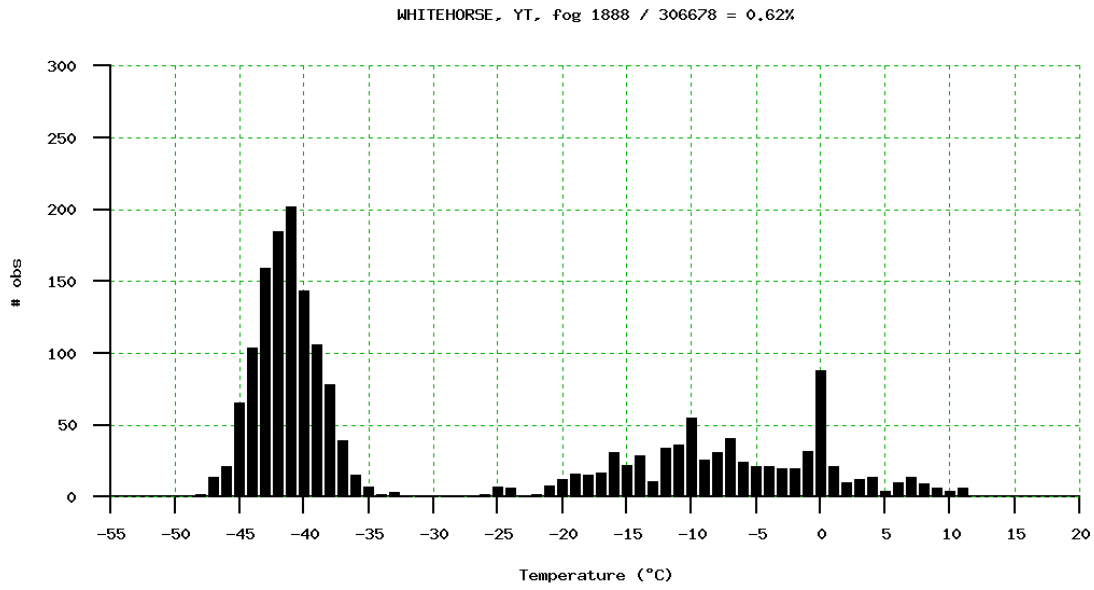


**Figure 4-7** Ice fog occurrence over White Horse based on 30 years of data.

Charlton and Park (1984) concluded that in the industrial area of Edmonton, deep ice fog conditions would generally set in at temperatures below -35°C. Burrows (2007, personal communication) remembers a subjective threshold of -27°F (~ -33°C) in the northern part of the city of Edmonton in the mid 1960s, below which dense ice fog would form.

*11. Sea fog or marine fog*

Sea fog is a particular category that deserves some attention because it forms in an environment fundamentally different from the land environment. Over land, the skin temperature is controlled by the diurnal cycle with short and long wave radiation, and by exchange between the air and the ground. Over the seas, the skin temperature (i.e. the sea surface temperature SST) is nearly constant, at least over time scales of a few days, and the diurnal cycle loses its importance.

The following graphic (U.S. Department of Agriculture, 1938, Chart 53) as reproduced by Lewis et al. (2004) shows the percentage of ship observations that reported dense sea fog (visibility < 1,100 yards) in the months of June, July and August for the years 1885 – 1933 (Figure 4-8). Strong maxima are apparent over the western Atlantic (30+ % near Newfoundland) and over the western Pacific (40+ % south of Kamchatka). Advection of warm moist air over the cold waters of these areas is the basic cause of these fogs.

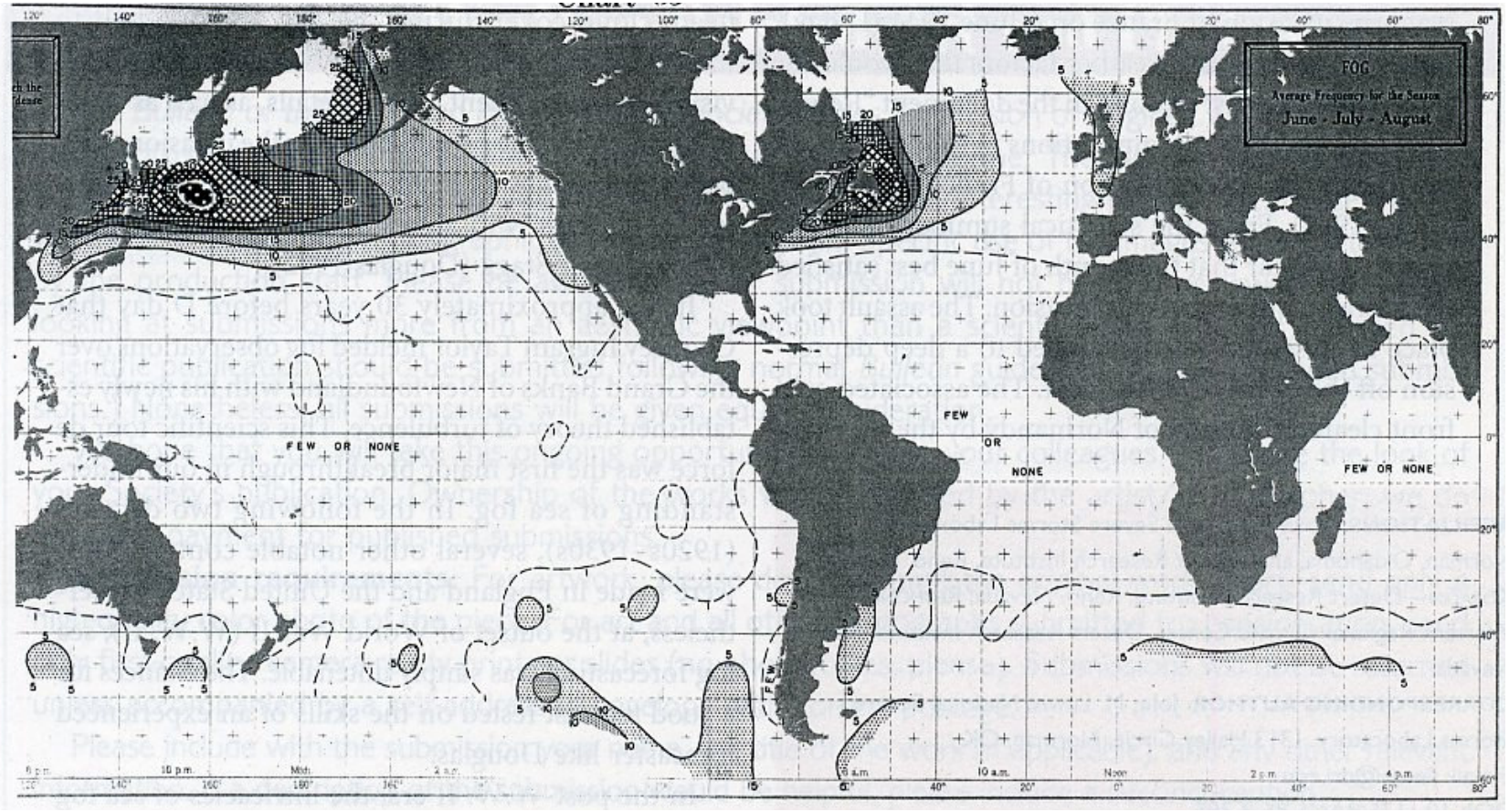


**Figure 4-8** Sea fog frequency [% of the observations indicating moderate to dense fog (not including mist)] in June, July, and August (1885-1933). Chart 53 from *Atlas of the Climatic Charts of the Oceans* (U.S. Department of Agriculture 1938). From Lewis et al. (2004).

Sea fog (also referred to as marine fog) forms over the sea when a cooling process occurs. Sea fog that is blown onto a coast is referred to as coastal fog. Sea fog can form if the SST is either lower or higher than the air temperature.

*i) Sea initially colder than the air*

Sea fog commonly forms through the advection fog process, due to cooling by the water below, which may be several degrees Celsius cooler than the air streaming above it. "It is thought that the fog forms when the SST falls below the dew point of the air moving over it" (Roach, 1995b). A classic example of this is shown in Figure 4-9 with warmer air flow from the west and southwest moving over the cool, tidally-mixed waters of the Gulf of Maine and Bay of Fundy on 02 June 2005. Fog along the Atlantic Coast of Nova Scotia is very common during June and July, and can be more prevalent during cool oceanic upwelling events when prolonged southwesterly winds blow parallel to the coast.

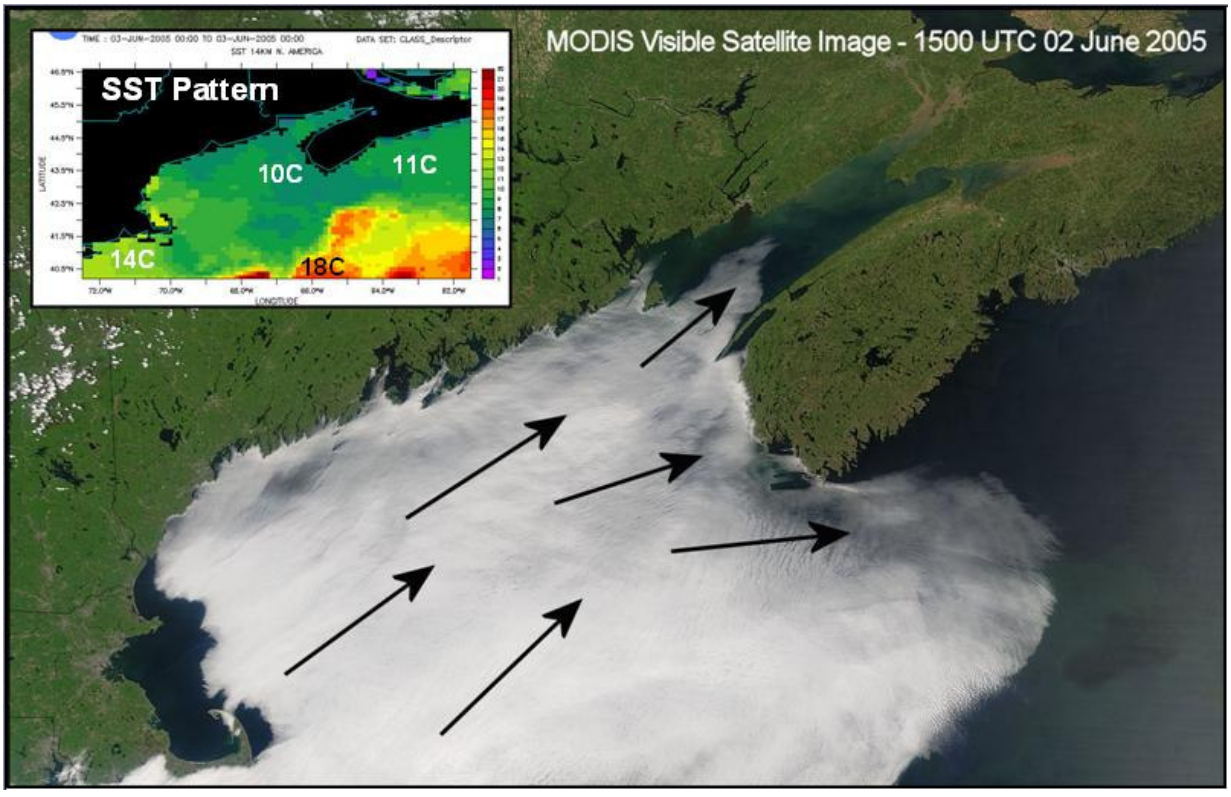


**Figure 4-9** MODIS satellite image of fog in the Gulf of Maine and Bay of Fundy on 02 June 2005. Sea surface temperatures (SSTs) at the time are shown in the inset. Black arrows denote the surface wind flow pattern.

There may also be a radiative contribution to the formation of sea fogs. Roach (1995b) has noted that "sea fog has been observed to form in relatively stagnant air near centres of slow-

moving anticyclones. This fog may be induced by a combination of moisture pick-up from the ocean and slow radiative cooling of the air mass, accelerated once fog forms."

*ii) Sea initially warmer than the air*

In this case an evaporation fog of the "sea smoke" type already discussed above can occur when the SST is much warmer than the air flowing over it. Usually this type of fog does not reduce visibility as significantly as radiation type fog because it usually appears as distinct "steam" columns rising from the water. Between the moist columns there are often drier areas without fog/condensation and the visibility reduction is often shallow as in Figure 4-10. Sometimes under the right conditions when there is also some radiational cooling, the sea smoke can take on the appearance of typical radiation fog (more vertical extent), with low visibilities over a small area near a warm lake or river valley for instance.

**Figure 4-10** Sea smoke over Halifax Harbour, 17 January 2004. Photo by Paul Pendergast (http://www.pendergast.ca/jan17).

*12. Combinations of processes*

Fog is generally not caused by one sole physical process, but rather by a combination of processes, in which one is perhaps dominant. For example, a common combination occurs when warm air travels over cold ground, followed by radiational cooling during the night. For example, many fogs could be categorized as "radiation-advection" fogs. In such cases, the changes related to advection (e.g. low-level cooling over a colder surface, moist advection) can result in an air mass in which fog will form once the air is carried to a region with favourable characteristics for radiation fog, or thicken an area of pre-existing fog. This scenario is

common in coastal areas, in which marine fog or a marine air mass can be advected to land by onshore flow, where favourable conditions for radiation fog may exist. Another example was mentioned in a previous section, in which upslope cooling often combines with pre-warm-frontal precipitation to produce widespread areas of fog. A combination of radiational cooling with sea smoke type conditions over warm lakes can occur in the fall when nights become longer but while the lakes are still relatively warm (Figure 4-11). This commonly occurs around the Halifax International Airport in Nova Scotia which is neighboured by many lakes. Flight operations are often affected by this type of fog since it can become particularly thick.

**Figure 4-11** Photograph of radiational fog that forms over a relatively warm lake during the early morning hours. (Lake Carroll, Carrollton, Georgia – photo by Ralph F. Kresge at http://www.photolib.noaa.gov/bigs/wea02054.jpg)

## 4.3 Synoptic considerations

### 4.3.1 Radiation Fog

Terminology: Radiation Fog, Ground Fog, Low Fog, Valley Fog, Shallow Fog

Formation process:

Nighttime cooling reduces the air temperature and - if the air is not initially too dry and if the right turbulent mixing conditions exist – then saturation occurs and water droplets condense onto available cloud condensation nuclei. This process, involving a delicate balance between radiative cooling and turbulent mixing, was described in detail in section 4.2 above. Radiation fogs form upward from the ground as the night progresses and are usually deepest around sunrise (Figure 4-12). However, fog may occasionally form just *after* sunrise when evaporation and mixing take place near the surface. See section 4.3.6 below for a discussion of this type of fog, known as "morning evaporation fog."

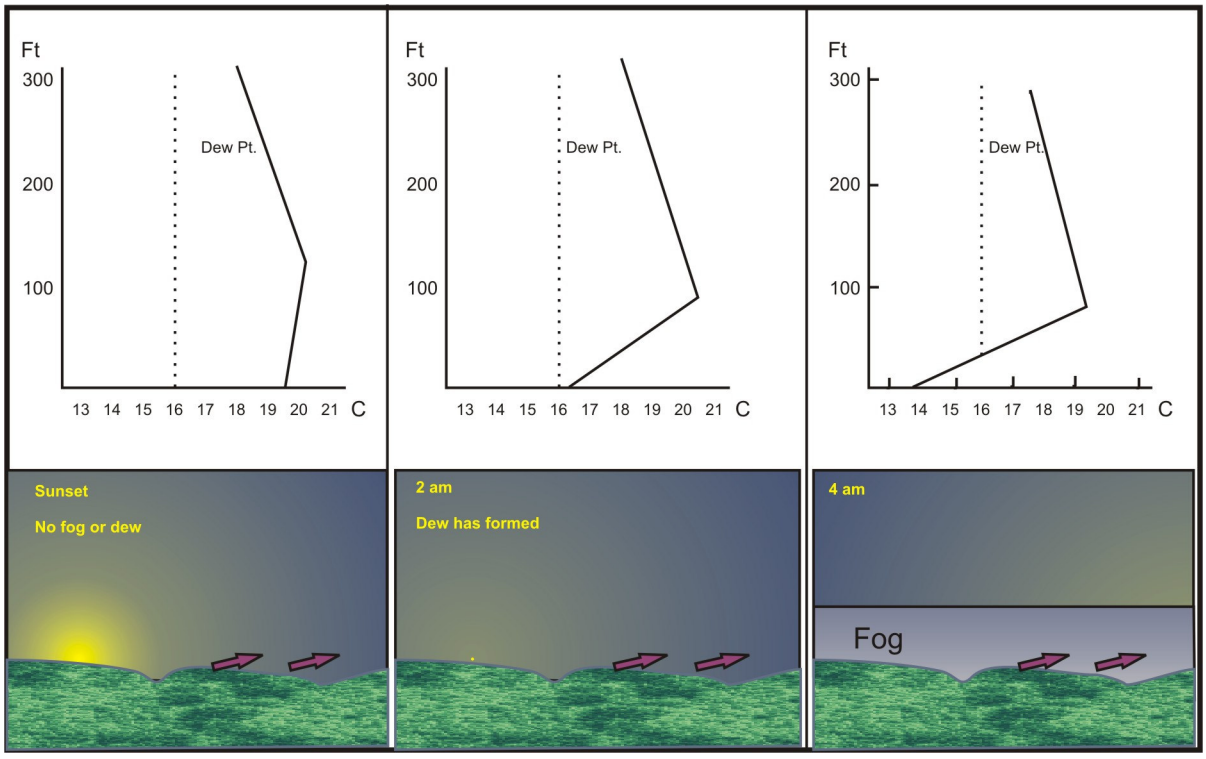


**Figure 4-12** Typical radiation fog formation: 1. Clear skies at night. 2. Sufficient moisture. 3. Light winds (adapted from MOIP 2006).

Favourable Conditions of Formation:

1. clear skies: to optimise the radiative cooling process, the longer the night, the longer the time of cooling and the greater the likelihood of fog. Hence, radiation fogs are most common over land in late fall and winter.
2. small dew point depression at sunset (T - Td): less cooling is required to form the fog.
3. light winds, < 10 knots, or slight turbulence: slight air movement brings more of the moist air in direct contact with the cold ground in order to distribute the cooling effect more rapidly through a deep enough layer.
4. mixing ratio value increases with height ($dr/dz > 0$) : for dense persistent fog.
5. wet surface : less cooling is required to form the fog.
6. local topography: valley or low spot with cold air drainage favouring the cooling of the air. Because colder air drains downhill and collects in valley bottoms, we normally see radiation fog forming in low lying areas (Figure 4-13). Radiation fog in these circumstances may be called valley fog.
7. condensation nuclei: the more the better for the condensation phase.

Unfavourable Conditions:

1. strong winds (> 10 kts): diffuse the water vapour available by mixing the moist air near the surface with drier air above, and may lift the fog to form stratus.
2. cloudy skies: limit the radiational cooling of the surface.
3. large dew point depression : this could require too much cooling for what is possible at night to allow the fog to form.
4. no wind in lowest few metres: promotes deposition of dew or frost.

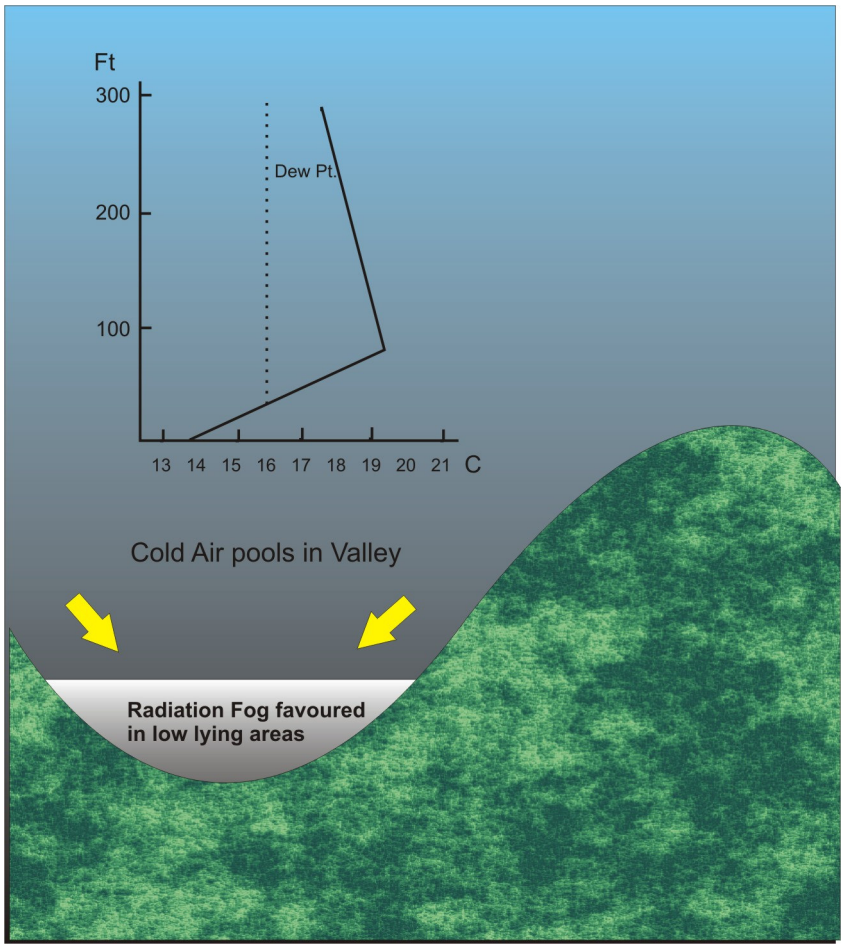


**Figure 4-13** Radiation fog favoured by a low lying area (adapted from MOIP 2006).

Characteristics and synoptic conditions:

1. Stable air: inversion
2. Can form or thicken at sunrise: the mixing caused by the heating of the air stirs up the moisture with cold air near the ground.
3. Drains to low lying areas: cold air is more dense
4. Usually burns off during the morning: as the incoming solar radiation increases and finally exceeds the outgoing long wave radiation, the $r_s$ (saturation mixing ratio) increases while the mixing ratio r remains the same
5. More common in high pressure areas: where light winds and clear skies prevail.
6. Can be initiated by aircraft: due to the release of condensation nuclei and water vapour in their exhaust.
7. Since radiation fog normally forms in the lowlands, hills may be clear all day long, while adjacent valleys are fogged in.

8. More radiation fog in fall and spring than in winter due to smaller supersaturation requirements.
9. Frequent in maritime coastal areas in the fall (due to extra available humidity).
10. When a high pressure system moves slowly over an area, radiation fog may form on many consecutive nights.
11. Note: Over a snow surface if $T_{AIR} < 0°C$ then the air must become supersaturated with respect to *frost point* for radiation fog formation

### 4.3.2 Advection Fog

Advection fog can occur over land or sea.

Formation process:

Advection fog forms as a result of advective cooling, and is often thicker and longer-lasting than radiation fog. As warm moist air is advected over a cold surface, it cools through conduction as it releases its heat to the cold surface. The cooling of the air to its dew point ($T_d$) causes saturation. The presence of condensation nuclei along with further cooling will produce condensation and therefore fog. This cold surface could be cold water, cold ground or an area covered with snow or ice. The surface must be sufficiently cooler than the air above so that the transfer of heat from air to surface can reduce the air temperature to the dew point temperature.

Favourable Conditions for formation:

1. High relative humidity: if the air is moist it requires less cooling
2. Stable stratification in lower atmosphere: warm air over a cold surface
3. Moderate winds (i.e., 8-17 knots: the fog will be less dense with lighter winds, and stronger winds will produce stratus or stratocumulus).
4. $T_{AIR} - T_{SFC}$ = large (i.e. the air is warm: this will optimize the advective cooling).
5. Large horizontal temperature gradient: this will favour the surface-air contrast in the cold air, and also the moderate winds.
6. In the lowest levels $dr/dz > 0$: (r is the specific humidity and z is height). If this condition is not met, turbulent mixing can bring down drier air and therefore decrease the possibility of fog)
7. Cold surface could be: land, snow, ice or cold sea or lake

Characteristics and synoptic situation:

1. Will persist until air mass or wind direction changes: a new wind direction may bring drier and/or cooler air, thus ending the conditions required for the advection fog to exist
2. May be stopped by land barriers (wind barrier effect)

3. May thin as ground heats: as the temperature increases $r_s$ (specific humidity) will increase and RH will decrease. Advection fogs prevail where two ocean currents with different temperatures flow next to one another. Such is the case in the Atlantic Ocean off the coast of the Atlantic provinces, where the cold southward-flowing Labrador Current meets the warm northward-flowing Gulf Stream. Warm southerly air moving over the cold water produces fog in that region throughout much of the year, and especially in the summer.
4. Summer: warm air over cold open arctic landmass.
5. Spring: warm air over cold (Great) Lakes.
6. Winter: mild air moving northward over snow cover or cold ground with frost.
7. In the case of sea fog, it tends to drift onshore, and, if the land is warm, the resultant turbulent and convective motion will dissipate fog or produce stratus. At night, the cooling of the land surface may well lead to the spread of fog far inland from the coast. In such a case there are both radiative and advective effects at work.

### 4.3.3 Upslope fog

Formation process:

Upslope fog forms as a result of adiabatic cooling by expansion of the air as it rises along a slope (Figure 4-14). Winds produce the initial motion upward along the slope. The cooling of the air to its dew point causes saturation. The presence of condensation nuclei with continued cooling will produce condensation leading to the fog. Basically, this fog is a cloud that touches the ground or more precisely, the ground rises to touch the cloud.

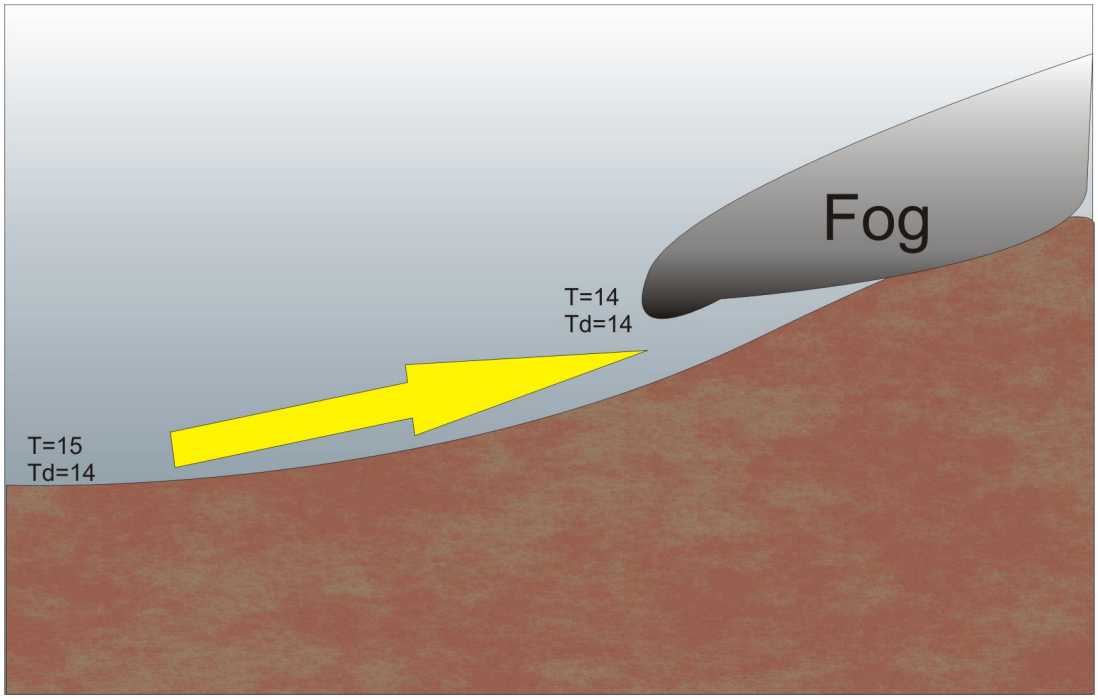


**Figure 4-14** Upslope fog and stratus (adapted from MOIP 2006).

Favourable conditions:

1. Hilly or mountainous terrain or sloping ground: so that the adiabatic cooling can take place as the air is forced to rise.
2. Upslope and/or onshore winds: the fog will be less dense with lighter winds and stronger winds will produce more mixing near the ground so that it may form some stratus or stratocumulus. The strength of the wind is important but its effect is dependent on several factors such as the slope itself, the RH of the air and the terrain roughness. Sometimes dense fog can form with strong winds (e.g. Cheyenne type fog in Colorado) if the air is saturated through a deep enough layer.
3. High relative humidity (small T-Td): requires less cooling.

4. Increase of moisture with height.
5. Stable air mass

Characteristics and synoptic situation:

1. Persist until air mass or wind direction changes.
2. Dissipates on leeward side due to subsidence.
3. Height of the slope is an important factor since Td will decrease by about 2 degrees per 1000 m.
4. May occur in easterly flow across the Prairies (e.g. YWG to YEG); to the north of synoptic low pressure systems; and in moist flow off the Atlantic to Appalachians;
5. It is closely related to local topography.
6. Will contribute to more widespread precipitation fog when precipitation is falling.

### 4.3.4 Precipitation fog : prefrontal (warm front) and post frontal (cold front)

Formation process:

**Prefrontal fog/warm front:** Fog in advance of a warm front is caused mainly by the increase of moisture in the underlying cold air resulting from the evaporation of pre-frontal rain. It can be augmented by cooling due to upslope flow if such upslope flow exists to the north of the warm front (Figure 4-15).

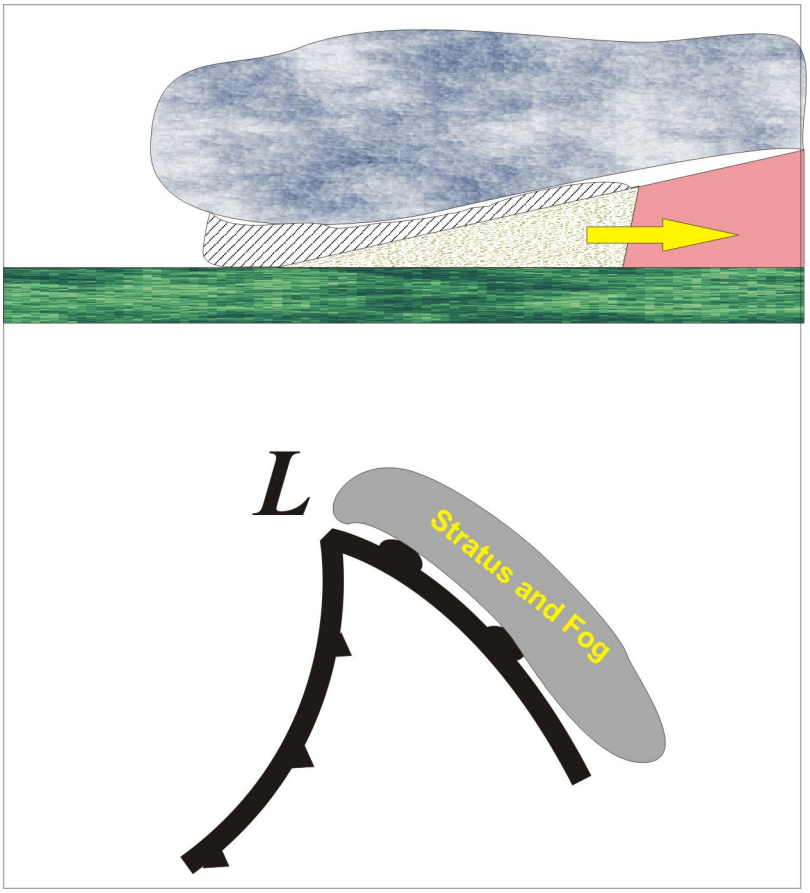


**Figure 4-15** Precipitation fog and stratus associated with a warm front (adapted from MOIP 2006).

In this process, relatively warm rain falls through a cold layer. This cold layer is nearly saturated. The mixing ratio of the cold air increases as precipitation evaporates within it. Consider the sounding below (Figure 4-16) which is typical for a warm front. Suppose rain begins falling from cloud based at the top of the inversion. The raindrops have a temperature $T_R$. Note that the rain remains warmer than the surrounding air all the way down to the surface. Consequently, the cloud base will gradually build down to the surface: as the warm rain

evaporates it initiates saturation, and condensation eventually occurs through the entire layer of colder air.

Characteristics and synoptic situation:

1. Prefrontal fog is associated with nimbostratus that produces rain for a few hours. During the rain, the base of the nimbostratus lowers to the ground to form the fog as the warm front approaches. The fog clears after the frontal passage.
2. Stratus fractus is formed by the same process as the prefrontal fog.
3. Prefrontal fog is often observed with drizzle.

*Forecasting hint 1*: The formation of stratus fractus in the precipitation ahead of the warm front can be a precursor for the occurrence of prefrontal fog.

*Forecasting hint 2*: Expect warm frontal fog when the temperatures ahead of the front are lower than the dew points behind the front.

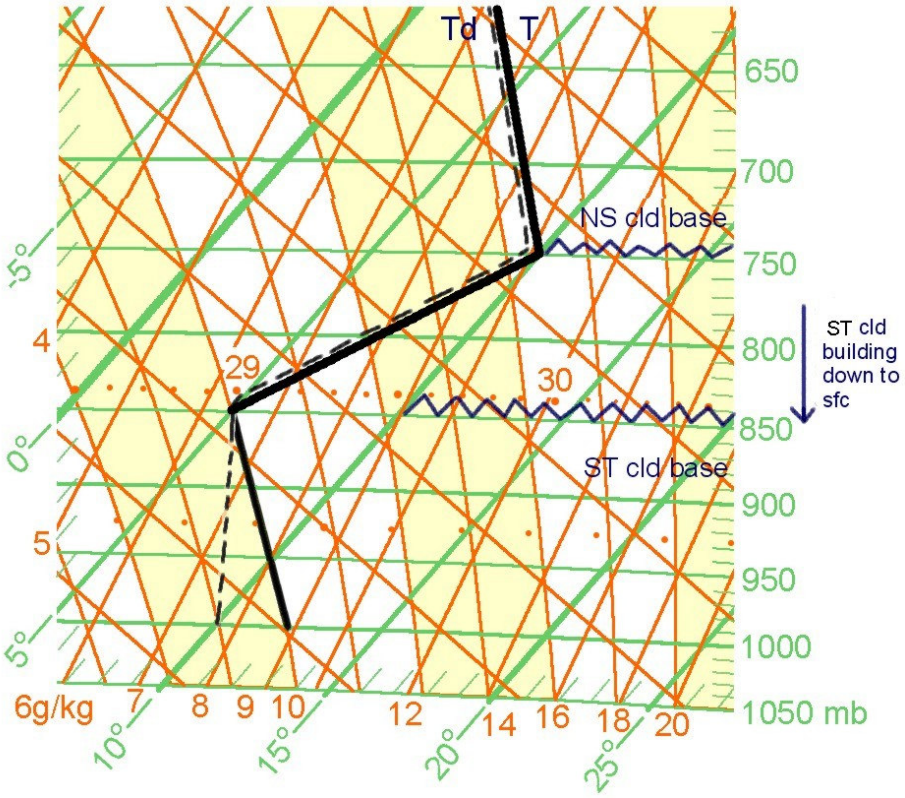


**Figure 4-16** Typical warm front sounding. Solid line is observed temperature, dashed line is dewpoint temperature ($T_d$) and ST is for the stratus cloud layer that is between 750 and 850 mb.

**Post frontal fog /cold front:** This type of fog can be the result of precipitation falling into cold, stable air, raising the dew point temperature and eventually saturating the air. It will form especially if the winds are light. This is also seen as a type of radiational fog which occurs over wet ground under clear skies and light winds after the passage of a cold front.

### 4.3.5 Stratus Build-Down fog

Terminology: Stratus build-down fog, cloud-base lowering fog, inversion fog

This type of fog occurs in the absence of precipitation, and so is fundamentally different from the precipitation fogs discussed in the previous section.

Formation process

Baker et al. (2002) describe the formation of this type of fog as follows: "While it is true that in the presence of stratus clouds surface radiative cooling is *reduced*, it is generally *not* eliminated, especially when the cloud layer is thin. Furthermore, the top of the stratus itself becomes a radiative cooling surface in the absence of clouds aloft. Mixing redistributes this heat loss downward, cooling the air below the cloud layer and lowering the condensation level. Cloud top cooling also promotes droplet growth and settling, which further promotes lowering of the cloud base. Since any upward transfer of heat from the ground counteracts this 'build-down' process, the most rapid 'build-downs' are associated with a cold underlying surface." Furthermore, they go on to explain that "snow-covered regions are especially vulnerable to stratus build-downs due to the excellent long wave radiative emissivity and poor thermal conductivity of snow. This leads to rapid boundary layer cooling since the surface radiative heat loss is uncompensated by the transfer of heat from the warmer soil below."

Clearly the radiative cooling of the stratus top is the original cause of stratus build-down fogs, but turbulent mixing also plays a central role. For the necessary radiative cooling to exist, the atmosphere above the stratus tops must be essentially cloud free, so that the outgoing long wave radiation has a free path to space. Furthermore, Peak and Tag (1989) emphasize that an inversion is necessary for this type of fog to form in the marine environment. They found that as long as the inversion is at or below 400 m, the marine layer is shallow enough for stratus to lower all the way to the surface.

The process is illustrated in Figure 4-17 below, adapted from Pilie et al. (1979).

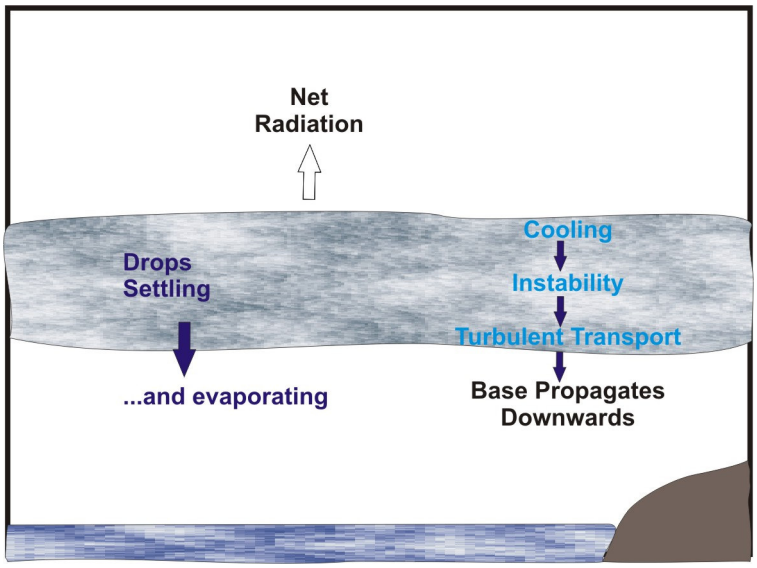


**Figure 4-17** Schematic representation of fog formation through the stratus-lowering process (adapted from Pilié et al, 1979).

Such fogs require, to start, the presence of stratus under a fairly strong and stable inversion. However the atmosphere must be fairly cloud free above the stratus deck so that long wave radiation can escape to space, allowing the cloud top to cool.

Stratus build down fogs can occur under persistent low level inversions in various situations, such as:

1. Over subtropical west coasts, in which there is semi-permanent low level subsidence under an anticyclone along with upwelling of cold water just off the coast (such as along the California coast in summer). In this situation a semi-permanent low level inversion is formed. “Because of turbulent mixing, a layer of stratus is usually present under the base of the inversion off the coast. Investigations of the inversion fogs that occur along the coast of California have shown that the diurnal variation of the height of the inversion is small compared with the variation in the height of the condensation level, and that the condensation level over land is above the inversion during the day and below the inversion at night. Thus, a layer of stratus or fog will be a normal occurrence over land during the night, when the inversion is sufficiently low and the relative humidity below the inversion sufficiently high, the subsequent nocturnal cooling will suffice to cause a stratus layer to form and build down to the ground, thus causing fog” (Petterssen 1956).
2. In mountain valleys (e.g. over western North America) in which cold air becomes trapped below warm air, separated by an inversion. Such fog can be very persistent due

to the valley walls which block the circulation of air from some directions. The effect is stronger in winter when the ground can be cold and/or snow-covered and the solar insolation is weak. Such fog is often referred to as valley fog. It can be thick and can persist for days, until the winds become strong enough to push it out and dissipate it.

3. Over the western Prairies during the cold season, with a quasi-stationary high over the eastern Prairies maintaining an easterly flow of cold air at low levels into the western Prairies, while aloft there is a westerly circulation of warmer air. In these cases a weak surface trough is often present just east of the mountains. A quasi-stationary low level inversion separates the cold air below from the warmer air above. Humidity accumulates under the inversion, partly due to the ascent in the upslope flow and partly due to low level convergence, with stratus forming due to turbulent mixing, and possible stratus build-down to fog occurring overnight with nocturnal cooling.
4. Over the western North Atlantic: while advection fogs dominate, some stratus build-down fogs do occur. Rogers (1988) found that in 68 cases of fog in that area, 62 were of the advection type, and 6 were of the stratus build-down type.

### 4.3.6 Morning Evaporation fog

This type of fog has not been found in traditional classifications, but recent synoptic experience has identified it as a minor but distinct type. For example, Saunders (1997) hints at this type of fog: “turbulence and added moisture due to the evaporation from the surface often give a sudden deepening soon after sunrise. Sudden fog formation may result if turbulence mixes cold surface air and warmer air aloft.”

Formation process

Fog may occasionally form just after sunrise when evaporation and mixing take place near the surface. This usually occurs at the end of a clear, calm night when radiational cooling has brought the air temperature down to the dew point in a shallow layer near the ground, so that a thick blanket of dew has formed on the surface. At daybreak, the sun’s rays evaporate the dew, adding water vapour to the air. A light breeze then stirs the moist air with the drier air above, causing supersaturation through the mixing of the moister and drier air, and hence forming the fog via the process discussed in section 4.2.1 (Figure 4-18).

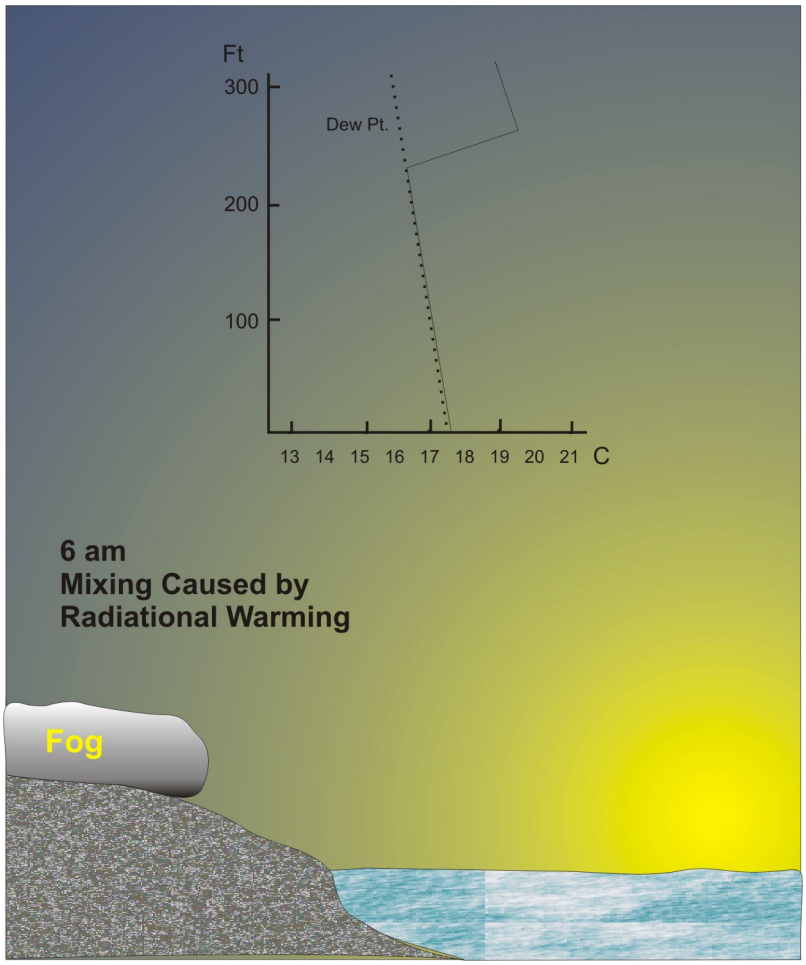


**Figure 4-18** Soon after sunrise with solar heating and turbulent mixing process (adapted from MOIP 2006).

Tardif and Rasmussen (2007) also discuss this type of fog. They describe it as being due to the evaporation of surface water and mixing in the surface layer. It can occur in situations which are close to those for radiation fog, but in which dew was deposited *without* the formation of radiation fog. In such cases, within one hour or so following sunrise, it can happen that the temperature increases, but the dew point increases even faster due to evaporation of the dew. The mixing can then lead to fog.

### 4.3.7 Arctic Sea Smoke

Arctic sea smoke, also called steam fog, forms as a result of evaporation. It occurs when cold air flows over much warmer water (Figure 4-19). As the warm water evaporates, it increases the water vapour content of the air above it. At the same time the water heats the air but the mixing ratio increases more rapidly than the saturation mixing ratio thus resulting in a state of supersaturation and condensation.

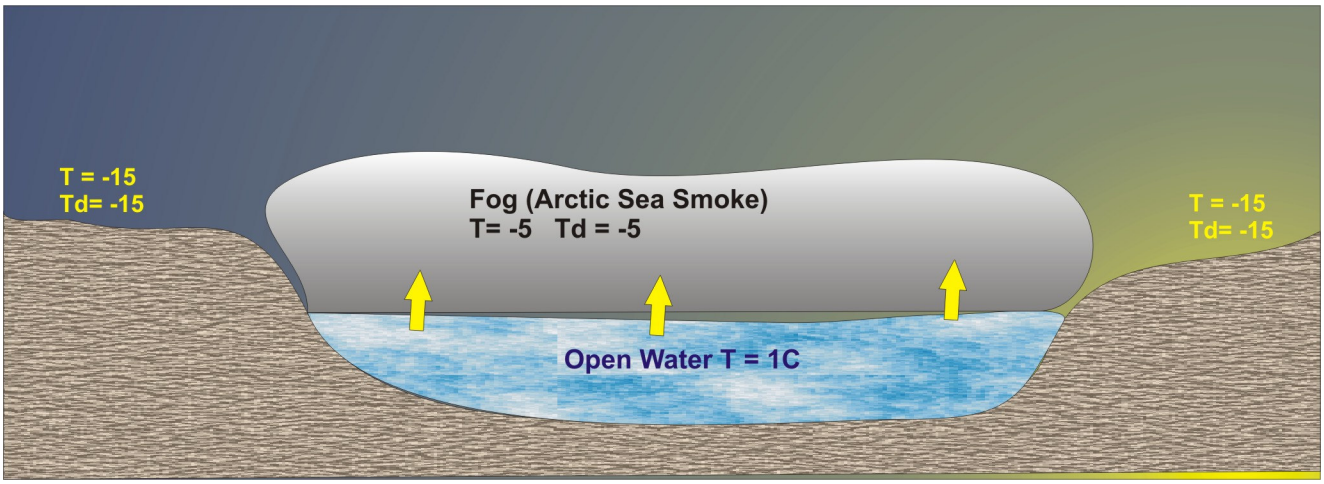


**Figure 4-19** Steam fog/Arctic sea smoke (adapted from MOIP 2006).

Favourable conditions:

1. early in the morning : cold air relative to water temperature
2. in autumn : cold air relative to water temperature
3. light winds : stronger winds will dissipate the water vapour concentration
4. high relative humidity : it requires less evaporation
5. high concentration of condensation nuclei : to favour the condensation process
6. in winter: Arctic regions over polynyas (open water areas) or coastal areas near open water (very cold air relative to water temperature)

Characteristics:

1. unstable layer near the water surface (since the water is warmer than the cold air)
2. the instability in the low levels favours evaporation as it produces upward motion, usually this portion is fog free
3. generally not dense over open water
4. lowest visibilities in Arctic sea smoke occur when the geography is favourable (e.g. fog forms and remains constrained in a narrow fjord)
5. coastal airports can be seriously affected
6. if the open water is very large with deeper instability then snow flurries and squalls will be favoured instead of steam fog .

### 4.3.8 Anthropogenic Ice Fog

Ice fog is formed solely of ice crystals. As described above, ice fog needs ice nuclei that can exist naturally or be added by anthropogenic activity (AA). The AA can introduce additional ice nuclei to the atmosphere that can enhance ice particle formation. Forecasters generally think of ice fog as forming only at very cold temperatures (e.g. < -30°C) and anthropogenic ice fog does fall in that temperature range also. However, ice fog in a more general sense can in some circumstances exist at much warmer temperatures (Gultepe et al. 2008) when RHi > 99% and IN are present (e.g. see Table 1) . Ice nuclei are generally scarce in cold regions and more common near inhabited areas. Anthropogenic activities such as combustion provide not only enough moisture to supersaturate the air, and but also nuclei for ice nucleation. Existing natural ice nuclei and/or those provided by the combustion then permit the formation of ice crystals leading to ice fog. A single aircraft that takes off may actually induce fog formation over an entire airfield. Ice fog crystals are in equilibrium with the ice of the snow cover below, and so ice fogs may be very persistent.

Favourable conditions for anthropogenic ice fog formation:

1. An adequate moisture supply in low levels: for example near settlements or power plants or with open water nearby.
2. Air temperature usually colder than -30$^{o}$C where source of ice nuclei (IN) is available (different threshold temperatures are applicable at different locations. Note that it may in some cases occur for T as high as -10°C (Gultepe et al. 2008).
3. A low level temperature inversion that inhibits the dispersion of particles
4. Surface winds less than 5 knots.
5. During a very cold period

Michael Shaffer discusses typical conditions in which anthropogenic ice fog occurs at stations in Yukon and northern BC at http://pnrinternal.pnr.ec.gc.ca/paawc/aviation/BC_ref/IceFog.htm. Purves (1997) also provided an illustrative case study of anthropogenic ice fog at Whitehorse. His study outlines general conditions favourable for ice fog at Whitehorse, and then discusses two ice fog events from January 1997.

### 4.3.9 Naturally-occurring Ice Crystal Fog

Ice crystal fog occurs naturally when IN exist at RHi>99% and usually T< -10°C (Gultepe et al. 2008). Natural IN always exists in the atmosphere and its effect is larger at T<-30°C with high supersaturation with respect to ice. Ice fog can be directly related to the natural transport of dust particles, biogenic particulates, and likely sulphate components particles that originates from the ocean. It is clear that origin and composition of IN are still debated and it is an open research area. A possible favourable synoptic pattern, assuming the availability of moisture, might be the weak low level convergence and upward vertical motion associated with a surface trough or a weak low. These ideas are speculation, and confident answers will have to await further research into the microphysics of ice crystal fog and stratus.

### 4.3.10 The Effect of Snow and Ice Surfaces on Fog

The presence of snow or ice on the ground implies a cold surface skin temperature, which is a condition that can be favourable for the formation and persistence of fog when advection of warm air and moisture advection occurs (Gultepe et al. 2008). However, in certain temperature ranges *liquid* fog droplets do not persist above snow or ice on the ground. The following summary discussion from Petterssen (1969, p 144) explains the effect:

> "Over snow-covered ground one often sees that the fogs prefer a belt within which the temperature is near freezing. The reason may be explained as follows. When the snow is melting, the air temperature above the snow is > 0°C, and the temperature of the air in contact with the snow is 0°C. There is, then, a temperature inversion at the ground, and the transfer of heat will be directed downward toward the snowy surface. The heat thus carried downward is consumed in the melting of the snow, without benefit to the surface."

Under normal conditions, the moisture content of the air increases when there is a temperature inversion above the snow. The transfer of moisture will then be directed downward, and the excess water vapour will condense on the snow. Thus, when snow is melting, heat and moisture are carried toward the snowy surface, and the process tends to cause the air to become drier. It follows, then, that fogs do not readily form over melting snow when the air temperature is **much over** freezing.

On the other hand, when the temperature of the snow is **much below** freezing, it becomes difficult for fogs to develop. The reason is that the saturation vapour pressure over cold snow is lower than over water. As a result, condensation will begin on the snow before the air becomes saturated. As will be seen from Figure 4-20, this effect is largest in the interval from -10°C to -15°C, and few liquid fogs survive cooling through this interval.

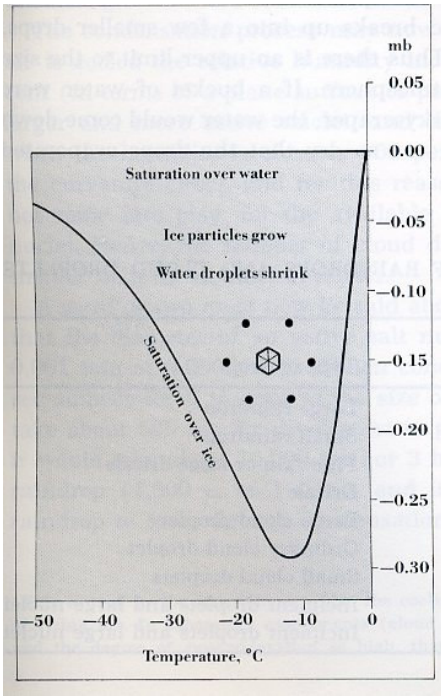


**Figure 4-20** "The saturation vapor pressure is lower over ice than over water. If both ice particles and cloud droplets exist in an undercooled cloud, the ice elements will tend to grow at the expense of the droplets." (Petterssen 1956, Figure 5.2).

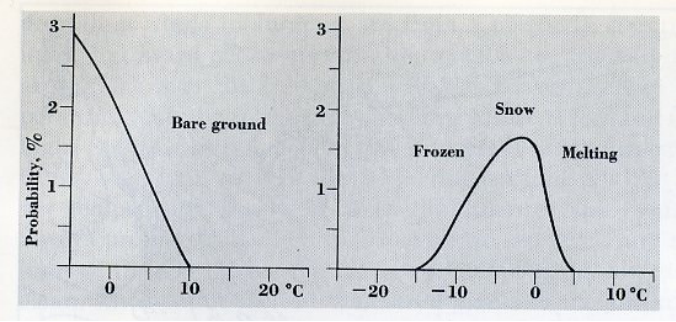


**Figure 4-21** Some characteristics of fogs at Oslo. In October, when the ground is bare, the probability of fog increases below 10°C and is highest at the lowest temperature (-5°C). During the winter months, when snow is present, the probability is highest in the vicinity of freezing, and fogs do not survive cooling below about -15°C." (Petterssen 1956, Figure 8.8)

The effect of snow cover is clearly shown in Petterssen's Figure 8.8 (reproduced as Figure 4-21). In October, when there is no snow on the ground, the highest probability of liquid fog is found at the lowest temperatures observed (0 to -5°C). In January, February and March, when snow is present, the highest probability is found in the vicinity of the freezing point, and liquid

fogs are absent when the temperature is above +5°C and below -10°C (but as in Gultepe et al., 2008, ice crystal fogs can exist below -10°C). In colder regions, where winter air temperatures are -30°C or lower, fogs consisting of ice crystals are common, as discussed above.

# 5 Fog dissipation and thinning

It is important to know the mechanisms by which fog has formed in order to forecast its dissipation. As a general rule, a change in the conditions that caused the fog, for example a wind shift in the case of advection fog, will bring about its dissipation.

As a rule, any of the following conditions will minimize the effect of fog:

1. prolonged sunshine/solar radiation
2. strong winds/turbulence
3. onset of precipitation
4. any other significant changes in the fog formation mechanisms that were responsible for the formation of fog.

## 5.1 Visibility in Precipitation and Fog

Fog visibility can be improved when precipitation occurs. Hydrometeors falling into pre-existing fog will typically scavenge-out cloud (fog) droplets thereby improving the overall visibility. This is of course not the same scenario as precipitation *inducing* fog when saturating the boundary layer.

### 5.1.1 Rain and Fog Together

Synoptic experience suggests that visibilities of 1 km or less in moderate rain and fog rarely occur. Higher visibilities (mist) in such situations are most common. Visibilities less than 1 km sometimes occur with heavy rain due to the direct effect of the rain itself. If fog exists and then rain begins, as noted above the visibility can improve due to the sweep-out effect.

### 5.1.2 Drizzle and Fog Together

Low visibilities are often recorded when drizzle and fog are reported together, probably because of the small size and greater number concentrations of drizzle droplets compared to rain drops (Gultepe and Milbrandt, 2010). Drizzle is sort of an “intermediate” form between rain and cloud droplets, but tends to be closer to cloud in its characteristics than to rain, so

perhaps it should not be surprising that its visibility effects are closer to those of fog than those of rain.

### 5.1.3 Snow and Fog Together

Snow and fog can be reported together, but conclusions about their relative effects on visibility are difficult to draw. If the snow is falling through a supercooled liquid fog or a mixed phase fog with significant liquid, then the snowflakes should grow at the expense of the liquid droplets, which will become less frequent and so cause less reduction of the visibility. It is possible that the snowflakes may sweep out some of the ice crystals of which the mixed phase fogs are composed, which also implies an improvement in visibility compared to that in the fog alone. On the other hand, the falling snow creates its own reduction in visibility. This is a difficult microphysical problem, and no hard and fast rules can be given.

Often in coastal climates such as in Atlantic Canada, wet snow can occur in the presence of fog at temperatures above zero (usually in the $0^{o}$C to $+2^{o}$C range). This is usually seen when the wind is onshore – i.e. in the presence of advection fog. In the United States visibilities of ½ SM or less with snow are always reported as SN FG (snow and fog) but often there is actually no fog. In Canada the inclusion of fog with snow is reserved for cases where the observer is convinced that the visibility is being reduced partly by fog. It is not often easy to differentiate between the two however.

### 5.1.4 Climatology and Observations of Precipitation and Fog Together

Visibility observations in which various types of precipitation and fog are recorded together are problematic because the recorded visibility is not necessarily the result of the combined effects of the precipitation and the fog. One way to remove this complication from climatological studies would be to examine only those cases for which fog alone was reported, as shown in Figure 5-1. Similar analyses for most other Canadian stations are available online at http://collaboration.cmc.ec.gc.ca/science/arma/climatology.

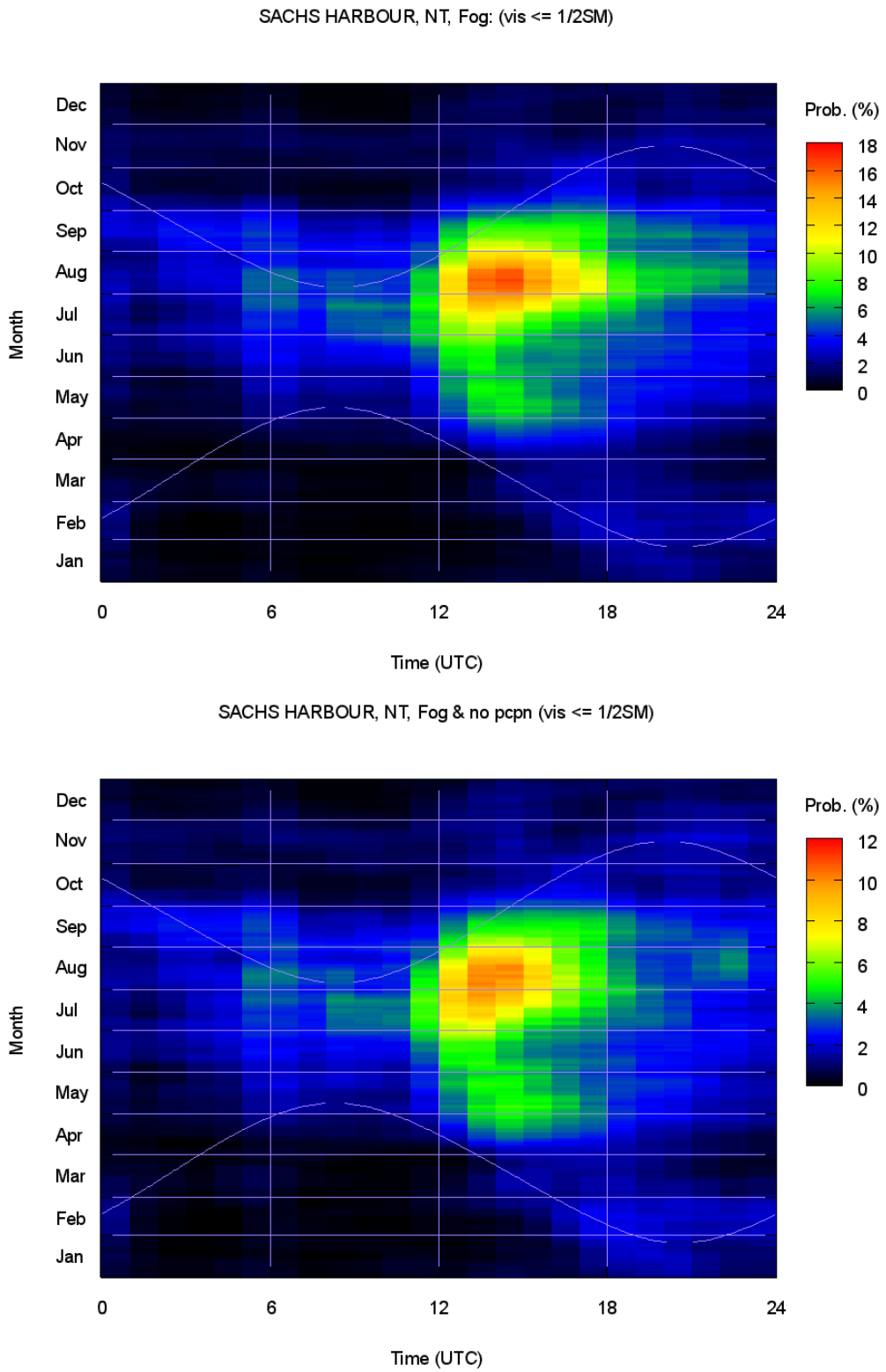


**Figure 5-1** Frequency of fog in Sachs Harbour, NWT, with and without precipitation (upper and lower).

## 5.2 Sunshine

Solar radiation can play two roles. The effect of sunshine as a dissipating mechanism depends on its ability to heat the air to reduce the relative humidity. The fog does not really "burn off"; rather, sunlight penetrates the fog and warms the ground, causing the air temperature in contact with the ground to increase. The warm air rises and mixes with the foggy air above, which increases the temperature of the foggy air. In the slightly warmer air, some of the fog droplets evaporate, allowing more sunlight to reach the ground, which produces more heating, which eventually causes the fog to completely disappear. If dew is present with fog, the solar effect can actually induce fog formation as described in section 4.3.6. The presence of evaporating dew may be sufficient to allow persistence of the fog for several hours longer than over a dew-free surface. Eventually solar heating causes the saturation vapour pressure to increase above the actual vapour pressure, even in spite of the evaporation of dew if available This leads to fog dissipation, first at the surface and then propagating upward. This is the origin of the term "fog lifting." The fog may lift to stratus, or it may dissipate without forming stratus.

The angle of the sun plays a critical role. The "critical" angle for the sun to have a positive effect will vary for many reasons. Also this critical angle will be related to time of day, time of year, and latitude of the location. Therefore, sunshine is a better mechanism for dissipation in the summer than the winter and better for low latitudes rather than high latitudes with increasing effectiveness from sunrise to noon as sun angle increases.

Furthermore, solar radiation causes mixing with drier air around the fog. It has been shown by satellite imagery (Roach et al. 1976), that radiation fog and stratus dissipates from its outer edges inward rather than the whole area simultaneously, as had previously been assumed. The reason for this is that the ground on the outside the fog area heats up more quickly than the ground inside. This generates a weak circulation which dissipates the fog by a process that has been called "inward mixing". The residual moisture can be significant: during the summer months lines of convective cloud can form along the early morning fog boundaries and spread out from there.

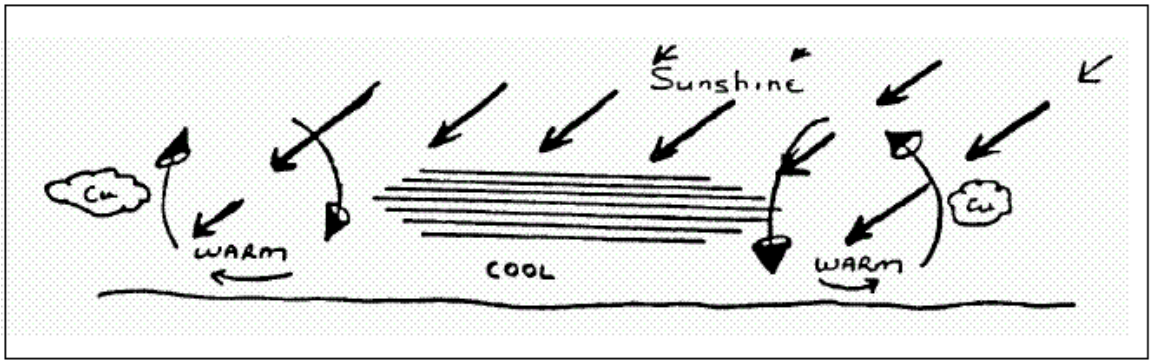


**Figure 5-2** Schematic of fog erosion mechanism from the edges (from MOIP 2006).

Figure 5-2 illustrates an example of the summertime "inward mixing" fog dissipation mechanism. As a consequence of this process of "outer edge" erosion, an important parameter in forecasting the time of radiation fog dissipation at a particular point is the location of the point relative to the fog boundary. The basic tool for this is high resolution satellite imagery (if available). If the fog is thick, with little sunlight penetrating it, and there is little mixing along the outside edges, the fog may persist through the day.

## 5.3 Strong Winds

Turbulent transport of heat and moisture plays an important role in the evolution of fog. However, in general the role of turbulence can be either constructive (contributing to the formation of fog) or destructive (contributing to the dissipation of fog, or hindering its formaation). Usually, significant turbulent mixing induced by strong winds mixes drier air with fog and dissipation occurs.

However, strong winds can in some cases contribute to fog formation. If the winds are in an upslope direction or the moist surface layer is capped by a strong inversion, then fog (or at least stratus) may indeed be enhanced by strong winds. Dense advection fog can also exist in marine environments or near coasts in the presence of strong winds.

Roach et al. (1976) infer from observations that too much turbulence hinders fog formation in the case of radiation fog. They came to this conclusion because lulls in wind were accompanied by maximum cooling, and major lulls were accompanied by periods of significant fog development. Conversely, increases in wind to greater than 2 m/s were associated with fog dispersal. They infer that as the wind speed decreases, turbulent transfer of moisture to the surface to form dew ceases. As a result, the moisture remains in the atmosphere, and as radiation cools the air, fog is formed. Alternately, at higher wind speeds, vertical mixing of drier air inhibits radiation fog formation.

## 5.4 Fog Dissipation

The forecaster must understand the processes involved in fog formation before considering when it is likely to dissipate.

When fog evaporates, the saturation mixing ratio is increased by an amount corresponding to the initial liquid water content of the fog. As you can verify from a tephigram, at 30°C, increasing the saturation mixing ratio by 5 g/kg corresponds to a temperature rise of about 3°C. However, at -30°C, increasing the saturation mixing ratio by the same amount involves a temperature rise of about 38°C! At low temperatures, much more heating is required to evaporate fog than is required at higher temperatures. Figure 5-3 shows the temperature increase required to dissipate fog at various temperatures and for fixed liquid water contents of 0.3 $g \cdot m^{-3}$ and 0.03 $g \cdot m^{-3}$.

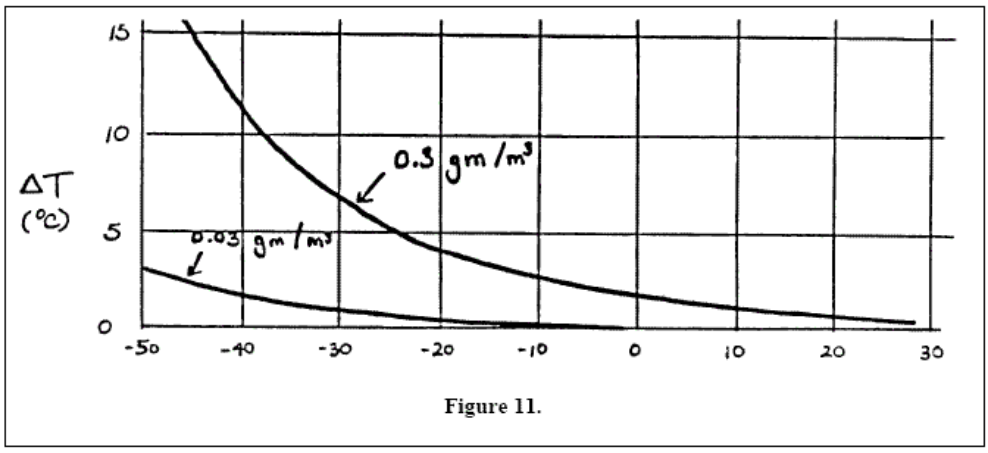


**Figure 5-3** Graph of the temperature increase required to dissipate fog at various temperatures, for liquid water contents of 0.3 $g \cdot m^{-3}$ and 0.03 $g \cdot m^{-3}$ (from MOIP 2006).

# 6 Recent fog microphysics research

## 6.1 Field programs

The Fog Remote Sensing and Modeling (FRAM) project was conducted over three regions of Canada and US. These locations were: 1) Center for Atmospheric Research Experiments (CARE), Egbert, Ontario 2005-2006, 2) Lunenburg, Nova Scotia June of 2006 and 2007, and 3) U.S. Department Of Energy (DOE) ARM Climate Research Facility at Barrow, Alaska, US during the Indirect and Semi-Direct Aerosol Campaign (ISDAC) field program April of 2008; FRAM C, FRAM-L, and ISDAC-FRAM-B, respectively. FRAM-C was undertaken in a continental fog environment while FRAM-L was in a marine environment. The FRAM-B was undertaken to study ice fog conditions. During the project, numerous in-situ measurements were obtained, including droplet and aerosol spectra, precipitation, and visibility. Analysis of satellite microphysical retrievals and visibility parameterizations suggested that improved scientific understanding of fog formation can lead to better forecasting/nowcasting skills benefiting both aviation and public forecasting applications.

**1. FRAM-C: Continental fog:**

The FRAM-C project was the first project of the FRAM series to study fog formation over a continental region. Other projects in Canada and the world have also focused on continental fog. The purpose of this project was to develop a list of instruments to be used in future field programs. Details on this project can be found in Gultepe et al. (2009).

**2. FRAM-L: Marine fog:**

Gultepe et al. (2006b and 2009) summarized the FRAM field project and preliminary results. The purpose of the FRAM field project was to characterize fog formation, evolution, and dissipation in continental and marine environments, and then to use the derived results in numerical simulations. Phase 1 of the project took place during the winter of 2005/2006 in southern Ontario. Phase 2 of the project took place during the summer of 2006 in Nova Scotia along the Atlantic coast. These phases focused on winter continental fog and summer marine fog, respectively. Observations include droplet, ice, and aerosol sizes and concentrations from optical probes, visibility from a present weather sensor (FD12P), liquid water path from a microwave radiometer (MWR), and inferred fog properties such as mean volume diameter, liquid water content, number concentration, and liquid water path from satellites. The results will be used to develop microphysical parameterizations which could be incorporated in numerical forecast models. During the winter of 2005/2006, an increased frequency of fog formation was observed in southern Ontario relative to the 30-year climatology. It is suggested that snow on the surface during several rain events caused this increase in frequency. Rain falling on a snow surface resulted in a release of latent heat which caused evaporation of snow, higher boundary layer saturations, and fog formation. The mechanisms for fog formation, along with some model simulations using the derived microphysical parameterizations, formed the foundation of FRAM-L, and this Handbook.

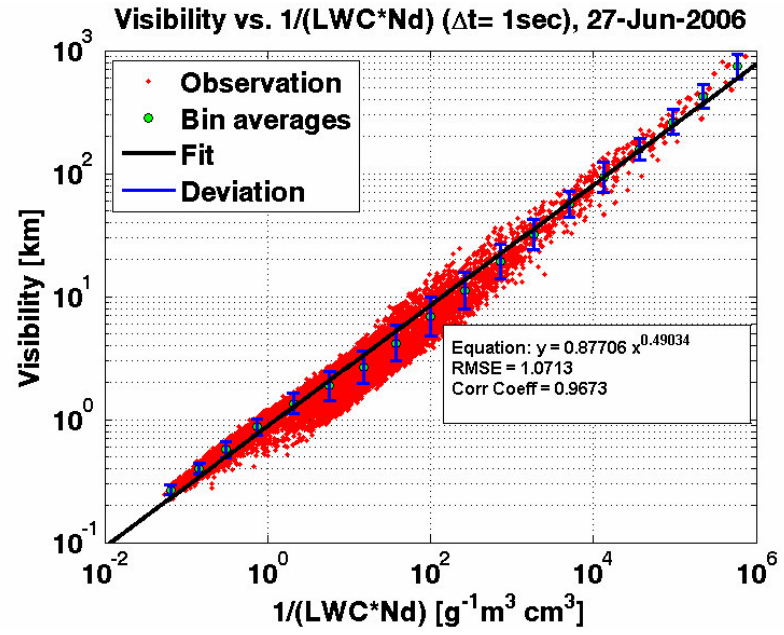


**Figure 6-1** Vis versus f(LWC, Nd) from the FRAM-L project (Gultepe et al, 2008).

A common relationship used to represent visibility reduction owing to precipitation or fog particles is given by Gultepe et al. (2006a) as follows:

$$VIS = f(\frac{k}{N_T LWC}) \tag{6-1}$$

Where k is a regression constant related to the hydrometeor type (fixed for warm fog), $N_T$ is the number of hydrometeors per given volume of air [$cm^{-3}$], and LWC is the water mass content.

**3. FRAM-B: Ice fog:** [1] During ISDAC (Indirect and Semi-Direct Aerosol Campaign) project which took place over the Barrow, Alaska, the FRAM instruments were located at the NSA (North Slope Alaska) site. The main observations obtained during FRAM-B were fog droplet spectra from a fog measuring device (FMD; DMT Inc.), *Vis* and precipitation rate (*PR*) from the VAISALA FD12P all-weather precipitation sensor and the OTT laser based optical distrometer called ParSiVel (*Par*ticle *Si*ze and *Vel*ocity), and relative humidity with respect to water ($RH_w$) together with temperature (*T*) from the Campbell Scientific HMP45 sensor. Table 1 in Gultepe et al. (2009) summarizes the Environment Canada (EC) instruments available during the FRAM project that took place in Barrow, Alaska. Liquid water path (*LWP*) and liquid water content (*LWC*) were obtained from a microwave radiometer (MWR; Radiometric Inc.). Fog coverage and some microphysical parameters such as droplet size, phase, and LWP were also obtained from satellites (e.g., GOES, NOAA, and Terra and Aqua MODIS products). Note that not all instruments were available for each phase of the FRAM projects.

Figure 6-2 shows an example of FD12P measurements during an ice fog event for April 10 2008. This sensor also measures the accumulated amount and instantaneous PR for both liquid and solid precipitation, and provides the *Vis* and precipitation type related weather codes given in the World Meteorological Organization (WMO) standard SYNOP and METAR messages. The FD12P detects precipitation droplets from rapid changes in the scatter signal. Based on the manufacturer's specifications, the accuracy of the FD12P measurements for *Vis* and *PR* are approximately 10% and 0.05 mm $h^{-1}$ respectively.

[1] In this section the term 'ice fog' refers to any fog composed of ice crystals, and is not limited to the traditional forecasters' connotation of 'ice fog' as anthropogenic ice crystal fog occurring only at very cold temperatures.

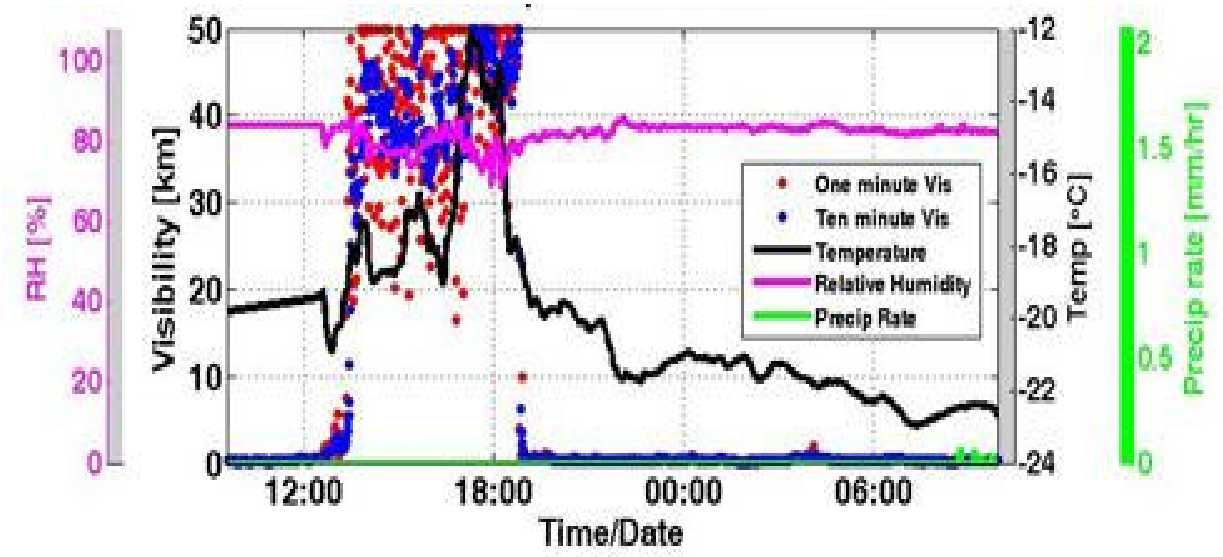


**Figure 6-2** Time series of FD12P measurements for RH, Precipitation Rate (PR), T, and Visibility for 10-11 April 2008 during FRAM-B project. The FD12P Weather Sensor is a multi-variable sensor for automatic weather stations and airport weather observing systems (VAISALA Inc.).

The fog-related microphysics parameters e.g. liquid water content (*LWC), ice water content (IWC)*, size, and droplet and ice crystal number concentration ($N_d$, and $N_i$) were calculated from the FMD spectra for both liquid and ice clouds. Although an ice particle counter was available, its measurement size range is likely beyond the upper limit of the typical fog particle size, e.g., 50 µm. The Climatronics Aerosol Profiling (CAP) aerosol probe within the sub-saturated conditions is used for measuring aerosol size and spectra between 0.3 and 10 µm. In saturated conditions, it measures nucleated particles' characteristics.

The ice fog case during FRAM-B lasted 4 days from April 9 to April 12 2008. During this fog event, *Vis* decreased to 100 m and project flights were cancelled. Ice fog forecasting is usually not performed with forecasting models because ice water content (*IWC*) and ice crystal number concentration ($N_i$) are not accurately obtained from existing microphysics algorithms. If both parameters were available from a high-resolution fog/cloud model, they could be used for delineating ice fog regions and forecasting *Vis*. Ice fog occurs commonly in northern latitudes when *T* is below -15°C (based on the Dr. I. Gultepe's observations in Barrow, Alaska (Gultepe et al. (2009) ). Ice fog usually forms when the *RH* becomes saturated with respect to ice ($RH_i$) without precipitation. Ice fog develops because of a deposition nucleation process that depends on nuclei size and concentration, and temperature. Previous reports have suggested that liquid droplets can be found at *T* down to about -40°C but it is not common to find droplets colder than -20°C.

## 6.2 Visibility parameterizations

Traditionally the visibility in fog has been related only to the liquid water content (LWC) of the fog (Kunkel 1984). However, Gultepe and Isaac (1997) and Gultepe et al. (2006a) have shown that the number concentration of droplets ($N_d$) is also very important for Vis calculation. For a given LWC, a large number of small droplets will result in a lower visibility than a small number of large droplets. These parameterizations can be used in NWP forecast models if the models include the necessary inputs as forecast variables. Note that the Kunkel parameterization was based on a very limited data set and needs to be replaced with new parameterizations (Gultepe et al. 2008; Gultepe et al., 2006a).

**1. Vis as a function of RHw**

Visibility is function of RH, fog LWC, and precipitation (e.g. snow and rain) as explained in Gultepe et al., (2006b; 2009). In the following equation Vis is obtained as a function of RHw. Vis is in km and RHw in %.

$$Vis_{FRAM-C} = -41.5\ln(RH_w) + 192.3 \tag{6-2}$$

**2. Visibility as a function of LWC and $N_d$**

The FMD measurements were used to obtain a relationship of Vis versus $N_d$ and LWC. During the analysis, it was found that LWC increases with increasing $N_d$ and the Vis decreases with increasing LWC and $N_d$ (Gultepe et al. 2006a). Based on these relationships and using 1 second interval observations, the following Vis parameterization equation was derived:

$$Vis = 1.002\left(LWC \bullet N_d\right)^{-0.6473} \tag{6-3}$$

**3. Visibility as a function of rain rate and snow rate**

Visibility as a function of rain and snow precipitation rates is also available, but is not shown here. Readers interested in more on this topic can consult Gultepe et al. (2006b, 2009), Gultepe and Milbrandt (2010), and Rasmussen et al. (1999).

**4. Model application**

Visibility reduction due to fog in a forecasting model is usually obtained using an equation similar to 6-3 in which $N_d$ is assumed as a constant or obtained from an empirical relationship. The LWC is obtained prognostically from the NWP model. This variable is available as QC from the GEM regional (in units of kg/kg). The $N_d$ is not normally an output parameter from a

model and is assumed as a constant (100 $cm^{-3}$) for marine clouds and 200 $cm^{-3}$ for continental clouds. Gultepe and Isaac (1997) suggested $N_d$ can be obtained as a function of temperature:

$$Nd = -0.071T^2 + 2.213T + 141.56 \quad (6\text{-}4)$$

where $N_d$ is in $cm^{-3}$ and T in °C. Note that large variability exists in this relationship and this equation can be strongly dependent on the type and amount of cloud condensation nuclei, not just temperature.

# 7 Satellite techniques

## 7.1 Channel differencing and multi-Spectral methods

Fog detection using remote sensing methods (satellites) can be important for aviation applications. Gultepe et al. (2007b) developed a method that uses multi-spectral GOES channel-differencing to overcome an issue with unavailability of GOES channel 2 data at night. It is explained below.

In this section, the analysis is divided into four subsections relating to surface observations, satellite data, model data, and statistical data analysis.

***a) Surface observations analysis***

Hourly observations from each of four weather stations were examined between the dates of March 1 and September 30, 2004 for warm fog events (T > -5ºC). Off-hour "special" reports were not included. For this comparison, only daytime events were selected, i.e. solar zenith angles in the satellite images were < 70º. Observed fog events at the surface were categorized as those that had at minimum three consecutive hours of fog (listed under the "Weather" column of the station reports) with at least some of those hours in the daytime. After matching these times with the available satellite and NWP data, 19, 25, 31 and 24 cases of fog (total of 99 cases) were identified at YOW (Ottawa), YQG (Windsor), YSB (Sudbury) and YYZ (Toronto), respectively. The same number of random no-fog events (99 cases) was also selected at each station to balance the comparison statistics with foggy cases. In this selection, it is assumed that the random sample of 99 no-fog events has the same distribution as the whole sample of 198 cases.

***b) Satellite data analysis***

The 198 events, including 99 foggy and 99 no-fog cases, were processed using the warm fog satellite detection scheme described below. Model data from the closest forecast hour were used in the algorithm. For example, when a satellite image at 1615 UTC is processed, model

data from the 16-h forecast were chosen and so forth. A 3 x 3 pixel area (15 km x 15 km) centered at each of the four weather stations was extracted for comparison against the surface observations for the corresponding hour. Results from the satellite scheme were considered "foggy" if at least 1 out of 9 pixels were classified as foggy by the detection scheme. If a large uncertainty occurred in an input parameter, the criteria given in Table 2 can likely eliminate the pixel from being considered foggy. The comparisons between surface observations and model values were made by using the model output, representing 15 km scale, over each weather station.

Warm daytime fog regions were identified in GOES-12 satellite imagery using the criteria given in Table 2. On a pixel-by-pixel basis, each satellite pixel was individually checked for the conditions specified in Table 2. In order for the scheme to detect the presence of low cloud/fog, the tests 1, 3, and 4 in Table 2 must be satisfied. The first test is an indicator of reflectance from cloud tops. The second test is an indicator of mid- and high-level clouds. The third test is a condition to specifically check for liquid water clouds. For this criterion, daytime channel 2 data are first separated into the shortwave (SW) albedo and infrared (IR) components. This separation is applied using the method given in Welch et al. (1992). This method is effective in discriminating water phase from ice phase using the SW albedo, although it is a rough approximation to the true channel 2 albedo. Next, the SW albedo component is used to identify liquid water phase clouds. For the fourth criterion, the channel 2 minus channel 4 IR temperature difference test is used as an indicator of the liquid water phase.

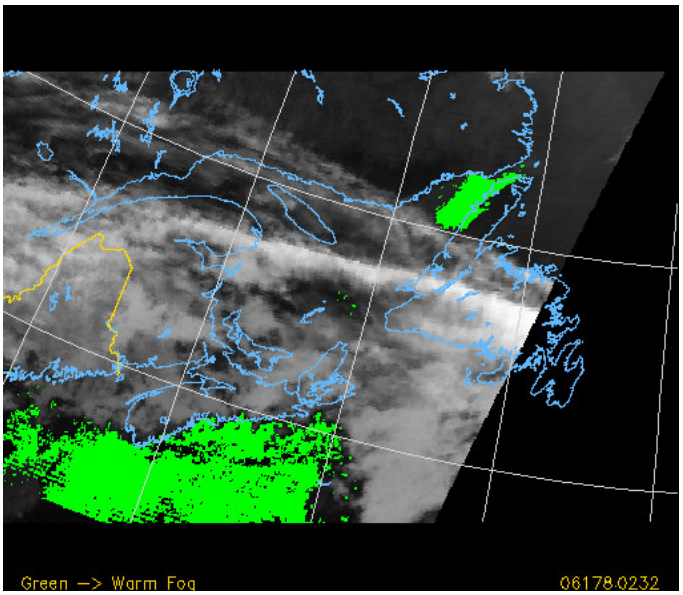


**Figure 7-1** Fog regions (in green) obtained using GOES observations and GEM model output on June 27 2006.

Following the cloud mask tests, all criteria 5-8 in Table 2 need to be satisfied for the satellite pixel to be considered foggy. The SZA (solar zenith angle) condition simply confirms daytime conditions. In test 6, it is assumed that $|Tch4-Tsc|<10°C$ approximately represents a maximum height of 1000 m if the dry adiabatic lapse rate is assumed. This assumption is made to increase the chance of detecting fog formation. It is clear that if the air is saturated and well mixed, the fog layer thickness can become more than 1000 m. The $Tch4 > -5°C$ condition is used for representing the liquid phase of fog because droplets are very commonly found at temperatures warmer than –5°C (Gultepe and Isaac 2004).

| # | Criteria | Explanation |
|---|---|---|
| 1 | Ach1 > 20% | Cloud detection |
| 2 | \| Tch4 – $T_{sc}$ \| > 10ºC | High level cloud detection |
| 3 | Ach2 > 8% | Liquid cloud detection |
| 4 | Tch2 – Tch4 > 10ºC | Liquid cloud detection |
| 5 | SZA < 70º | Day time cloud/fog detection |
| 6 | \|Tch4-Tsc\| <10ºC | BL cloud/fog detection |
| 7 | Tch4 > -5ºC | Warm fog detection |
| 8 | RHw> 80% | BL fog/cloud detection |

**Table 2** Criteria used in the fog algorithm (Gultepe et al. 2007b). The model based screen temperature is shown as ($T_{sc}$). A represents albedo and SZA is defined as solar zenith angle. The RHw is the relative humidity with respect to water based on model runs. The ch1, ch2, and ch4 represent channel 1, 2, and 4 from GOES data. The BL is the Boundary Layer.

***c) Model data analysis***

The occurrence of fog over small scales is possible when RHw (~80%) from a large-scale model (e.g. < 50 km) is less than 100% as shown in Gultepe et al (2007b). This value (80%) can be increased when high-resolution models (with grid size less than 1 km) are applied for fog forecasting.

Screen-level temperature was obtained from an interpolation between the surface skin temperature estimated using the land surface scheme (Belair et al. 2003) and the air temperature at the first atmospheric model level around 50 m. The interpolation is done using surface layer stability functions. Surface screen temperature comparisons between 2 model runs with 15 and 24 km resolutions have been studied and related information can be found at http://www.msc.ec.gc.ca/cmc/op_systems. These comparisons indicate that differences in $T_{sc}$ were negligible. For this work, using a Lagrangian bi-cubic interpolation method, numerical model data were interpolated to the same ground resolution as the post-processed satellite data (5 km).

## 7.2 Low cloud detection and nowcasting using satellite observations

Ellrod and Gultepe (2007) summarized a method to detect low clouds that is based on satellite observations. A simple algorithm (shown by the flow diagram in Figure 7-2) has been developed to show how an enhanced GOES low cloud product (hereafter referred to as the Low Cloud Base (LCB) product) may be generated to display areas of possible IFR ceilings. Details on product generation are described in Ellrod (2002). In the final image (Figure 7-3), possible IFR cloud base heights are color-coded red, while other areas of low clouds are

coloured green, and cirrus is shaded black or blue. Cloud-free regions are displayed as gray scale. The algorithm is generated for each pixel, so in areas where there are variable cloud conditions, or instrument noise due to cold IR temperatures, there may be difficulty in interpreting the image and matching the cloud base category with ground observations. The LCB images are currently produced in real time for each hour at night for all CONUS regions. Six sectors are currently available: Two over the Western United States from GOES-11, and four covering the Eastern United States from GOES-12.The sectors are remapped into Lambert Conformal projection, true at 30$^{o}$N and 50$^{o}$N. Observed cloud ceilings (ft) at METAR sites are plotted on the image for comparison. Both single images and animated loops may be accessed at http://www.star.nesdis.noaa.gov/smcd/opdb/aviation/fog.html. An example is shown in Figure 7.3.

Results of an idealized model of a radiation fog based on a thermal profile described by Turton and Brown (1987) is shown in Figure 7-3. 'A' is the dry stable layer above the fog, 'B' is the portion of the inversion containing the fog, and 'C' is the well-mixed layer formed by weak convection, with warming at the surface and radiative cooling at the top.

Certain problems associated with interpretation of the original fog images (Ellrod 1995), such as the presence of obscuring higher cloud layers, and false signatures due to low emissivity soils such as coarse sands (Sutherland 1986) will also affect the new product. In North America, the latter effect is chiefly a problem in southwestern deserts, especially in the Gran Desierto north of the Gulf of California. Additional problems may occur in mountainous areas where METAR stations are sparse, leading to possible errors in cloud height category due to interpolation of low elevation temperature data into higher terrain.

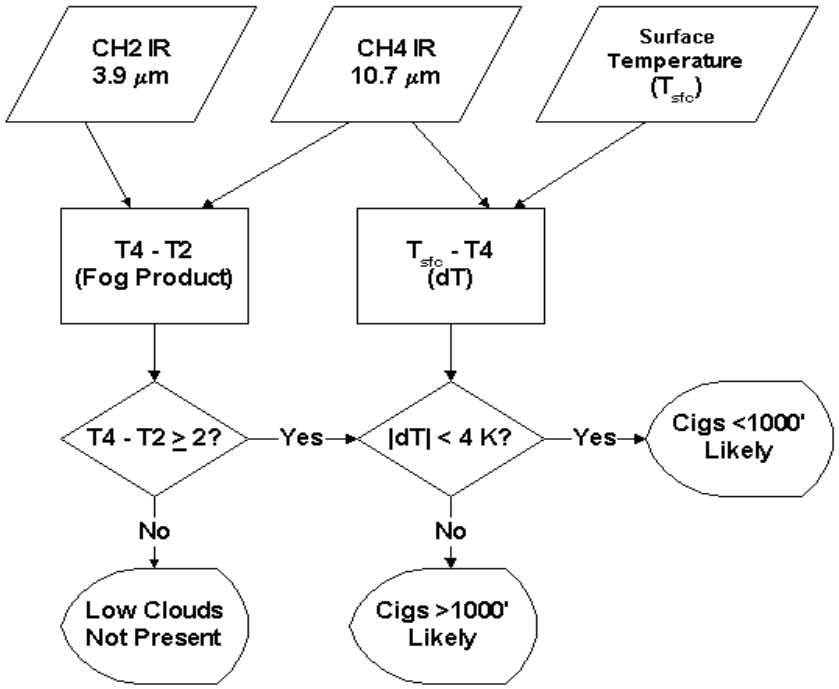


**Figure 7-2** Flow chart showing an experimental procedure for estimating cloud base conditions at night using a GOES bi-spectral IR technique and surface temperatures from METAR sites. $T_{sfc}$ is surface temperature, T4 is Channel 4 IR temperature, and T2 is Channel 2 IR temperature.

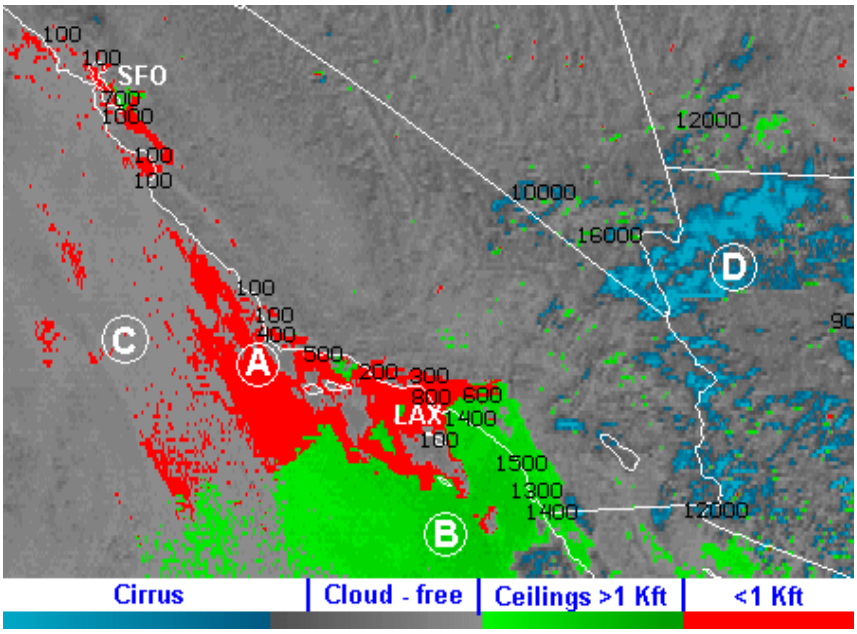


**Figure 7-3** GOES Low Cloud Base product on 19 October 2000 at 1200 UTC. Circled letters refer to: A) stratiform clouds with IFR cloud base heights, B) stratiform clouds with cloud bases > 1000 ft, C) partially undetected stratiform clouds, and D) cirrus clouds.

# 8 Fog prediction using NWP models

## 8.1 General concepts

One of the most important tools in operational weather prediction is guidance from numerical weather prediction (NWP) models. These models are essentially number-crunching computer programs which predict the future state of the atmosphere based on an estimate of the present state. Several times a day, data from a variety of measurements – from ground-based to satellite measured, in situ and remotely sensed – are collected and assimilated to produce estimates of the true state of the atmosphere at a given moment in the form of gridded analyses. An analysis serves as the initial condition (i.e. input data) for the NWP model. Using numerical methods to solve the equations that describe atmospheric motion, models predict the future state of each atmospheric quantity in small, finite time steps (on the order of minutes to tens of minutes) repetitively until the solution at the final forecast time is obtained.

There are many NWP models, appropriate for various length and time scales, from cloud-resolving models which "see" individual clouds and generally run no longer than 24 h, to medium-range global models which typically run from 1-2 weeks. Depending on the type of

model, different types of parameterization schemes are used to predict the effects of physical processes, such as the formation of fog.

## 8.2 The Canadian GEM model

### 8.2.1 Overview

The operational model used by the Canadian Meteorological Centre (CMC) is the Global Environmental Multiscale (GEM) model (Côté et al. 1998). As the name implies, the GEM can be used on a wide range of spatial scales for a wide variety of meteorological interests. Various horizontal grid configurations are available to model the atmosphere from the microscale to a global scale. For the prediction of fog, forecast fields from the GEM regional and GEM-LAM (Limited Area Model) systems are considered in section 9 of this Handbook.

### 8.2.2 The regional configuration

The configuration of the GEM model used to produce short-term (48-h) deterministic forecasts is generally referred to as the "regional" model. This configuration uses a global grid with variable horizontal grid-spacing, for a region of uniform horizontal resolution over the forecast area and a gradually decreasing resolution (increased horizontal grid-spacing) away from this region. This is illustrated in Figure 8-1. The horizontal grid-spacing over North America is approximately 15 km (as of November 2009).

**Figure 8-1** The variable-resolution horizontal grid of the operational regional configuration of the GEM model, with a uniform horizontal grid-spacing of 0.1375° (~15 km) over the central window**.**

The horizontal resolution of a NWP model is important for determining the type of parameterization scheme that is appropriate for the representation of clouds and the prediction of precipitation. With a horizontal grid-spacing of 15 km, individual convective storms cannot

be resolved. The effects of convection – that is, the redistribution of temperature, moisture, and momentum and the formation of precipitation at the ground – are represented by a "convective parameterization scheme" (CPS). The CPS in the regional GEM model (as well as the "global" configuration, used for medium-range ensemble forecasts) is the scheme of Kain and Fritsch (1993), which is based on the removal of convective available potential energy (CAPE) over a convective time scale.

### 8.2.3 The condensation scheme in the regional GEM

Clouds produced by synoptic-scale forcing are parameterized by the Sundqvist et al. (1989) condensation scheme. In this parameterization, condensation occurs and clouds are formed once the relative humidity in a model grid box exceeds a threshold value. This threshold relative humidity varies in the vertical and is 80% at the lowest model level. A portion of the humidity is then removed and considered to be condensed mass (a prognostic model variable for the total condensate *mass mixing ratio*). After the amount of condensation is computed, the relative humidity is then reduced towards the threshold value. The phase of the condensed mass is diagnosed simply as liquid if the ambient temperature $T > 0°C$ and ice if $T < 0°C$. This means that at a given grid box, there may be cloud (liquid or ice) with a relative humidity (*RH*) greater than the threshold value but less than 100%. Physically, this is interpreted to mean that there are subgrid-scale clouds (with *RH*=100%) over a *portion* of the grid box, with subsaturated and cloud-free air over the remaining portion, and that the grid-scale *RH* represents the *average* value over the area. The condensed mass can then be transported in the model by the 3D wind field. The Sundqvist scheme predicts precipitation to occur instantaneously at the ground if the condensate mixing ratio exceeds a certain threshold. Thus, precipitation is not an advected quantity with this scheme; condensed water mass in the column is simply removed and an instantaneous precipitation rate at the surface is given.

In the sense that liquid fog is defined simply as small cloud droplets near the surface, it may be regarded that fog can be "explicitly" predicted by the regional GEM by the condensate field from the condensation scheme. However, experience has shown this to be of limited success in practice since the low vertical resolution of the model creates problems for predicting liquid water near the surface. As part of the FRAM project, a new set of rules-based fog forecast techniques has been developed for use with the GEM regional model. It is described in section 9.

### 8.2.4 High-resolution LAM configuration

The GEM is also capable of running in a "limited-area model" (LAM) configuration, in which the model grid is a "rectangular" area over a specific region of the globe. An example of a possible grid is illustrated in Figure 8-2. Generally, the initial conditions of a LAM come from a numerical forecast from a larger-scale (e.g. global) model, though a LAM can also be initialized from a gridded analysis or output from another LAM grid that encompasses the area of the smaller grid. One of the main advantages of a LAM over a global model configuration is that smaller grid-spacing (higher resolution) can be used without the need to run the model over the entire globe, which would be very computationally expensive due to the large number of grid points. In general, reducing the horizontal grid-spacing by a factor 2 increases the computational cost of the model by a factor of 16. Thus, a LAM configuration is a very useful feature of a NWP model for applications that require high resolution, such as weather prediction in mountainous regions where there is a need to properly resolve orographic peaks and valleys.

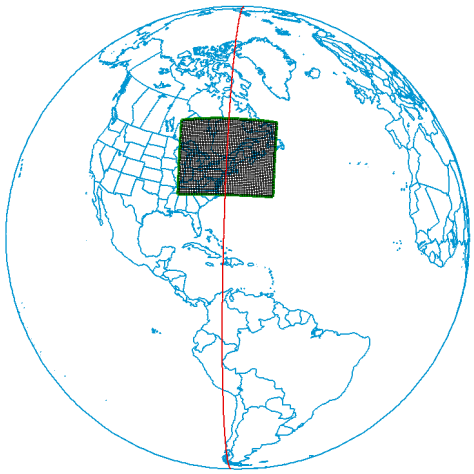

**Figure 8-2** Hypothetical GEM grid with a LAM configuration.

The CMC currently (as of November 2009) runs a LAM configuration of the GEM model over four domains in Canada (see Figure 8-3) in experimental mode. The domains are located over south-central British Columbia and Alberta, southern Ontario and Quebec, the Nova Scotia region, and the region over southern Baffin Island. Although the official status of these GEM model domains is "experimental" (as opposed to "operational", which implies a guaranteed forecast product for clients), the model is run in real-time forecast mode and can be referred to by meteorologists in Canada for operational forecasting. With increasing computer resources and the ability to run high-resolution model grids regularly, such configurations will play an increasingly important role in operational centres around the world.

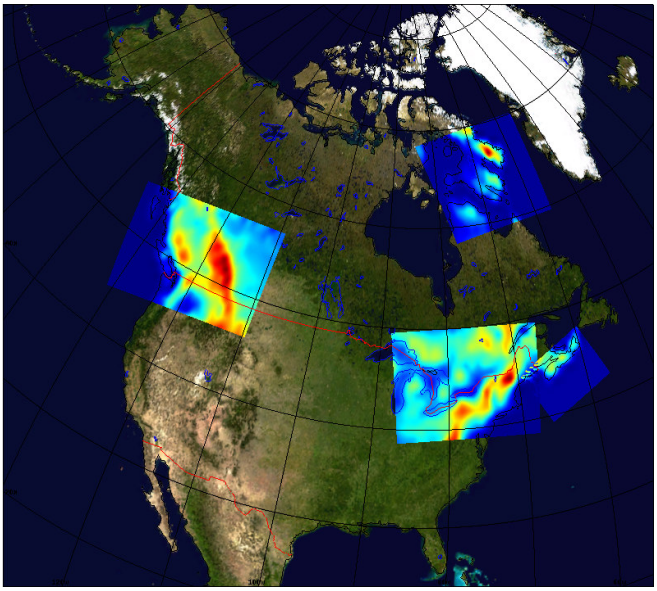

**Figure 8-3** The four limited-area domains for the quasi-operational LAM-2.5 configuration of the GEM model as of 2008, each with a horizontal grid-spacing of 0.0225° (~ 2.5 km). The color in the domains indicates topography.

The initial (and lateral) boundary conditions for each of the domains come from the model forecast fields from the regional GEM configuration. In this sense, the LAM grids are "driven" by the regional model. Each grid has a horizontal grid spacing of approximately 2.5 km. This configuration is thus often referred to as the GEM -LAM-2.5. At this resolution, the model begins to resolve individual thunderstorms. This changes the type of cloud schemes that are appropriate. A subgrid-scale CPS, such as the one in the coarser-scale regional model, is no longer used, and the condensation scheme is considerably more detailed and capable of simulating fog.

### 8.2.5 The explicit cloud microphysics scheme in the GEM-LAM

The type of condensation scheme used in a high-resolution (cloud-resolving) model, including the GEM-LAM, is referred to as an *explicit cloud microphysics* scheme. A "cloud" scheme is a physical parameterization which predicts the effects of a complex set of cloud microphysical processes. Cloud schemes are invoked when a model grid element reaches saturation (hence they are referred to as "explicit" schemes) or when condensate is already present in a grid element. Through the calculations of processes involving phase changes of the water substance, such as condensation or melting, the model dynamical fields (i.e. temperature, pressure and vertical air velocity) are affected by latent heating and cooling due to phase

changes, causing changes in buoyancy. The dynamics are also affected by precipitation loading, whereby downward vertical air motion is induced due to the weight of the condensed water/ice. There is also a feedback through the radiation scheme, which uses liquid and ice water contents predicted from the cloud scheme to compute cloud optical properties. The microphysics scheme also contributes to the total model precipitation at the surface and, depending on the complexity of the scheme, can provide details about the precipitation type.

As of April 2008, the Milbrandt and Yau (2005) microphysics scheme has been used in the four experimental LAM-2.5 domains. In this parameterization, the hydrometeor-size spectrum is partitioned into six separate categories – *cloud* (small liquid droplets), *rain*, *ice* (pristine crystals), *snow* (large crystals and aggregates), *graupel* (rimed crystals), and *hail*. In the current (as of November 2009) version of the scheme used in the experimental GEM-LAM-2.5, the mass mixing ratio of each hydrometeor category is a prognostic model variable, implying that it evolves in time, is advected by the 3-D wind field, and precipitates. In a research version of the scheme, the total number concentration of each hydrometeor category is also a prognostic variable. This added complexity provides better prediction of mean particle sizes of the hydrometeor categories, which is important for some applications, including the prediction of visibility through fog.

To understand how the model would predict liquid fog, it is useful to consider how the microphysics scheme predicts the mixing ratio of the cloud water, $q_c$. Ignoring changes due to advection (transport by the model wind field), the prognostic equation for *cloud* water, giving the rate of change due to microphysical processes, is:

$$\left.\frac{dq_c}{dt}\right|_S = VD_{vc} - CN_{cr} - CL_{cr} - FZ_{ci} - CL_{ci} - CL_{cs} - CL_{cg} - CL_{ch}, \qquad (8\text{-}1)$$

where the terms on the right-hand-side of the equation are: condensational growth, conversion to *rain*, accretion by *rain*, homogeneous freezing, accretion by *ice*, accretion by *snow*, accretion by *graupel*, and accretion by *hail,* respectively.

Thus, liquid water (excluding *rain*) forms and grows by condensation only, and interaction with all other hydrometeor categories results in depletion of *cloud* water. It must be emphasized that the scheme will produce cloud water by condensation if and only if the relative humidity of a model grid box reaches 100%, either due to an increase in the specific humidity or decrease in the temperature. However, the microphysics scheme has no information about its neighbouring grid points or about the meteorological situation other than the current values of the atmospheric state variables which it is supplied. Thus, in order for liquid fog to form correctly in the model, the temperature and humidity must be correct.

Similarly, the prognostic mixing ratio of *ice* crystals, $q_i$, is predicted by a similar predictive equation as for $q_c$, where the sources if *ice* mass are nucleation, freezing of cloud droplets, and depositional growth with depletion resulting from sublimation, melting, and collection from other hydrometeor particles.

For given values of the prognostic hydrometeor variables relevant to fog, the visibility can be parameterized using empirical equations such as the ones discussed in section 6. For example, equation 6-3 can be applied for visibility (*VIS*) through liquid fog, which gives *VIS* as a function of the cloud liquid water content (*LWC*) and the cloud droplet number concentration ($N_d$), based on empirical relations obtained from measurements during the FRAM project. $LWC = \rho q_c$, where $q_c$ is predicted by the microphysics scheme, and an assumed value of the cloud droplet number concentration, $N_d$ is used. The current version of the Milbrandt-Yau scheme uses fixed values of 80 $cm^{-3}$ for maritime regions and 200 $cm^{-3}$ for continental regions. In the research (double-moment) version of the scheme, $N_d$ is a prognostic quantity so no assumed value is required, and thus in principle a better prediction of *VIS* is possible since *VIS* though liquid fog depends on both *LWC* and $N_d$. The scheme also parameterizes reduction of *VIS* due to rain and snow, also based on empirical relations obtained from FRAM observations. An example of the parameterized *VIS* fields is shown in the horizontal and vertical cross-sections in Figure 8-4 and Figure 8-5, respectively.

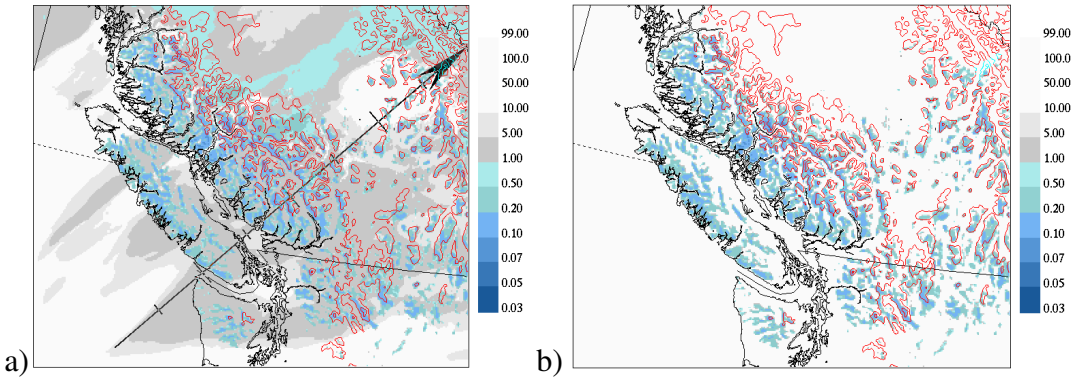


**Figure 8-4** Fields of parameterized *VIS* from a GEM-LAM-2.5 simulation at the lowest prognostic model level (approximately 40 m AGL) due to reductions from a) the combined effects of liquid fog, rain and snow; and b) liquid fog only. Units are in km. Red contours depict elevations of 1500 and 2000 m.

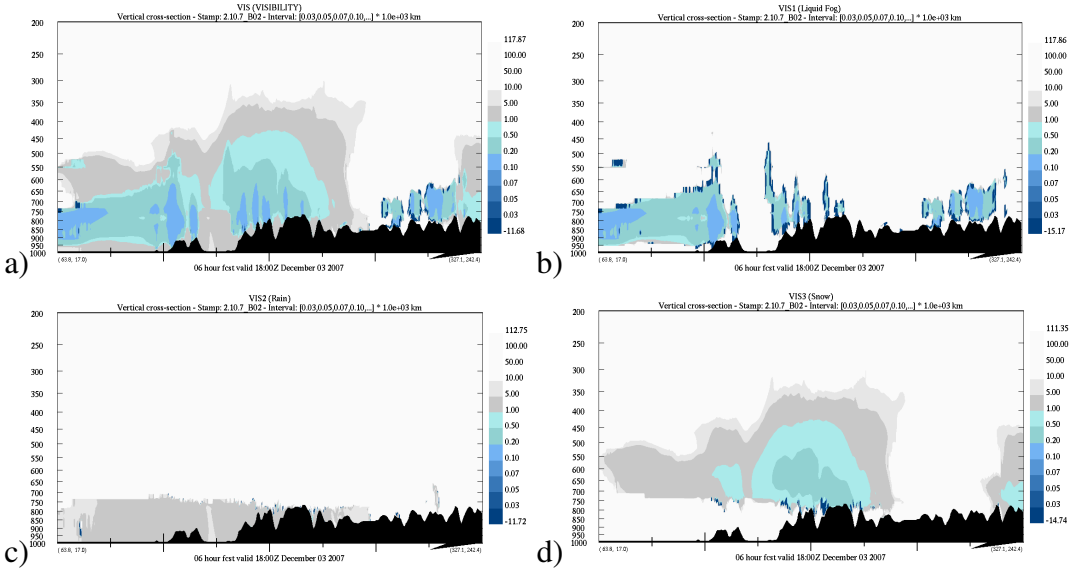


**Figure 8-5** Vertical cross-sections (corresponding to the arrow in Figure 8.4a) of *VIS* due to reductions from a) the combined effects of liquid fog, rain and snow; and b) liquid fog only; c) rain only; and d) snow only. Units are in km.

It must be recognized that NWP models in general, including the GEM, have some intrinsic limitations pertaining to the explicit prediction of fog, at least as they are typically run operationally. In particular, the vertical resolution of the planetary boundary layer is generally insufficient to properly capture the processes that lead to the production of relatively high liquid water contents near the surface. This is illustrated in Figure 8-6 and Figure 8-7, which show the cloud water mixing ratio field from a GEM-LAM-2.5 model run. In Figure 8-6 the cloud water field at the 3rd lowest model level is shown. Figure 8-7 depicts vertical cross-sections, corresponding to the arrows in Figure 8-6 on pressure levels (left) and on model levels. The vertical coordinate of the GEM model is terrain-following, so no underlying orography is visible in the model level cross-sections. In both sets of cross-sections, it is apparent that the model is simulating low-level stratus cloud which, in reality, was responsible for coastal fog at the surface for this case. However, at the lowest few model levels, including the level closest to the ground, the model is almost completely dry. Thus, although the stratus cloud was captured relatively well by the model, it does not accurately capture the liquid fog very near the surface. This is due in part to the lack of sufficient vertical resolution in the configuration of the GEM-LAM-2.5. This current limitation must be borne in mind when using explicit output fields from the GEM-LAM-2.5 for fog forecasting. In the future, as computer resources increase and high-resolution NWP model forecasts become a more mainstream tool for operational weather prediction, this aspect of the model will likely improve.

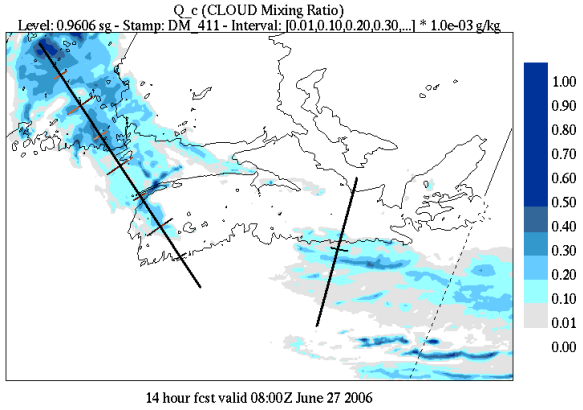


**Figure 8-6** Cloud water mixing ratio from 3rd lowest model level for a GEM-LAM-2.5 simulation of a case of coastal fog. Units are in g $kg^{-1}$.

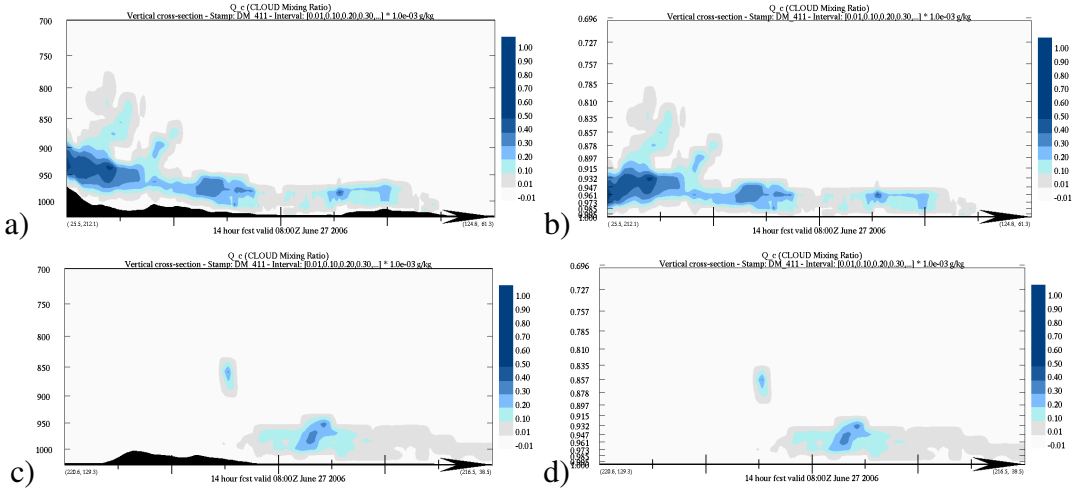


**Figure 8-7** Vertical cross-sections of the cloud water mixing ratio corresponding to the left line [a) and b)] and the right line [c) and d)] in Figure 8-6 on pressure levels [a) and c)] and terrain-following model levels [b) and d)]. Units are in g $kg^{-1}$.

## 8.3 The NCEP RUC model approach

The Rapid-Update Cycle (RUC) model (Benjamin et al. 2004) is one NWP model from the U.S. National Center for Environmental Prediction (NCEP) which uses a similar type of explicit cloud microphysics scheme as the LAM configuration of the GEM model, in which the mass mixing ratios of four hydrometeor categories – *cloud* (liquid), *rain*, *ice*, and *snow* – are predicted. The algorithm of Stoelinga and Warner (1999) is used to compute the extinction coefficients corresponding to hydrometeor mixing ratios, based on empirical and theoretical relations. These are then summed and used to compute the visibility, in a similar manner to the GEM-LAM-2.5. Other NCEP models use similar methods to parameterize visibility.

### 8.4 1-D fog models

Some researchers have used special 1-D numerical models to study the development, evolution and dissipation of fog (generally radiation fog) in certain situations and to compare the results with the observations (e.g. Turton and Brown 1987; Duynkerke 1991; Bergot and Guédalia 1994; Guédalia and Bergot 1994; Koracin et al. 2001; Bergot et al. 2005; Tardif, 2007). These models have the advantage of being able to include a very high vertical resolution and a detailed account of lower boundary layer effects and possibly detailed surface and sub-surface effects as well, while being able to run in a reasonable amount of time. However, these models currently remain as research tools, and must be initialized using 3-D information such as advected fields from a separate analysis or larger-scale NWP model, and the solutions are valid only for a single point.

# 9 Tools and resources

This chapter covers many of the tools available to Canadian forecasters.

The GEM regional, GEM-LAM, and other models will be discussed including American products which are available to Canadian forecasters and cover at least the southern regions of the country.

### 9.1 Fog Diagnosis

Fog and stratus are highly variable in time and space, and lie close to the surface, beneath other cloud layers. For these general reasons, diagnosis can be difficult. The following sections briefly summarize the diagnostic possibilities.

#### 9.1.1 Traditional human weather observations

Such observations give the best detail and confidence about the presence of fog and stratus. However, over land in Canada these stations are generally very far apart, so spatial resolution of the observations is poor. Many of these stations have been replaced by automatic observing instruments, for at least part of the day. Partial observing programs, in which human observations are available only in the daytime hours, are common in some regions, particularly in the North. For these cases the temporal resolution of the observations is inadequate as well.

#### 9.1.2 Automatic observation stations

These stations are becoming more and more common, but often report only the most basic weather elements (temperature, pressure, dewpoint, wind). In such cases, the report at best

might support an uncertain deduction about the presence of fog or stratus. Full Automated Weather Observing System (AWOS) devices found at many airports incorporate a visibility sensor which attempts to simulate the visibility characteristics of the human eye. The sensor used typically uses a forward scattering approach, in which a pulsed light source is detected by a sensor and algorithms are used to convert the measured extinction of the light source into a visibility measurement. Such sensors do not have a directional capability and assume that the visibility measurement is homogeneous in all azimuths. When combined with information from the ceilometer sensor, the forecaster can generally deduce information about the nature of the obstruction to vision. However, the information from these systems can be open to interpretation, and forecaster training and experience are generally required to make the most of the data. Interpretation of these measurements is particularly problematic in cold Arctic conditions when ice crystals are present. In these conditions forward visibility sensors will tend to under-report the extinction whereas the ceilometer will over-report the extinction due to the ice crystals.

### 9.1.3 Ship observations

Ship observations often lack specific information about visibility and ceiling. The information they provide is often more general. Ships that conduct ocean, ice and atmospheric research do tend to provide more detailed information. This was true of both the US Coast Guard (USCG) icebreaker Healy and the German research ship Polar Stern that operated in the Arctic ocean in the summers of 2008 and 2009. The Healy also provided useful web cam images that were available in real time at http://mgds.ldeo.columbia.edu/healy/reports/aloftcon/2008.

### 9.1.4 Summary Charts of Observations

#### 9.1.4.1 HAL F/ST Summary Observation Charts

These charts were developed in the Hydrometeorology and Arctic Lab by Andrew Giles to support the development work of the rules-based fog and stratus forecasts that are described in section 9.2.6 of this Handbook. They are can be found at http://chinook.edm.ab.ec.gc.ca/~gilesa/STFOGmaps.html.

Here is an example:

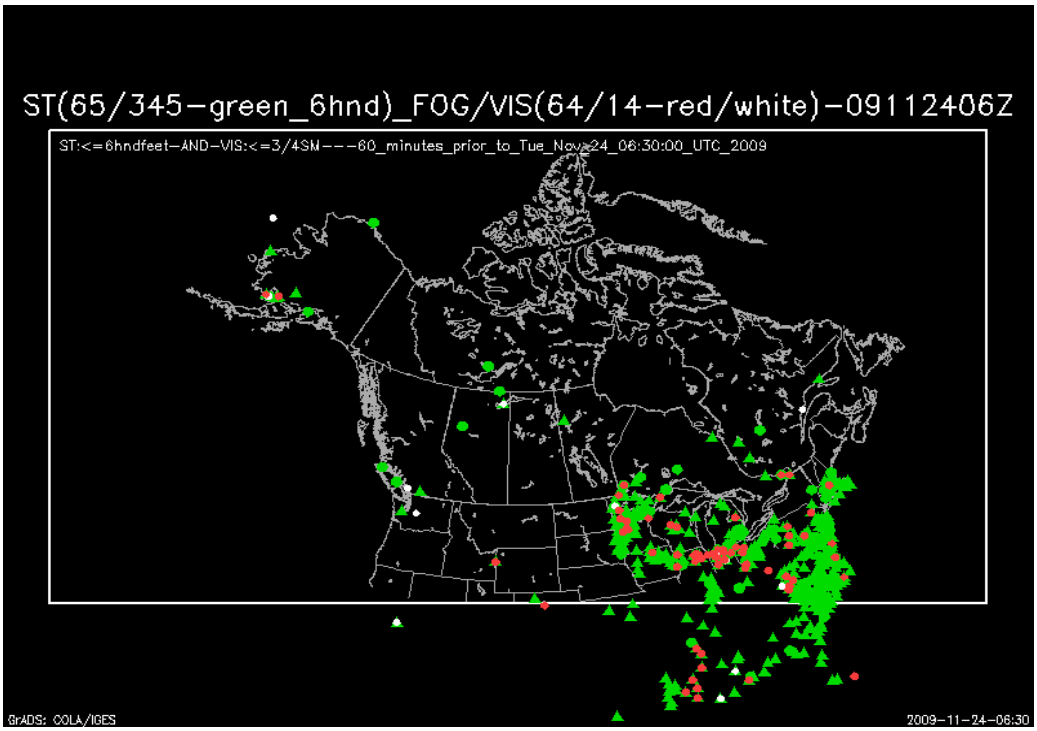


**Figure 9-1** HAL F/ST summary observation chart.

The charts are available hourly, in real time. For each hour, all North American observations in the period of plus or minus half an hour centred on that hour are considered. A green dot indicates a station that observed a ceiling of 600 feet or lower. This will be generally a stratus ceiling, though an obscured ceiling in precipitation is also a possibility. A red dot indicates an observation of fog with a visibility of ¾ SM or lower. The red dot is slightly smaller than the green dot, so that a station reporting both conditions will be indicated with the red dot surrounded by a thin green border. Cases for which the obscuring phenomenon can not be defined (e.g. an autostation report with a reported visibility but no indication of the obscuring phenomenon, which could be snow, for example, rather than fog) will be included as a white dot. White dots need further interpretation on the part of the user. If the observing station is an automatic station, then it is indicated as a triangle rather than a circle in these charts.

Fog observation charts from ships in Canadian waters and adjoining oceans can be found at http://chinook.edm.ab.ec.gc.ca/~gilesa/shipdisplay.html. In these charts, coloured dots indicated three separate observed visibility ranges, as specified in the label. Since many ships do not include observations of visibility, coloured crosses indicate three separate ranges of temperature – dew point spread (T-Td), where available, as a rough proxy for visibility. An example is shown in Figure 9-2 (some autostations in Greenland also appear in this chart).

Subsets of these charts, covering an eastern Canadian window, can be found at http://chinook.edm.ab.ec.gc.ca/~gilesa/eastfog.html.

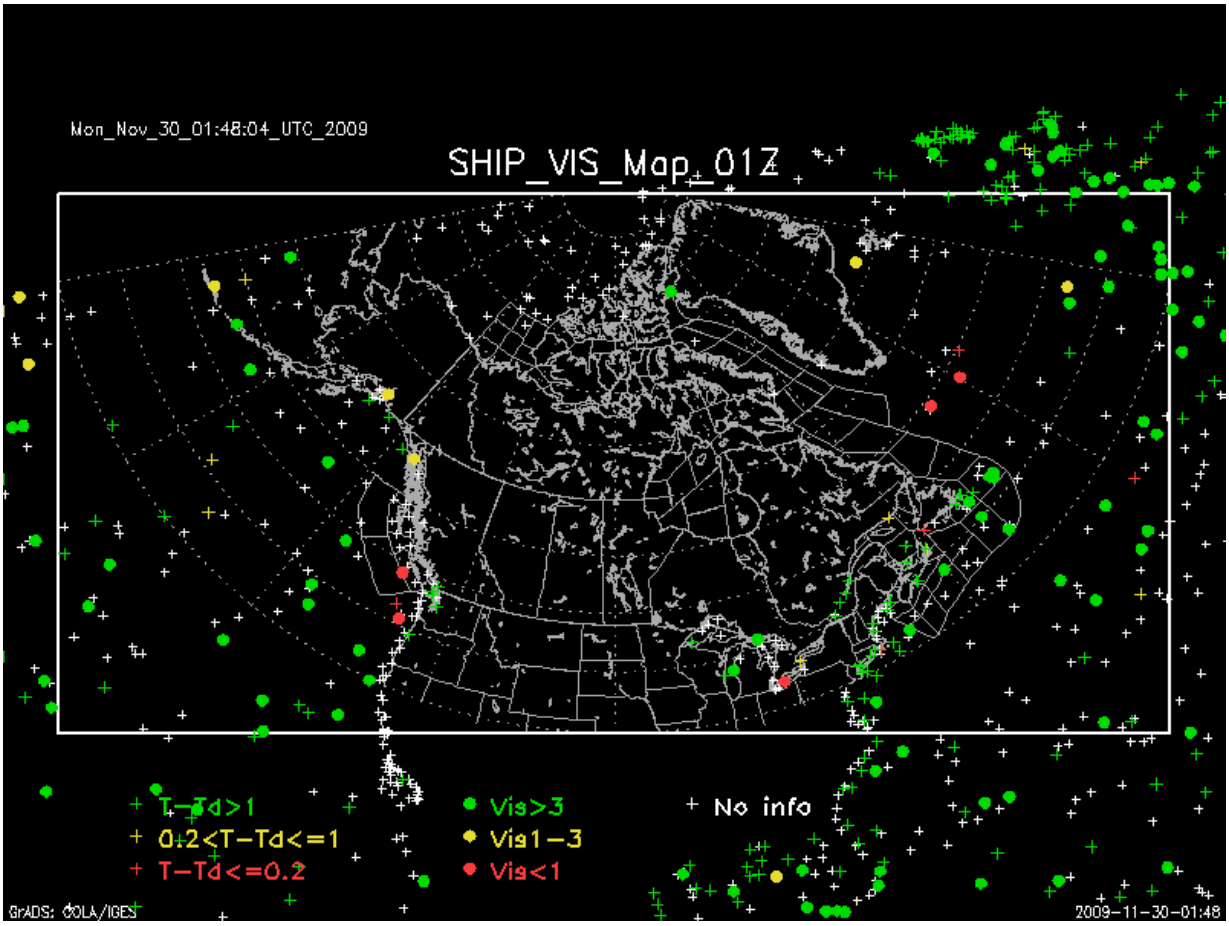


**Figure 9-2** HAL summary ship observation chart for Canadian waters and adjoining oceans.

### 9.1.5 Web Cams

Web cameras are a very useful resource for the forecaster. When available (during the daylight hours) they can help "fill in the holes" between traditional observing stations, and can give the forecaster a good "feel" for what is happening at particular locations. Updates every few minutes give good temporal resolution. Web cams can therefore be quite useful for fog diagnosis in particular, although they do not provide numerical estimates of the visibility. One might be able to interpret the presence of low stratus in some cases as well. The following sites have groupings of webcams and they can be found in Appendix A.

### 9.1.6 Satellite Imagery

Satellite imagery offers a wide variety of possibilities for fog and stratus diagnosis, but there are also many limitations. The fog and stratus may be covered by higher clouds, or may

blend in with the surface features, or may be invisible to some channels because they lie under a strong low level inversion with temperatures that are much warmer somewhat higher up in the atmosphere. However, channel-differencing techniques are showing some promise in certain situations when satellite data is integrated with model observations (Gultepe et al. 2007b). However, even if they do correctly identify a region of fog or stratus, they do not give information on the visibility within that fog, or the height of the stratus base above the surface. Some of these limitations were discussed in chapter 7.

## 9.2 Fog Forecasting and Nowcasting

### 9.2.1 Climatological Tools

Fog and stratus episodes can be of short or long duration. One example of an uncommon long-duration episode took place in southwestern British Columbia and in western Washington State in December, 1999. Air traffic at airports in southwestern BC was disrupted during the period from 00 UTC Dec 22 through 00 UTC Dec 29 in what has been called "the Christmas 1999 fog and stratus episode" (McCay 2000). The return periods of prolonged fog events are described by Hansen et al. (2009), with an example provided in Figure 9-3.

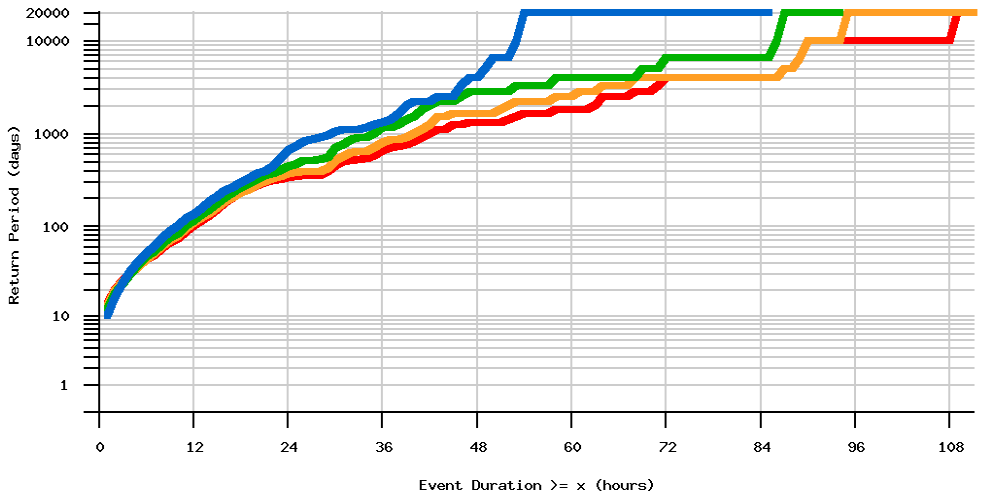


**Figure 9-3** Return periods of prolonged fog events at Vancouver International Airport based on all hourly observations for the years 1953-2007, inclusive. The *y*-axis is return period in days; the *x*-axis refers to events ≥ *x* hours duration. For instance: events ≥ 1 day duration have a return period of approximately 300 days; events ≥ 2 days duration have a return period of approximately six years. The blue curve describes unbroken events only; green curve includes events with breaks no longer than one hour; orange curve includes events with breaks no longer than two hours; and red curve includes broken events with breaks no longer than three hours. See Hansen et al. (2009) for further description and an online archive of analyses for most major airports in Canada.

Another tool called WIND-3 is used to help forecast ceiling and visibility based on the analog method (Hansen 2007). An example of a forecast guidance product is shown in Figure 9-4. For each airport in Canada, at each hour, the system produces 24-hour forecasts of ceiling (in blue) and visibility (in red). The system uses the analog method: predictions for the current case are based on the most similar past cases. Conditions other than ceiling and visibility, which help to predict ceiling and visibility, are determined by GEM model guidance, namely: wind direction and speed, humidity, and weather (rain, snow, and so on). Thirty years of recent hourly observations for each airport are searched and those with the most similar conditions are identified, the values of ceiling and visibility in those cases are summarized, and the results are plotted as guidance for aviation forecasters, as shown here.

The raw numbers (actual analogous past observations) are plotted in the frame at the bottom, which forecasters may inspect if they like. More often they refer to the graph at the top. In this graph: the horizontal axis shows time from 0 to 24 hours. The left vertical axis is for ceiling, with values in hundreds of feet, and ticks at significant thresholds. Likewise, the right vertical axis is for visibility, in statute miles. So for example, conditions above 1000 feet and 3 miles are VFR flight conditions, and below are IFR flight conditions.

For each hour, a probabilistic forecast is made, for ceiling in blue and visibility in red, as shown here. The past analog values of ceiling and visibility range from lower to higher values. Consider ceiling (in the blue color band) between the two green arrows. Values range as low as 2 hundred feet, and as high as 15 hundred feet. The median value, shown by the dark blue line, is 1000 feet. This is the most probable range of ceiling to expect for this forecast time for given forecast wind, weather and humidity, based on past cases.

Every new observation triggers the production of a new chart. For example, a sudden lowering of ceiling leads to the production of a corresponding chart. However, often conditions are variable or volatile, and a forecaster may choose to disregard a single observation, believing it to be anomalous and unrepresentative of a trend. In such a case the forecaster may choose to not forecast persistence. A running archive of the latest 24 graphs is available in case a forecaster wants to refer to a previous diagram rather than the latest (anomalous) one. To access the charts on the website, position the mouse cursor over the x-axis of the chart (like the one shown in Figure 9-4) and pan from left to right to scan through recent diagrams.

The system also helps to forecast ceiling and visability with shading-dependent degrees of confidence. For example, here after 12 UTC, even the lowest values among past analogs are well into the VFR category.

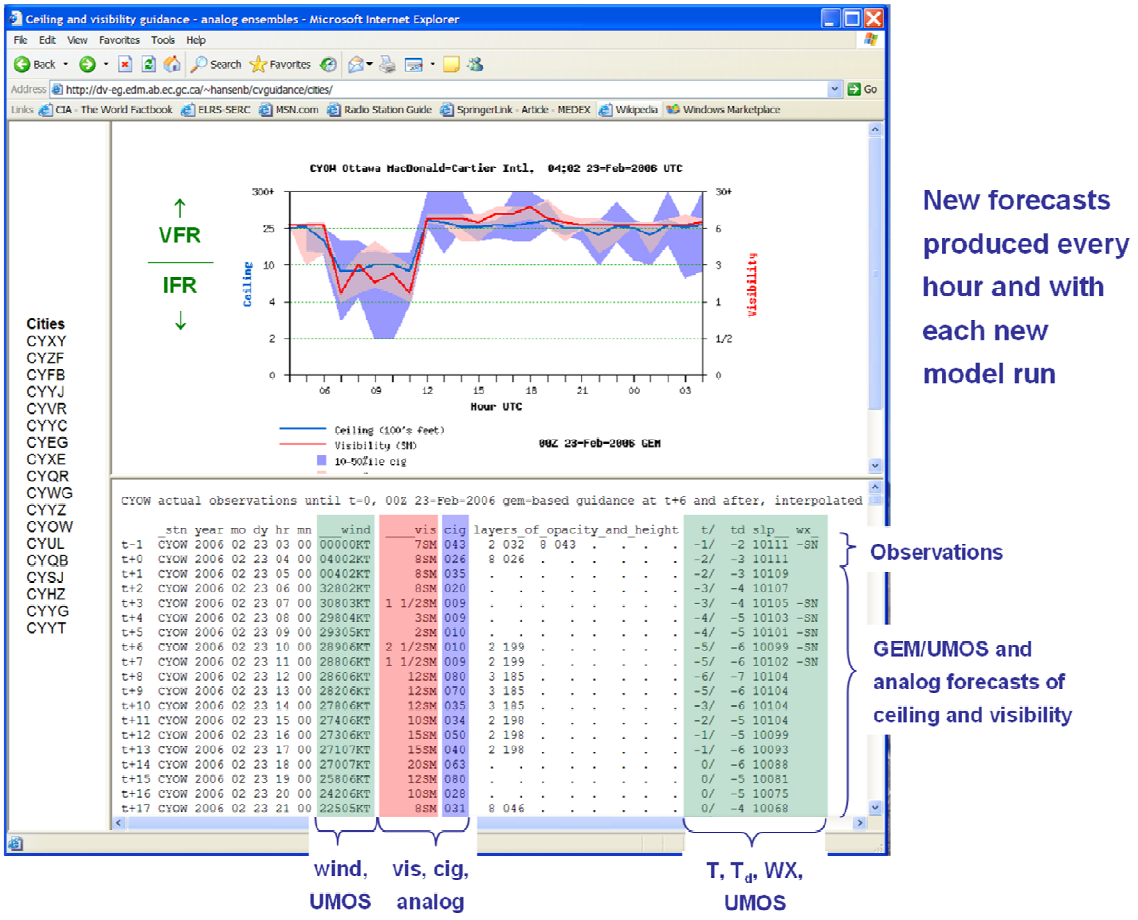


**Figure 9-4** Forecast of ceiling (blue) and visibility (red) based on the analog method.

Forecasters have identified weaknesses in WIND-3 guidance in two types of cases. Both types of cases are recognizable in context, and forecasters can treat the guidance with appropriate discretion and subjective adjustments in such cases:

- *Volatility in cases where persistence seems more likely*. Fog events (periods with consecutive hours of fog) last on average 3 to 6 hours, varying from location to location and time of year. Therefore when WIND-3 forecasts fog to dissipate within the first three hours, the forecaster should regard the guidance with discretion. In cases where all conditions are barely changing (fairly constant wind, humidity, and precipitation, or lack of precipitation), ceiling and visibility will usually persist.
- *Poor input leading to poor output*. WIND-3 is driven by forecast conditions provided by the GEM model and UMOS: wind direction, dry bulb temperature, dew point temperature, and precipitation (e.g. the green highlighted data in Figure 9-4). For example, the input guidance might predict an unrealistically rapid upward trend in the temperature-dew point

spread (e.g. when the wind is forecast to become offshore). In this case, the forecaster would not expect the spread to grow to more than 2 degrees if the real winds were remaining onshore, while the input guidance is forecasting a spread of 5 degrees. In such a case, WIND-3 will forecast ceiling and visibility based on analogs with a 5 degree spread, output which is as unrealistic as the input. A forecaster familiar with the current weather map could look at the WIND-3 guidance and discern such a case, and subjectively adjust: a lower spread than shown implies a lower visibility than shown.

#### 9.2.1.1 FogSpecs

FogSpecs is a simple climatological technique. Climatological records from various stations have been analyzed to indicate average times of early formation, likely formation, max occurrence, likely dissipation and late dissipation. This has been done for each month of the year. In any month, the five separate times for each station for that month are integrated into the operational TAFtime window, at the lower right. TAFtime is an application that provides aerodrome information and NWP forecast information, along with some climatological information, for aerodromes across the country for which TAFs are written. The presentation is compact for high "glance value". FogSpecs times are found at the lower right of the TAFtime window. To see TAFtime, go to http://pnrinternal.pnr.ec.gc.ca/CMAC-West/site_reference/siteref.html?site=yxd&resource=4_pan and click on CMAC-W or CMAC-E and then click the TAFtime button. The five times supplied by FogSpecs can be used for short term forecasting of both fog formation and dissipation at individual observing stations.

General Fog Specs information and forecasts are found at: http://pnrinternal.pnr.ec.gc.ca/paawc/public/wxelement/fog. Available FogSpecs sites are found at http://pnrinternal.pnr.ec.gc.ca/CMAC-West/site_reference

Figure 9-5 below shows a typical FogSpecs curve. In this case the times 09/11/12/15/18 are the five climatological times created by the FogSpecs analysis. These numbers are repeated in the small rectangle at the lower right of the image, which represents the way the FogSpecs data have been integrated into TAFtime. By its design, FogSpecs provides an estimate of both fog formation and dissipation time.

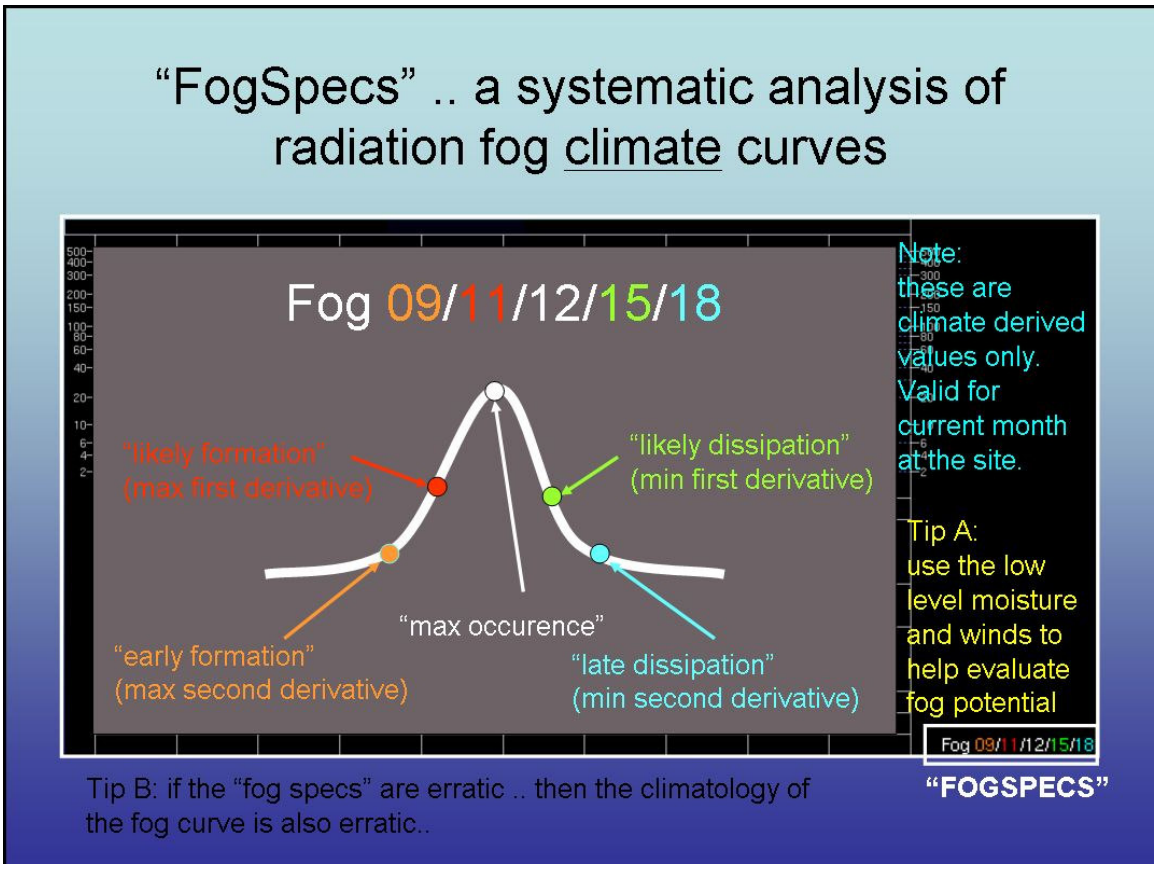


**Figure 9-5** FogSpecs analysis of radiation fog.

#### 9.2.1.2 Robert Rowson's Climate Manager Routines

Robert Rowson (Prairie and Northern Region) has built routines to access and display climatological data on ceiling and visibility from Climate Manager (Climate Manager Percent Occurrence of Ceilings and Visibilities). Probabilities and frequencies of occurrence for ceiling and visibility for various stations with various filtering possibilities (e.g. by wind direction and speed) are available. See http://dv-eg.edm.ab.ec.gc.ca/~rowsonr/percent.html.

### 9.2.2 FogDex

The FogDex is a radiation fog formation index developed by Anke Kelker in 2002. Information can be found at http://dv-eg.edm.ab.ec.gc.ca/~suttonl/fogdex_main.html.

### 9.2.3 Merv Jamieson's UPS Fog Station Forecasts

This was the first work in Canada on the UPS fog method. It includes forecasts for stations in western and northern Canada, but does not include some of the modifications such as the ground skin temperature. See http://dv-eg.edm.ab.ec.gc.ca/~jamiesonm/fog.

The more recent Toth/Burrows rules-based UPS forecast is described in section 9.2.6 of this Handbook.

### 9.2.4 SCRIBE Rules for Fog Forecasting

#### 9.2.4.1 Public SCRIBE

Most text forecast products in Canada (prepared by the Meteorological Service of Canada) are generated using a software package known as SCRIBE. This software converts forecaster-manipulated graphical "concepts" from the user interface to standardized text. The software will automatically generate these graphical "concepts" directly from the GEM regional model output variables such as surface air temperature, wind, cloud cover, etc. The latest rules for fog concept generation in "Public" SCRIBE (where T = model surface air temperature and Td is model surface dew point):

Radiation fog must satisfy the following criteria:

- $T > -3.0^{o}C$
- cloud cover $\leq$ 2/10 coverage;
- winds < 14 km/h;
- temperature inversion where $T \leq T_{(eta=0.97)}$ ;
- T-Td spread $\leq 1.0^{o}C$

Fog with or following precipitation must satisfy:

- temperature close to or above zero;
- light winds and low ceiling;
- little or no T-Td spread;
- precipitation at current time or in recent past.

The ice fog concept will be generated under similar criteria as radiation fog criteria above, but when $T < -27^{o}C$ and the low level temperature inversion is strong. Advection fog is not handled in Public SCRIBE at the time of this document.

#### 9.2.4.2 Marine SCRIBE

The standard "Marine" SCRIBE rules used to generate a visibility concept for fog or mist is more sophisticated than for Public SCRIBE, and are outlined below in algorithm format (SST = sea surface temperature):

If Td > SST then:

If the sea/lake ice cover < 50% AND
the Td-SST > 8°C AND
T-Td = 0.0°C then:

**Visibility is set to 0 nm**.

Else if the ice cover < 60% AND
Td-SST ≥ 3°C AND
T-Td ≤ 2°C then:

**Visibility is set to 1.6 nm.**

Else the **Visibility is set to 6 nm.**

Else if T-Td ≤ 1°C AND
Surface wind speed < 10 knots during the 3 hour period AND
Ice cover < 60% AND
T < SST-8°C:

If T-Td = 0.0°C:

**Visibility is set to 0 nm.**

Else **Visibility is set to 1.6 nm.**

Else the **Visibility is set to 12 nm.**

All marine forecasts that are issued by the MSC contain the following statement regarding fog at the beginning of the forecast: "Fog implies visibility less than 1 mile." This value is apparently an important threshold for many marine operations (Ted McIldoon, ASPC, internal communication).

Both "Prairie and Northern" and "Atlantic" forecast regions have noted that SCRIBE under- forecasts advection fog and mist concepts. After some investigation of the knowledge base rules it appears that the current thresholds (as of October 2008) used to generate advection fog are too restrictive. There are several options being considered for the December 2008 v1.2 release to address the deficiency.

The National Labs in Edmonton and Halifax are currently working (as of Fall 2008) on several projects (the FRAM project being the primary one) aimed at improving visibility guidance using both numerical and statistical methods. The long term solution is to integrate one or more of these methods into SCRIBE either directly via the "Matrices" (raw code used to

generate the graphical “concepts”) and/or calculated within the rules using a rules-based approach. This option may be included in a future release.

The short-term solution (and the solution approved for v1.2) is to introduce an option for regions to use a "more relaxed thresholds" for the production of visibility concepts. The new set of rules has been developed in conjunction with the Prairie and Northern Region (Andrew Giles and Ed Hudson) and has been tested through two marine seasons in the Arctic. The new set of rules can be optionally activated by the regional forecast office:

If Td-SST > -1°C then:
- If the ice cover < 50% AND
- Td-SST > 6°C AND
- T-Td ≤ 1°C :
  - **Visibility is set to 0 nm.**
- Else if the ice cover < 80% AND
- Td-SST ≥ 3°C AND
- T-Td ≤ 3°C:
  - **Visibility is set to 1.0 nm.**
- Else **visibility is set to 6 nm.**

Else if T-Td ≤ 2°C AND
Surface winds are light during the 3 hour period AND
Ice cover < 60% AND
T < SST–4°C:
- If T-Td=0.0°C:
  - **Visibility is set to 0 nm.**
- Else **Visibility is set to 1.0 nm.**

Else the **Visibility is set to 12 nm.**

*Additionally, for Arctic sea smoke:*

If surface wind speed < 10 knots (~ 20 km/h) AND
Ice cover < 60% AND
T < SST–3°C
- If T-Td ~=0°C
  - **Visibility is set to 0 nm**
- Else if T-Td~=1°C
  - **Visibility is set to 1.6 nm**

#### 9.2.4.3 Marine SCRIBE Test Rules – Summer, 2009

A test of modified rules was done at the ASPC in the summer of 2009, based on rules provided by G. Toth from his experience with the GEM Regional F/ST forecast system. The operational forecasters felt that the existing rules described in the previous sections often did not forecast enough fog. The modified rules are:

```
ES=T-Td
IF  ICE <= 70%
THEN
      IF (Td >= SST + 3)
      THEN
            IF ES <= 1.5            Vis = 0
            IF 1.5 < ES <= 3        Vis = 1
            IF 3 < ES <= 6          Vis = 6
            IF 6 < ES               Vis = 12

      ELIF (SST <= Td < SST +3)
      THEN
            IF ES <= 0.5            Vis = 0
            IF 0.5 < ES <= 2        Vis = 1
            IF 2 < ES <= 4          Vis = 6
            IF 4 < ES               Vis = 12
      ELIF (Td < SST)
      THEN
            IF ES <= 1.0            Vis = 1
            IF 1 < ES <= 2          Vis = 6
            IF 2 < ES               Vis = 12
      FI
FI

IF ICE > 70%
THEN
      IF (Td >= SST + 3)
      THEN
            IF ES <= 0.5            Vis = 0
            IF 0.5 < ES <= 2        Vis = 1
            IF 2 < ES <= 4          Vis = 6
            IF 4 < ES               Vis = 12
      ELIF (SST <= Td < SST +3)
      THEN
            IF ES <= 1.0            Vis = 1
            IF 1 < ES <= 2          Vis = 6
            IF 2 < ES               Vis = 12
      ELIF (Td < SST)
      THEN
            IF ES <= 1.0            Vis = 6
            IF 1 < ES               Vis = 12
      FI
```

These rules were run in parallel and produced test SCRIBE output available to the forecasters. Initial verification results from the ASPC in the summer of 2009 indicate that these rules do indeed produce more fog than the other SCRIBE rules. Further verification is planned to allow the tuning of these rules.

### 9.2.5 Visibility diagnosed from model output

#### 9.2.5.1 Kunkel (1984)

The Kunkel (1984) parameterization that is commonly used for fog forecasting is

$$\beta = 144.7\ C^{0.88} \qquad (9\text{-}1)$$

where β is the visibility extinction coefficient and C is the cloud water mass concentration. As mentioned earlier, Gultepe et al (2006a) has suggested a new equation (Eq. 6-3) based on detailed fog observations. As described in Section 6, Kunkel's equation, which does not consider $N_d$, can include very large uncertainties. Gultepe et al., (2009) based on the FRAM field projects suggested a new Vis=f(LWC, $N_d$) relationship that should replace the Kunkel equation. Gultepe et al. (2006a) suggested that (without inclusion of $N_d$ in the parameterizations) uncertainty in Vis can be more than 50%.

#### 9.2.5.2 Texeira (1999)

In Kunkel's equation 9-1, it turns out that a liquid water mixing ratio of 0.016 g/kg corresponds to a visibility of approximately 1 km. Texeira (1999) used this mixing ratio value as obtained from the ECMWF model to create a climatology of model fog, which he then compared to the actual climatology. In the rules-based F/ST forecast system described in section 9.2.6, one of the experimental forecasts (titled QC2) presents simply the GEM regional model cloud water mixing ratio at model level eta = 0.995. The 0.016 contour is highlighted in this chart.

#### 9.2.5.3 Stoelinga and Warner (1999)

Stoelinga and Warner (1999) used Kunkel's equation 9-1 in their visibility work. It is based on the more general equation 9-2.

Gultepe et al. (2006a) summarized Vis versus LWC and Nd parameterizations as described in section 6 of this handbook. As is shown in Gultepe and Milbrandt (2009), it is suggested that the integration of extinction coefficients for RH and fog LWC (rainfall or snowfall rate) should be summed, then used for the computation of Vis in the following equation given by Stoelinga and Warner (1999):

$$Vis = -\ln(0.02) / \beta_{ext} \qquad (9\text{-}2)$$

where 0.02 represents a threshold for brightness contrast.

### 9.2.6 Rules-Based Forecasts of F/ST using GEM regional Model Output

#### 9.2.6.1 Introduction

As part of the FRAM project, a new automated technique for forecasting fog (F, visibility 1 km or less) and low stratus (ST, ceiling 500 feet or less) has been developed at the MSC's Hydrometeorology and Arctic Lab (HAL) in Edmonton. The technique takes advantage of the forecast fields from the GEM regional model. They are operational products available regularly over a large geographic area that covers Canada, the northern continental US and adjoining portions of the Atlantic, Pacific and Arctic oceans. The goal was to produce forecasts over this large region (rather than at specific locations) for periods from 1 hour through 48 hours into the future. A sample forecast chart is shown in Figure 9-6.

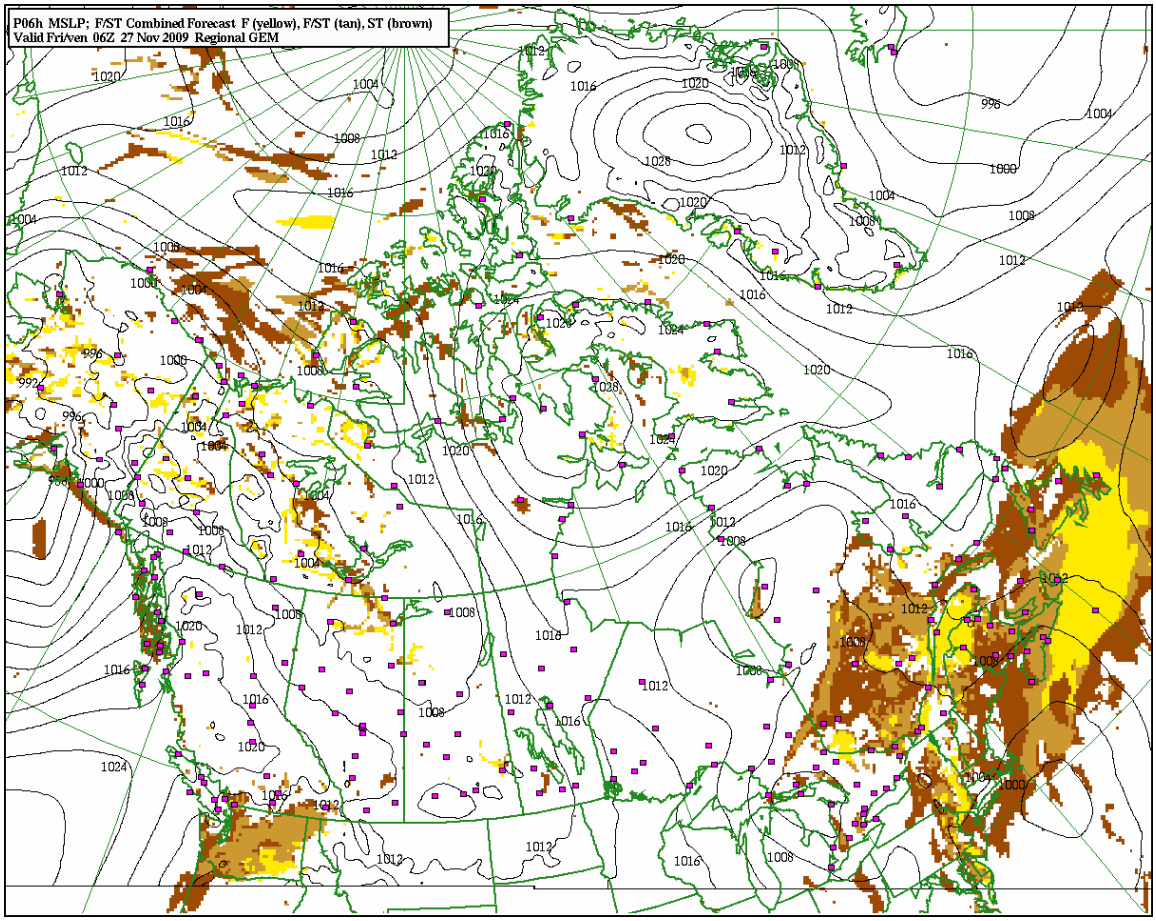


**Figure 9-6** Sample of combined F/ST forecast in the national window (Toth/Burrows rules-based forecast based on GEM regional output). Fog most probable areas are in yellow. Stratus most probable areas are in brown. In the tan areas either F or ST is possible. See Figure 9-7 for the corresponding augmented combined forecast chart.

In this section, the various forecast rules that feed into these forecast charts are summarized. The description is very general rather than detailed. The idea is to give the reader a flavour of what goes into the system. The charts are found at: http://halmetmodel1.edm.ab.ec.gc.ca/F+ST/F+ST.html. This web page is divided into four sections:

*1. Primary Automated Experimental Fog and Stratus Forecasts*

In this section the nine component forecasts (described below in section 9.2.6.4) are combined to create the combined F/ST forecasts.

*2. Combined F/ST Forecasts from Section 1 Components*

The nine component forecasts of section 1 are combined to produce charts in the first subsection of this section (Combined F/ST – full window). For a given grid-point, any of the components forecasting the fog or stratus will be included as a F or ST or F/ST point in this chart. For each grid point the presence of as few as one component forecast of F results in the assignment of an intermediate F/ST category to that point. The final version of the forecast chart is produced by examining the bulk Richardson number at each intermediate F/ST point. If it is large enough (experiments are ongoing as this is being written at the end of November, 2009, but with values typically around 1.0) then the point is defined as a F most probable point (yellow in the chart). Otherwise it remains as a F or ST probable point (tan in the chart). The brown points remain as ST most probable points. See Figure 9-6 for an example.

The second set of charts in this section repeats the information contained in the first set, but add to it model precipitation information that has been found useful in defining areas of low stratus ceilings or obscured low ceilings in snow. A brief description of these additions is found below. Since this expansion to a combined forecast brings in extra information from a second calculation done at a later time, it is available only an hour or two after the basic combined forecast.

In addition to the full geographical window, there are also four zoomed windows in this section that contain the basic combined forecast. They are for the Atlantic, Pacific, Arctic and Prairies regions.

*3. Other Experimental Automated Fog and Stratus Forecasts*

This is a group of different component forecasts that are being tested. They are *not* integrated into the combined forecast of section 2. They are briefly described below.

*4. Other Model Fields Potentially Useful in F/ST Forecasting*

These charts do not contain F/ST forecasts. Rather, they are ancillary charts of GEM regional model variables that have potential use in the forecasting of F and ST. The following information is included:

*a. T at Level eta = 1.0*

This is the hourly GEM regional temperature at the model diagnostic screen level eta = 1.

*b. Snow Depth and 50% Ice Cover Line*

These charts present in colour the snow depth (a dynamic variable that can change during the model run) and a blue line showing the analyzed 50% ice line (unchanging during the model run). Over the ocean or resolved lakes this line refers to 50% sea ice cover. Over the land, the blue line can be interpreted as showing where unresolved lakes have 50% ice cover. Assuming that there is usually a sharp gradient of ice between completely open water and completely ice-covered water, then one can roughly interpret the 50% line as follows: lakes/ocean north of the line are ice-covered, while those south of the line are ice-free.

*c. Precipitation Type*

These charts present the hourly forecast precipitation type using a combination of the Bourgouin area method and the Baumgardt top-down method (as seen in COMET). This approach differs in that it analyzes multiple above-freezing layers and below-freezing layers aloft and generates a precipitation type in those layers. It also applies rules to GEM regional model output to forecast drizzle, freezing drizzle, and snow grains. These charts can be found at http://hal-bobk.edm.ab.ec.gc.ca/HAL_Winter/Winter_Fields/Winter_Fields.html.

*d. Hourly Precipitation Amounts*

These charts present the hourly accumulated total precipitation amounts, in mm of water equivalent directly from GEM regional.

*e. Hourly Dubé Solid Precipitation Amounts*

These charts present the hourly accumulated solid precipitation amounts, in cm, as calculated by the Dubé (2003) method from GEM regional forecast data.

The F/ST forecast charts are designed to forecast areas in which **dense fog (visibility <= ½ SM)** and **low stratus (ceiling <= 500 feet)** are probable, or in which either is possible. Many different rules are applied to GEM regional output to determine the forecast areas of fog and stratus. These rules will be outlined very briefly in the sections below. A combined forecast chart is also produced. The charts are available hourly for P01 through P48. At the time of writing (November 2009) these forecasts have an experimental status. This means that they are

not supported 24/7, and are subject to further development. However, it is expected that the system as described here will not change much in the future.

#### 9.2.6.2 GEM Regional Model Variables Used in the Rules-Based Forecasts

A wide variety of GEM regional model variables are use in the rules. Some are from the model's free atmospheric levels (the second eta level and above), some are from the model's diagnostic level eta = 1 and others are from the model's land surface package known as ISBA. The model diagnostic level eta = 1 corresponds to about 1.5m above the model surface ("screen" level) while the first free atmospheric level, eta = 0.995, corresponds to a level of about 40m.

#### 9.2.6.3 Background thresholds for the Rules-Based Forecasts

Basic rules that apply to all the fog types are summarized below.

*Vertical Gradient of Humidity*

If the model specific humidity decreases from eta level (.995) to eta level (.985) then no fog is forecast.

*Amount of Humidity*

This is a criterion for the actual amount of humidity. If the specific humidity at eta level (.995) is below 0.004 kg/kg, then no fog is forecast. This value of specific humidity would typically correspond to a surface dew point of -30$^{o}$C based on a standard atmosphere.

*Presence of Snow at Certain Temperatures*

It is well-known that in the absence of increasing moisture through moisture advection, fogs do not readily form over melting snow when the air temperature is much above freezing, and also that when the temperature of the snow is much below freezing, it becomes very difficult for fogs to develop. See section 4.3.10 of this document for a brief explanation.

In the forecast rules, the surface is considered to be snow-covered if the GEM regional model snow depth SD is >= 3 cm. Otherwise the rules consider that no snow is present. In the absence of moisture advection, the rules specify no fog if model temperature (eta = 1) < -10°C or model temperature (eta = 1) > +5°C. Otherwise fog is possible. However, if the model moisture is increasing fast enough in time or in space, then fog is possible even in those temperature ranges.

*Fog/Stratus Differentiation*

Basic procedure:

Baker et al. (2002) state that "the real requirement for radiation fog is not lack of *wind*, per se, but lack of *turbulence*, which can result from various combinations of stability and boundary layer wind speeds." They use this idea to include a method to differentiate between fog and low stratus, using values of what they termed a "modified Richardson number MRi." This number is identical to the stability ratio SR presented by Munn (1966, p 82). According to Baker et al, If the MRi <=0.025, then the situation is "mixy" and the turbulently-mixed boundary layer favours ST over F (if saturation occurs). If MRi >= 0.040, then the low level winds are decoupled from the winds aloft and the unmixed boundary layer supports cooling and favours F rather than ST. The intermediate values are marginal for fog. Toth and Burrows (developers of the F/ST displays) found that the GEM regional bulk Richardson number RB is almost exactly 10 times the MRi. Their rules drop the "intermediate" category: in the first pass, over solid surfaces, if low level saturation occurs, then RB ≤ 0.25 results in stratus, and RB > 0.25 results in fog.

However, Baker et al. also note that in some situations the thresholds must be lowered: "MRi thresholds must be adjusted downward for situations where significant surface airflow is needed to force boundary layer cooling (e.g. advection and upslope fogs). For the relatively common radiation/advection hybrid fog near coastlines with onshore flow, MRi = 0.015 is the threshold for 'mixy'."

With this in mind, the development of the rules-based system over marine areas included sensitivity tests using various values of the threshold RB value to differentiate between F and ST. Subjective evaluations led to the conclusion that an RB threshold of 0.10 over marine areas rather than 0.25 gave the best results. One other modification relates to the vertical motion in the lowest layers of the atmosphere. If the model forecasts downslope flow and enough subsidence then RB is not relevant because no F or ST is forecast. If there is upslope flow and with enough ascent then if conditions are stable, F is forecast independently of the threshold RB value, while if conditions are unstable, convection is assumed and no F/ST is forecast.

Final Calculations*:* In verifying the results of the basic procedure that gave a yes-no F/ST forecast, it was realized that there would inevitably be some F observations in the forecast ST area, and some ST observations in the forecast F area. In other words, there is an element of uncertainty. To better address this fact, as mentioned above, a final version of the F/ST forecast chart is produced by examining the bulk Richardson number at each "intermediate" F/ST point. If it is large enough, F is the most probable outcome (yellow in the chart). Otherwise is a point

(tan colour) where F or ST are possible. Brown areas are those where ST is most probable. See Figure 9-6 for a sample chart.

*Onshore/Offshore Flow*

If there is offshore (onshore) flow over the model coastlines then the solid surface rules (marine rules) apply along the coast.

*Skin Temperature of Solid Surfaces*

Baker et al. (2002) mention that if there is saturation and F or ST is expected, then F is more likely if the skin temperature is relatively cold, and ST is more likely if the skin temperature is relatively warm. The GEM regional skin temperature over ground and over sea ice (variables I0 and I7) is used to make these modifications through a comparison with the crossover temperature described in the UPS fog section below.

#### 9.2.6.4 Rules for each Basic Fog Category (Those that Contribute to the Rules-Based Combined Forecast)

*UPS Fog*

The UPS (United Parcel Service) Fog technique was developed by Baker et al. (2002). It is designed to forecast radiation fog or combined radiation/advection fog and is applied over solid surfaces (not open water). It assumes that at the warmest time of day (generally around mid-afternoon) the lowest levels of the boundary layer are well mixed and the surface dewpoint temperature is representative of the average dewpoint through that mixed layer. This surface dewpoint at the warmest time of day is known as the crossover temperature Tx. The technique states that if the air temperature cools to below Tx then the air is saturated and fog is likely, assuming no significant moisture advection. Baker et al. also present a rule to differentiate between fog and stratus.

Baker et al. obtained their crossover temperatures from actual observations. The rules-based system uses only GEM regional model data, so takes its value of Tx directly from the model: Tx over any solid surface gridpoint is the minimum model Td at eta=0.995 during the warmest daytime hours.

After obtaining this value of Tx, certain modifications to it are applied, as follows:

1. Increase Tx for available moisture from the portion of resolved or unresolved lakes in the tile around the grid point;
2. Increase Tx if enough liquid precipitation has fallen during the past 6 hours (calculate the model liquid precipitation in the last 6 hours);

3. Increase Tx for upslope flow (cooling is caused by the vertical motion, so the crossover temperature doesn't have to be as low as it would otherwise to get fog);
4. Account for a change in airmass

The UPS technique implicitly assumes that there is no change in airmass at a given point between the time of minimum Td during the afternoon mixing period and the time of the forecast. We attempt to account for any change in airmass by examining the change in theta-w at eta=0.995 between the moment of minimum Td and at the valid time of the forecast.

If the theta-w decreases (e.g. a cold front passed by) then we want to reduce the crossover temperature (i.e. harder to get saturation and therefore more difficult to get fog). If theta-w increases (e.g. a warm frontal passage) then we want to increase the crossover temperature (easier to get fog).

Baker et al. (2002) noted that if the temperature descends to below 3 degrees F colder than the crossover temperature, then fog with a visibility of ½ mile or less (or stratus depending on the Richardson number criterion) can be expected. In the rules-based system, saturation is expected and F/ST are possible if the model temperature at eta level 1.0 descends to below Tx.

The UPS scheme is then summarized as follows. For each solid surface gridpoint:

1. Calculate the final crossover temperature Txf;
2. If a forecast model temperature at some time is less than Txf, then that point is determined to be saturated at that time;
3. For each saturated point, apply the Bulk Richardson number criterion and any modifications as described above to determine whether the UPS forecast is for F or ST;
4. If model rain rate at that time and point is >= 2mm/hr, and if the forecast from step 3 is for ST, then change the forecast to F (the ST builds down to F at the surface due to the rain);
5. If the model solid precipitation rate at that time and point is >= 2 mm/hr water equivalent, and if the forecast from step 3 is for F, then change the forecast to ST (the snow will "sweep out" some of the fog and improve the visibility, but that there still would be a low ST ceiling).
6. Make the adjustment for particularly cold or warm skin temperatures as compared to the crossover temperature.

NOTE: The UPS fog forecast and the marine fog forecast described in the next section are presented in one single forecast chart. This is possible since the UPS F/ST forecast is valid only over solid surfaces, while the marine F/ST forecast is valid only over water bodies.

*Marine Fog*

The marine fog rules apply only over water bodies, where the model SST is available. The rules are relatively simple, and finally boil down to the very basic "moist air over cold water." If "moist enough" air is over "cold enough" water, then dense fog or low stratus are possible.

*Advection Fog over Solid Surfaces*

Like the marine fog, this is also an approximate case of moist enough air over a cold enough surface which also has a certain amount of surface moisture. The atmospheric moisture comes from the model dewpoint at level eta = 1. The surface temperature is the model's skin temperature from the land surface scheme. The surface moisture also comes from the land surface scheme.

After the basic calculations are finished, then a further test is applied to account for cases in which the skin is particularly warm (or particularly cold) with respect to the crossover temperature. This is the same modification that is applied to the results of the UPS F/ST calculation. A particularly cold surface makes fog more likely, while a particularly warm surface makes stratus more likely. It should be noted that the suite of F/ST products do not account for direct advection of fog from sea to land.

*Radiation Fog*

Despite the fact that the UPS technique is designed for radiation (and the hybrid radiation-advection) fog forecasting, it was found that it can miss some cases of pure radiation fog, so a separate radiation fog rule set was formulated. If the model has enough outgoing long wave radiation from the surface combined with enough condensation at the surface combined with enough moisture from the skin, then fog or stratus are forecast.

*Ice Edge Fog*

This is a simple advection rule for the case where the wind is blowing a moist enough air mass onto an ice-covered area (defined as 50% coverage or greater). If the dew point at eta = 1 is greater than the sea ice temperature, then fog or stratus can occur.

*Cold Frontal ST*

Low stratus can occur under a cold frontal inversion with northwesterly winds if enough rain is falling. We attempt to define the areas behind cold fronts through the calculation of temperature advection and humidity advection at level eta = 0.995. If there is enough cooling or enough drying, then we assume that the grid point is behind a cold front. In that case, if the

model rain in the last 6 hours is 5 mm or greater, then ST is forecast. None of the background rules apply, since this is a “top-down” occurrence rather than a “ground-up” occurrence.

*Visibility Calculated Directly from Model RH*

These charts present the visibility calculated directly as a function of model RH (with respect to water at temperatures above -8°C, and with respect to ice at temperatures below -8°C) at model level eta=0.995 according to the formula Vis = -0.0177RH**2 + 1.462RH + 30 (Vis in km, RH in %) or Vis=f(RHw) from Gultepe et al. (2009). The “VISR raw” charts on the web page contain the result of this calculation with the visibility in km. The "VISR component" charts contain the contribution of the VISR calculation to the combined F/ST forecast. Over solid surfaces any forecast of 2 SM (3.2 km) or less is included in the combined charts. Over open water, any forecast of ½ SM (0.8 km) or less is included in the combined charts.

*Inversion Fog*

This calculation essentially searches for low-level temperature inversions that are strong enough and have enough humidity beneath them. Points that meet these criteria will have F or ST. Furthermore, if enough rain is falling then the forecast stratus can be lowered to fog. A moist layer depth is calculated, and the mean RH in the layer is calculated. Fog or stratus are forecast if the mean RH in the moist layer is greater than a certain threshold. Moisture flux convergence in the moist layer is also calculated. If the convergence is positive, then the threshold is lowered, making it easier to get fog or stratus.

#### 9.2.6.5 Rules for ST Lowering to F

In the presence of an inversion, stratus can lower to fog. This can happen if there is no rain when there is enough long wave radiative cooling. Falling rain can also make this happen, and rules for stratus lowering to fog are applied in the presence of an inversion for the case of either light rain (up to 1 mm/hr) or moderate to heavy rain (1 mm/hr or more). Some of the basic ideas for these rules come from the work of Peak and Tag (1989) and of Rogers (1998).

*Near-Surface Saturated Layers*

Low ST or F can occur in the real atmosphere as a result of a very thin saturated layer very close to the surface. The model tends to smooth out such conditions and to be too dry in such layers. This chart attempts to identify such situations through an examination of the forecast vertical profiles in the lowest model levels.

#### 9.2.6.6 Other Experimental Rules Being Tested

The third section of the HAL F/ST forecast web page contains forecasts made from other rule sets that are being tested. As of November 2009, there are five such rule sets for the following categories.

*"Cold" F/ST Potential Areas*

This chart contains the results of two separate calculations, described in the two following subsections.

*Anthropogenic Ice Fog*

These areas, shaded in green or red, are areas in which anthropogenic ice fog at very cold temperatures might be possible if there are adequate sources of humidity and/or ice nuclei. The forecaster will have to evaluate whether or not this is the case. The definition of these areas is as follows: for northern regions where the communities are very small (N of 57N by our definition) the chart indicates areas where the model forecasts T ≤ -41°C and wind speed ≤ 3 kt (at eta level = 1) (red areas). For areas south of 57N where the communities are larger, the T threshold is not as cold: -35°C rather than -41°C (green areas).

*Naturally-occurring Ice Crystal Fog*

These areas, in tan shading, are areas in which the model forecasts T(eta = 1) <= -10°C AND QC(eta = 0.995) > 0.05 g/kg. (NOTE QC is the model cloud water content, both liquid+solid water, assumed to be mostly ice at T < -10°C).

*VSN1*

These charts present the visibility calculated as a function of both model liquid water content (obtained from the model total cloud water) and $N_d$ (number density of cloud particles) where $N_d$ is calculated as a function of model temperature (see equation 9 of Gultepe et al. 2006a]). It would be better to have $N_d$ as a model variable, but this is not available in the GEM regional.

*VSN2*

These charts are similar to VSN1, except that $N_d$ is simply fixed at 80 $cm^{-3}$ over open water and 200 $cm^{-3}$ over solid surfaces. This is done because there is much uncertainty in the calculation of $N_d$ as a function of temperature in the VSN1 calculation. However, it turns out that the two forecasts of visibility are similar overall.

*QC2*

The GEM regional cloud water at level eta = 0.995 can be used as a proxy for visibility (e.g., in the Kunkel (1984) parameterization, a value of 0.016 g/kg corresponds approximately to a visibility of 1 km). Teixeira (1999) used the value of 0.016 from the ECMWF model to create a model climatology of fog. In these experimental charts the GEM regional QC2 is displayed and the brown areas are those for which QC2 >=0.016. Subjectively, these areas are overdone in cold Arctic airmasses.

#### 9.2.6.7 The Augmented F/ST Forecast Chart

Through verifications of various situations, Toth and Burrows found that low ST ceilings (sometimes obscured ceilings but often with a reported cloud base) can often occur in the presence of falling snow, drizzle or freezing drizzle. The basic rule set did not account for this possibility. Therefore, the basic combined forecast chart is "augmented" by precipitation information in a separate calculation that runs a couple of hours after the basic combined chart becomes available. In the augmented chart, several contours (0.30, 0.50, 0.75 and 2.0 cm) of Dubé frozen precipitation hourly accumulations diagnosed from GEM regional model data are added to the basic F/ST forecast data. It has been found that low ST ceilings can occur with hourly amounts of as little as 0.30 cm. It has been similarly found that low ST ceilings can occur in the presence of drizzle or freezing drizzle. The augmented charts therefore include orange contours that identify diagnosed drizzle areas. The diagnosis is done using the Burrows technique (HAL internal project, unpublished as of November, 2009) for any hour in which at least 0.05 mm water equivalent of precipitation is forecast to fall by the GEM regional model.

An example of an augmented combined F/ST forecast chart is found in Figure 9-7. It corresponds to the combined forecast presented in Figure 9-6.

The user must remember that the augmented chart is available only a couple of hours after the basic combined chart.

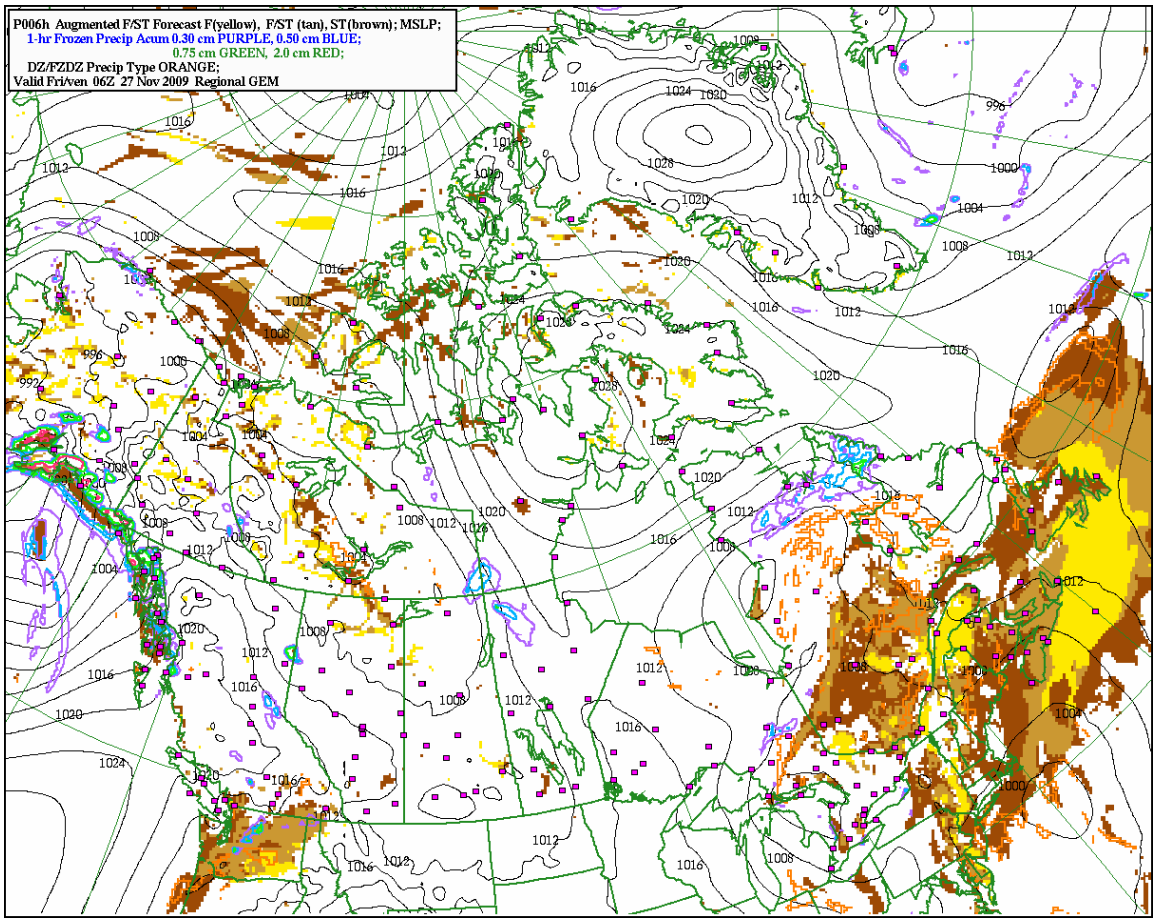


**Figure 9-7** Sample of augmented combined F/ST forecast in the national window (Toth/Burrows rules-based forecast based on GEM regional output). Fog most probable areas are in yellow. Stratus most probable areas are in brown. In the tan areas either F or ST is possible. Dubé (2003) diagnosed hourly solid precipitation amounts are in purple, blue, green or red contours (see the legend for values) and Burrows-diagnosed areas of drizzle or freezing drizzle are in orange contours. See Figure 9-6 for the corresponding combined forecast chart (without the precipitation contours).

### 9.2.6.8 Performance of the Rules-Based System: Subjective Evaluation Results

The developers of the System have conducted ongoing evaluation of the forecasts as part of the development process. There have also been some comments on the combined charts from operational forecasters, mostly in Edmonton (the HAL is co-located with the forecast offices) but also from Vancouver and Montreal. An operational evaluation of various fog forecasting techniques, including the combined charts of the rules-based system, was carried out in the Atlantic region during the summer 2008 east coast fog season. The information in this section has been synthesized from all these sources.

Experience with the Toth/Burrows automated F/ST forecasts has shown that the system does have some forecasting skill. Here are a few comments on the performance of the system:

1. The system attempts to forecast where fog (visibility ½ mile or less) and low stratus (ceiling 500 feet or less) are probable. A third category present areas where either is possible. The development of the system has been completely subjective, so no numbers are available (yet) to define what "probable" means. An extension of the project (possibly in 2010) will verify the forecasts at a set of manned observing stations to verify the performance of the system at those stations. However, as mentioned above, subjective examination of many cases shows that the system does have a certain level of forecast skill in many situations.
2. The differentiation between fog and stratus is based on the Richardson number criterion as originally presented by Baker et al. (2002) and as modified by Toth and Burrows as described above. No formal verification of these rules has been carried out. Subjective verification indicates some skill in the chart using the following interpretations of the forecast areas: brown (ST most probable); yellow (F most probable); and tan (F or ST possible). See Figure 9-6 for an example of the forecast chart.
3. The performance of the system over the Atlantic ocean was felt to be reasonable by the Atlantic region forecasters who participated in the evaluation of the system in the summer of 2008. As mentioned above, they felt that "the techniques worked quite well over water." However it was noted that in coastal areas the system had a tendency to bring fog in from the water to the land too slowly, and then to forecast it to recede from the land back out to the sea too quickly. A few forecasters in Vancouver have made the same general comments about reasonable performance of the system over the waters of the Pacific. One could speculate that a similar problem to the one outlined above for Atlantic coastal areas also exists over Pacific coastal areas. Another important performance note is that the system is dependent on the GEM regional model topography and land-sea mask. This means that detailed topographical features are not resolved, so that the system does not correctly handle the details of fog and stratus that depend on detailed coastal topography of both the east and west coasts.
4. Two research ships (the Healy and the Polarstern) sent weather observations from the Arctic ocean in the summer of 2008. The Healy also supplied hourly webcam images available on the web. Examination of some of those images and weather reports indicated that the fog and stratus were highly variable in space and time. The tentative conclusion was that the fog/stratus forecast system does not perform as well over the

open water of the Arctic ocean as it does over the Atlantic and Pacific oceans. The broad outline of the forecasts was often good, but the details were often incorrect. A more detailed verification of the F/ST forecasts over the Arctic ocean in the summer of 2009 was commenced in the fall of 2009. It is ongoing. Initial tentative results indicate that F/ST are common in the Arctic pack ice. The system seems to have more skill over the pack ice areas of the Arctic ocean than over the open water areas. This work will continue, and it is hoped to have some numerical results some time in 2010.

5. A similar comment applies to the performance of the system in complex mountainous terrain. It has been noted, for example, that the system has more problems in the sharp narrow valleys of BC than in the wider valleys. Furthermore, the system can forecast relatively large areas of fog and stratus along the ridges of the higher terrain. This can be interpreted as clouds covering the upper mountain levels, and these forecasts can spill over into adjacent valley areas where fog and stratus are in fact not observed.
6. Cases of pure radiation fog were at times missed in the summer of 2009. A modified set of rules was then implemented which seemed to improve things in a few test cases. Other changes were made as the summer progressed. Slow progress is being made in this area.
7. The UPS fog routine can occasionally forecast a sudden significant expansion of a fog/stratus area from one hour to the next. A subjective look at some of these cases indicates that they are cases in which the forecast system has been too slow to forecast fog or stratus. In such cases, it seems that the UPS fog routine is attempting to "catch up" with what should have been forecast in the last few forecast hours.
8. It has been noted that the GEM regional model can be too dry at the very lowest model levels in the case of a marked low level inversion, and that the inversion itself can be too weak. This impacts the forecast rules for inversion fog which use both the strength of the inversion and the humidity in the inversion. One example of this is in very moist maritime-tropical airmasses that can arrive in the area of the Great Lakes from the south. The fog/stratus forecast system tends to underestimate the area covered by fog or stratus in this situation. The same type of problem can occur in the cold season. For example, in the fall a subsidence inversion can get set up over the West. In such cases the model can again be too dry with too weak an inversion in the lowest model layers. The result can be an underforecasting of the fog/stratus areas in these situations. If a weak surface trough is also forecast to be present, then it is more likely that the system is underforecasting the fog/stratus areas.

9. In the winter there can be openings and leads in the Arctic ice which supply local moisture that can support fog or stratus. The model generally does not know about these leads, and so has no chance of forecasting the associated fog and stratus.
10. As a general rule, it seems that "cold" fog and stratus, composed of ice crystals, are harder to forecast than "warm" fog and stratus, compose of water droplets (supercooled or otherwise). In general, then, the performance of the system is probably weaker in cold airmasses than in warm airmasses. For anthropogenic ice fog at very cold temperatures, one experimental chart included in the F/ST forecast page http://halmetmodel1.edm.ab.ec.gc.ca/F+ST/F+ST.html does forecast areas where there is the potential for anthropogenic ice fog, given enough local input of moisture and/or ice nuclei. The forecaster must examine this chart separately, since it is not integrated into the overall combined forecast chart.
11. The basic system was not designed to forecast low obscured ceilings or low stratus ceilings in falling snow. This problem was noticed with the arrival of the cold season in the fall of 2008. This can happen in organized systems in which snow is falling, or in snow squalls or lake effect snow. It was found that certain hourly accumulations of snow from the Dubé (2003) technique are a reasonable indication of such low ceilings in snow. This change has been added to a new chart labelled on the F/ST forecast page as "Combined F/ST plus Potential Areas of Low ST or Obscured Ceilings due to Precipitation." The additions to this chart go a long way to solving the weakness of the basic system in snow.
12. It can happen that rain falling into the atmosphere behind a cold front can cause conditions to be humid enough that low stratus ceilings can form. Rules that attempt to treat this situation have been implemented, but the system still seems to underestimate the stratus in this type of situation.
13. It was noticed that the original system would dissipate F/ST too fast in the morning, particularly in cases of dense and widespread F/ST. Extra rules to extend the forecast in these cases have been implemented, and have had a positive effect.

#### 9.2.6.9 Performance of the Rules-Based System: Objective Evaluation Results

At the time of writing of this document (November 2009), no objective evaluation results are available. The next phase of the project will be to obtain such results, by interpolating the forecasts to the locations of a set of Canadian observing stations and then comparing the forecasts with the observations. Some results might be available in 2010.

### 9.2.7 Fog "shootout" evaluation – Atlantic Canada (summer 2008)

*Overview:* During the summer of 2008 forecasters and research meteorologists at the Atlantic Storm Prediction Centre (ASPC), Newfoundland and Labrador Weather Office (NLWO) and the National Lab for Coastal and Marine Meteorology (hereafter "National Lab") participated in the FRAM Project. A summary of the overall objectives of this project were to:

1. Improve description of fog environments across Canada (marine focus for the Atlantic Region)
2. Develop microphysical parameterizations for model applications (particularly the GEM-Limited Area Model, GEM-LAM)
3. Develop remote sensing methods for fog detection (nowcasting)
4. Further our capabilities related to ground-based fog-measuring instrumentation
5. Integrate observations with model output to predict and detect fog areas and particle phase.

A number of observing and numerical prediction products were developed by members of the FRAM group. These products included:

1. GOES Satellite Detection: (Ismail Gultepe) combining GEM model output with satellite channel differencing to highlight areas with fog.
2. GEM-LAM (Jason Milbrandt) new microphysical scheme: with direct outputs of cloud liquid water content and visibility.
3. Conditional fog and ceiling climatology (Bjarne Hansen): including conditional probabilities and an air parcel back trajectory climatology.
4. Post processing rules-based approach (Gary Toth & Bill Burrows): combining GEM regional model outputs with post processing rules to forecast areas of fog / stratus.

The focus of the evaluation by forecasters was to:

1. Determine the usefulness of the techniques to operational forecasting
2. Provide feedback to the developers for possible improvements
3. Provide evidence/advice for possible implementation of techniques into forecast operations

A complete summary of that evaluation can be found at http://wiki.whxlab.dart.ns.ec.gc.ca/WHXLabWiki/FOG_Shootout_2008

*Summary:*

A forecaster evaluation of the Toth/Burrows fog product was done in the ASPC in the summers of 2008 and 2009. Generally, the techniques worked quite well over water for marine fog studies, but certainly had limitations over land in 2008 (the scheme did not handle the

advection of fog from the sea to land). The techniques were not reliable enough to use as predictors for the retreat of fog to the coast during the warm season. In 2009 some improvements were made in this regard.

The GEM-LAM moisture/visibility diagnostics at the lowest computational level, used during the 2008 evaluation of the model, were generally not helpful for forecasting. Most likely, this was due primarily to the limited vertical resolution in the boundary layer, which is typical for operational NWP models. As seen in section 8, however, there may be useful information regarding low-level moisture at slightly higher levels. To adapt to this realization, the evaluation had to be conducted again (during the summer of 2009) using moisture and derived fields from other levels in the boundary layer, not just the lowest computational level. It is clear that model based fog prediction is the ability of the model to treat boundary layer processes. In this respect, model and observation comparisons are in progress and being published (Yang et al. 2009 and Gultepe et al. 2009).

Satellite based fog forecasting can work accurately when high level clouds are not present. However, this is usually not the case. This may result in large uncertainties in the use of satellite-based schemes (Gultepe et al. 2007b). One particular advantage of the Gultepe product was its ability to identify nocturnal fog in the absence of mid- and upper-level cloud when conventional near-infrared imagery would be difficult to analyse.

Conditional climatology and back-trajectory products have been generated and more time is needed to effectively evaluate these products. The output is more probabilistic in nature and takes into account climatological conditions, which is an attractive attribute to any forecast product. Climatology of fog events at various locations can lead to better understanding of fog forecasting. Details on fog climatology are given by Hansen et al. (2007 and 2009) and can also be found on their supplementary websites.

Complex processes at various time and space scales play an important role for improved understanding of fog events and more work in this area is needed. One approach to solve this issue is to integrate the model based data with observations such as done in Gultepe et al. (2007b) and perform more objective analysis.

### 9.2.8 Fog “shootout” evaluation – Atlantic Canada (summer 2009)

An evaluation of the F/ST system was carried out in 2009, similar to the 2008 evaluation. Results can be found at
http://wiki.whxlab.dart.ns.ec.gc.ca/WHXLabWiki/FOG_Shootout_2009.

# Appendix A: Web-based resources for fog and stratus forecasting

All websites referred to in the text of this document are listed as follows.

Climate Manager Percent Occurrence, Percent Occurrence of Ceilings and Visibilities, http://dv-eg.edm.ab.ec.gc.ca/~rowsonr/percent.html

COMET Met Ed website, http://www.meted.ucar.edu

Fog & Stratus Forecasting (Daryl Pereira), http://dv-eg.edm.ab.ec.gc.ca/~pereirad/method_fcsting_fogst_files/frame.htm

Fog (glossary definition), Arctic Climatology and Meteorology, National Snow and Ice Data Center, http://nsidc.org/arcticmet/glossary/fog.html

Fog Forecasting: tips, tricks, techniques, by Dave Carlsen, http://pnrinternal.pnr.ec.gc.ca/pspc/fog/fogpage.html

Fog Material, Prairie and Arctic Storm Prediction Centre/Canadian Meteorological Aviation Centre, http://pnrinternal.pnr.ec.gc.ca/paawc/public/wxelement/fog

Fog occurrence related to temperature, http://arxt39.cmc.ec.gc.ca/~armabha/clim/temp_dirn

FogDex: A Radiation Fog Formation Index, http://dv-eg.edm.ab.ec.gc.ca/~suttonl/fogdex_main.html

HAL Experimental Fog Forecasting Products, http://halmetmodel1.edm.ab.ec.gc.ca/F+ST/F+ST.html

HAL Winter Weather Experimental Model Fields, http://hal-bobk.edm.ab.ec.gc.ca/HAL_Winter/Winter_Fields/Winter_Fields.html

JANUARY 17, Halifax Harbor -18c with sea smoke, http://www.pendergast.ca/jan17

Marine observation maps of Eastern Canada, http://chinook.edm.ab.ec.gc.ca/~gilesa/eastfog.html

Nighttime Fog and Low Cloud Images, From GOES and NOAA Polar Satellites, http://www.star.nesdis.noaa.gov/smcd/opdb/aviation/fog.html

Operational analysis and forecast system / Système opérationnel d'analyse et de prevision, http://www.msc.ec.gc.ca/cmc/op_systems

Picture of radiation fog, http://www.photolib.noaa.gov/bigs/wea02054.jpg

Site reference, Prairie and Arctic Storm Prediction Centre/Canadian Meteorological Aviation Centre, http://pnrinternal.pnr.ec.gc.ca/CMAC-West/site_reference

Stratus and fog maps, Hydrometeorology and Arctic Lab, http://chinook.edm.ab.ec.gc.ca/~gilesa/STFOGmaps.html

Transportation Safety Board of Canada - AVIATION REPORTS,
http://www.tsb.gc.ca/en/reports/air

UPS fog product (Merv Jamieson), http://dv-eg.edm.ab.ec.gc.ca/~jamiesonm/fog

USCG Icebreaker Healy, webcam archive,
http://mgds.ldeo.columbia.edu/healy/reports/aloftcon/2008

Webcam collections,
Alberta: http://chinook.edm.ab.ec.gc.ca/~gilesa/ama-cam.html
British Colombia: http://chinook.edm.ab.ec.gc.ca/~gilesa/bc-cam.html
East Coast: http://www.stormpost.com/cams_nl.pl

Whitehorse, Ice fog study, http://pnrinternal.pnr.ec.gc.ca/paawc/aviation/BC_ref/IceFog.htm

WHXLab Wiki for Fog Remote Sensing and Modelling (FRAM) Project,
http://wiki.whxlab.dart.ns.ec.gc.ca/WHXLabWiki/FOG_Shootout_2008

http://wiki.whxlab.dart.ns.ec.gc.ca/WHXLabWiki/FOG_Shootout_2009

# References


Aratus, 1921: Aratus*;* In W. Heinemann (Ed.): *Callimachus and Lycrophon,* London, and Harvard University Press, Cambridge, Mass. 644 p.

Aristotle, 1952: Meteorologica / with an English translation by J. D. P. Lee; In W. Heinemann (Ed.), *Loeb classical library*. Cambridge, Harvard University Press.

Azevedo, A., and D. L. Morgan, 1974: Fog Precipitation in Coastal California Forests. *Ecology*, **55**, 1135–1141.

Baker, R., J. Cramer, and J. Peters, 2002: Radiation fog: UPS Airlines conceptual models and forecast methods. 10th Conference on Aviation, Range, and Aerospace Meteorology.

Bélair, S., R. Brown, J. Mailhot, B. Bilodeau, and L.P. Crevier, 2003: Operational Implementation of the ISBA Land Surface Scheme in the Canadian Regional Weather Forecast Model. Part II: Cold Season Results. *J. Hydrometeor.*, **4**, 371–386.

Bendix, J., B. Thies, T. Nauss, and J. Cermak, 2006: A feasibility study of daytime fog and low stratus detection with TERRA/AQUA-MODIS over land. *Meteorological Applications*, **13**, 111–125.

Benjamin, S. G., D. Dévényi, S. S. Weygandt, K. J. Brundage, J. M. Brown, G. A. Grell, D. Kim, B. E. Schwartz, T. G. Smirnova, T. L. Smith, and G. S. Manikin, 2004: An hourly assimilation–forecast Cycle: The RUC. *Mon. Wea. Rev.,* **132**, 495–518.

Bergot, T. and D. Guédalia, 1994: Numerical forecasting of radiation fog. Part I: Numerical model and sensitivity tests*. Mon. Wea. Review*, **122**, 1218–1230.

Bergot, T., D. Carrer, J. Noilhan, and P. Bougeault, 2005: Improved site-specific numerical prediction of fog and low clouds: a feasibility study. *Wea. Forecasting*, **20**, 627–646.

Bissonette, L. R., 1992, Imaging through fog and rain. *Opt. Eng.*, **31**, 1045–1052.

Bonancina, L. C. W., 1925: Notes on the Fog of January 10th-12th, 1925. *Meteor. Mag.*, **60**, 7–8.

Bott, A. and T. Trautmann, 2002: PAFOG: A new efficient forecast model of radiation fog and low level stratiform clouds. *Atmos. Res.,* **64**, 191–203.

Bott, A., 1991: On the influence of the physico-chemical properties of aerosols on the life cycle of radiation fogs. *Bound.-Layer Meteor.*, **56**, 1–31.

Bowling, S. A., T. Ohtake, and C. S. Benson, 1968: Winter Pressure systems and ice fog in Fairbanks, Alaska. *J. Appl. Meteor.*, *7*, 961–968.

Byers, H. R., 1944. *General Meteorology*. New York, McGraw.

Byers, H. R., 1959. *General Meteorology*. McGraw-Hill, 481 p.

Capon, R., Y. Tang, P. Clark and R. Forbes, 2007: A 3D high resolution model for local fog prediction. NetFAM / COST722 Workshop on Cloudy Boundary Layer, Toulouse, France. Available online at http://netfam.fmi.fi/CBL07/capon.pdf.

Cermak, J. and J. Bendix, 2007: Dynamical nighttime fog/low stratus detection based on Meteosat SEVIRI data–a feasibility study. *Pure Appl. Geophys.*, **164**, 1179–1192

Charlton, R. and C. Park, 1984: Observations of Industrial Fog, Cloud and Precipitation on Very Cold Days. *Atmos.–Ocean*, **22**, 106–121.

Choularton, T. W., G. Fullarton, J. Latham, C. S. Mill, M. H. Smith, and I. M. Stromberg, 1981: A field study of radiation fog in Meppen, West Germany. *Quart. J. Roy. Meteor. Soc.*, **107**, 381–394.

Cober, S. G., G. A. Isaac, A. V. Korolev, and J. W. Strapp, 2001: Assessing Cloud-Phase Conditions. *J. Appl. Meteor.*, **40**, 1967–1983.

Côté, J., S. Gravel, A. Méthot, A. Patoine, M. Roch, and A. Staniforth, 1998: The operation CMC-MRB Global Environmental Multiscale (GEM) model. Part I: Design considerations and formulation. *Mon. Wea. Rev.*, **126**, 1373–1395.

Croft, P. J, 2003: Fog; in Encyclopedia of Atmospheric Sciences, J. R. Holton, J. A. Curry and J. A. Pyle Editors, Academic Press, pgs. 777–792. Available online at http://curry.eas.gatech.edu/Courses/6140/ency/Chapter8/Ency_Atmos/Fog.pdf.

Curry, J. A., O. Pinto, T. Benner and M. Tschudi, 1996: Evolution of the cloudy boundary layer during the autumnal freezing of the Beaufort Sea. *J. Geophys. Res.,* **102**, 13851–13860.

Dubé, I., 2003. From mm to cm: study of snow/liquid ratio over Quebec, Technical Note, Meteorological Service of Canada (Quebec Region), 127 p.

Duynkerke, P. G., 1991: Radiation fog: a comparison of model simulations with detailed observations. *Mon. Weather Rev.*, **119**, 324–341.

Ellrod G. P., 2002: Estimation of low cloud base heights at night from satellite infrared and surface temperature data. *Natl. Wea. Dig.*, **26**, 39–44, 1/2.

Ellrod, G. P. and I. Gultepe, 2007: Inferring low cloud base heights at night for aviation using satellite infrared and surface temperature data. *Pure Appl. Geophys.*, **164**, 1193–1205.

Ellrod, G. P., 1995: Advances in the detection and analysis of fog at night using GOES multispectral infrared im agery. *Wea. Forecasting*, **10**, 606-619.

Environment Canada, 2007: Tornadoes. Avialable online at http://www.mb.ec.gc.ca/air/summersevere/ae00s02.en.html.

Etkin, D. A. and A. Maarouf, 1995: An overview of atmospheric natural hazards in Canada. In: Proceedings of a Tri-lateral Workshop on Natural Hazards. Etkin, D. (ed.). Merrickville, Canada, pgs. 1-63 to 1-92.

Fuzzi, S., M. C. Facchini, G. Orsi, J. A. Lind, W. Wobrock, M. Kessel, R. Maser, W. Jaeschke, K. H. Enderle, B. G. Arends, A. Berner, A. Solly, C. Kruisz, G. Reischl, S. Pahl, U. Kaminski, P. Winkler, J. A. Ogren, K. J. Noone, A. Hallberg, H. Fierlinger-Oberlinninger, H. Puxbaum, A. Marzorati, H.-C. Hansson, A. Wiedensohler, I. B. Svenningsson, B. G. Martinsson, D. Schell, and H. W. Georgii, 1992: The Po Valley Fog Experiment 1989. An Overview. *Tellus 44B*, 448–468.

Fuzzi, S., P. Laj, L. Ricci, G. Orsi, J. Heintzenberg, M. Wendisch, B. Yuskiewicz, S. Mertes, D. Orsini, M. Schwanz, A. Wiedensohler, F. Stratmann, O. H. Berg, E. Swietlicki, G. Frank, B. G. Martinsson, A. Günther, J. P. Dierssen, D. Schell, W. Jaeschke, A. Berner, U. Dusek, S. Z. Galambo, C. Kruisz, N. S. Mesfin, W. Wobrock, B. Arends, and B. H. Ten, 1998: Overview of the Po Valley fog experiment 1994 (Chemdrop). *Contr. Atmos. Phys.*, **71**, 3–19.

Gazzi, M., V. Vincentini, and C. Pesci, 1997: Dependence of a black target's apparent luminance on fog droplet size distribution. *Atmos. Environ.*, **31**, 3441–3447.

Gazzi, M., T. Georgiadis, and V. Vincentini, 2001: Distant contrast measurements through fog and thick haze. *Atmos. Environ.*, **35**, 5143–5149.

Gadher, D. and T. Baird, cited 2007: Airport Dash as the Fog Lifts, The Sunday Times, Dec 24, 2006. Available online at http://www.timesonline.co.uk/tol/news/uk/article1264290.ece.

George, J. J., 1951: Fog; in Malone, T. F. (Ed.), *Compendium of Meteorology*. American Meteorological Society, 1334 p.

Georgii, W., 1920: Die Ursachen der Nebelbildung. *Annalen der Hydrographie und Maritimen Meteorologie*, **48**, 207-222.

Girard, E. and J.-P. Blanchet, 2001: Simulation of Arctic Diamond Dust, Ice Fog, and Thin Stratus Using an Explicit Aerosol–Cloud–Radiation Model. *J. Atmos. Sci.*, **58**, 1199-1221.

Glickman, T. S. (Ed.), 2000: *Glossary of Meteorology*. 2nd ed. Amer. Meteor. Soc., 855 p. Accompanying webpage available online at http://amsglossary.allenpress.com/glossary.

Gotaas, Y. and C. S. Benson, 1965, The effect of suspended ice crystals on radiative cooling. *J. Appl. Meteor*, **4**, 446-453.

Guédalia, D. and T. Bergot, 1994: Numerical forecasting of radiation fog. Part II: A comparision of model simulation with several observed fog events. *Mon. Wea. Review*, **122**, 1231–1246.

Gultepe, I., and Isaac, G. A., 1997: Relationship between liquid water content and temperature based on aircraft observations and its applicability to GCMs. *J. Climate*, **10**, 446–452.

Gultepe, I., Isaac, G.A., and Cober, S.G., 2001: Ice crystal number concentration versus temperature for climate studies. *Inter. J. of Climatology*, **21**, 1281–1302.

Gultepe, I., and G. Isaac, 2004: An analysis of cloud droplet number concentration (Nd) for climate studies: Emphasis on constant Nd. *Q. J. Royal Met. Soc.*, **130**, Part A, No. 602, 2377–2390.

Gultepe, I., M. D. Müller, and Z. Boybeyi, 2006a: A new warm fog parameterization scheme for numerical weather prediction models. *J. Appl. Meteor.*, **45**, 1469–1480.

Gultepe, I., S. G. Cober, P. King, G. Isaac, P. Taylor, P., and B. Hansen, 2006b: The Fog Remote Sensing and Modeling (FRAM) Field Project And Preliminary Results. AMS 12th Cloud Physics Conference, July 9-14, 2006, Madison, Wisconsin, USA, Print in CD, P4.3.

Gultepe, I., R. Tardif, S. C. Michaelides, J. Cermak, A. Bott, J. Bendix, M. D. Müller, M. Pagowski, B. Hansen, G. Ellrod, W. Jacobs, G. Toth, and S. G. Cober, 2007a: Fog Research: A Review of Past Achievements and Future Perspectives; in Gultepe, I. (Ed.): 2007a: Fog and Boundary Layer Clouds: Fog Visibility and Forecasting. Springer, 316 p.

Gultepe, I., M. Pawgoski., and J. Reid. 2007b: Using surface data to validate a satellite based fog detection scheme. *Wea. Forecasting*, **22**, 444–456.

Gultepe, I. and J. Milbrandt, 2007: Microphysical observations and mesoscale model simulation of a warm fog case during FRAM project, *Pure Appl. Geophys.*, 1161–1178.

Gultepe, I., P. Minnis, J. Milbrandt, S. G. Cober, L. Nguyen, C. Flynn, and B. Hansen, 2008: The fog remote sensing and modeling (FRAM) field project: Visibility analysis and remote sensing of fog. SPIE Remote Sensing Applications for aviation weather hazard detection support. Conference 7088-Proceedings of SPIE Vol. 7088. 13-14 August. 12 p.

Gultepe, I., G. Pearson, J. A. Milbrandt, B. Hansen, S. Platnick, P. Taylor, M. Gordon, J. P. Oakley, and S. G. Cober, 2009: The Fog Remote Sensing and Modeling Field Project. *Bull. Amer. Meteor. Soc.*, **90**, 341–359.

Gultepe I., and J. Milbrandt, 2010: Probabilistic parameterizations of visibility using observations of rain precipitation rate, relative humidity, and visibility. *J. Appl. Meteor. Climatology,* January issue, In Press.

Hansen, B., I. Gultepe, A. McCay, and A. Ling, 2009: Return periods of prolonged fog events in Canada, 43rd Congress of the Canadian Meteorological and Oceanographic Society, Halifax, NS, 1-4 June 2009. Available online at http://collaboration.cmc.ec.gc.ca/science/arma/duration_statistics.

Hansen, B., I. Gultepe, P. King, G. Toth, and C. Mooney, 2007: Visualization of seasonal-diurnal climatology of visibility in fog and precipitation at Canadian airport. AMS Annual Meeting, 16th Conference on Applied Climatology, San Antonio, Texas, 14-18 January 2007, In CD volume. Available online at http://collaboration.cmc.ec.gc.ca/science/arma/climatology.

Houghton, H. G. and W. H. Radford, 1938: On the local dissipation of warm fog. *Papers Phys. Ocean. Meteor.*, ***6***, No. 3, 63 p.

Hyvarinen, O., J. Julkunen, and V. Nietosvaara, 2007: Climatological tools for low visibility forecasting. *Pure Appl. Geophys.*, **164**, 1383–1396.

Jiusto, J. E., R. J. Pilie, W. C. and Kocmond, 1968: Fog Modification with Giant Hygroscopic Nuclei. *J. Appl. Meteor.*, **7**, 860–869.

Kain, J. S. and J. M. Fritsch, 1993: Convective parameterization for mesoscale models: The Kain-Fritsch scheme. The Representation of Cumulus Convection in Numerical Models. *Meteor. Monogr.*, No. 46, Amer. Meteor. Soc., 165–177.

Kloesel, K.A., 1992: A 70-year history of marine stratocumulus cloud field experiments off the coast of California. *Bull. Amer. Meteor. Soc.*, **73**, 1581–1585.

Köppen W., 1917: Landnebel und seenebel, Part II. *Annalen der Hydrographie und Maritimen Meteorologie*, *45(10)*, 401–405.

Köppen, W., 1916: Landnebel und seenebel, Part I. *Annalen der Hydrographie und Maritimen Meteorlogie*, *44(5)*, 233–257.

Koracin, D., J. Lewis, W. T. Thompson, C. E. Dorman, and J. A. Businger, 2001: Transition of Stratus into Fog along the California Coast: Observations and Modeling. *J. Atmos. Sci.*, **58**, 1714–1731.

Kornfeld, B. A. and B. A. Silverman, 1970: A comparison of the warm fog clearing capabilities of some hygroscopic materials. *J. App. Meteor.*, **9**, 634–638.

Kunkel, B. A., 1984: Parameterization of Droplet Terminal Velocity and Extinction Coefficient in Fog Models, *J. Climate Appl. Meteor.*, **23**, 34–41.

Leipper, D. F., 1994: Fog on the US west coast: A review. *Bull. Amer. Meteor. Soc.*, **75**, 229–240.

Lewis, J. M., D. Koracin and K. Redmond, 2004: Sea Fog Research in the United Kingdom and United States: A historical essay including outlook. *Bull. Amer. Meteor. Soc.*, **85**, 395–408.

Lindgrén, S., and J. Neumann, 1980: Great Historical Events That Were Significantly Affected by the Weather: 5, Some Meteorological Events of the Crimean War and Their Consequences. *Bull. Amer. Meteor. Soc.*, **61**, 1570–1583.

ManObs, 2006: Manual of Surface Weather Observations, Meteorological Service of Canada, Environment Canada. Available online at http://www.msc-smc.ec.gc.ca/msb/manuals_e.cfm.

McCay, A., 2000: The Christmas 1999 Fog and Stratus Episode. Available online at http://dv-eg.edm.ab.ec.gc.ca/~mccaya/stratus/fog_n_stratus.html.

Mensbrugghe, V., 1892: The formation of fog and of clouds; Translated from *Ciel et Terre*, Symons's Monthly Meteorological Magazine, **27**, 40–41.

MOIP, 2006: Meteorologists Operational Internship Program (MOIP) Training Module 3.1C on Fog Formation and Dissipation. MSC Internal Document. Available online at http://neige.wul.qc.ec.gc.ca/qww_domaf/TrainingWeb.

Meyer, M. B. and G. G. Lala, 1986: FOG-82: A cooperative field study of radiation fog. *Bull. Amer. Meteor. Soc.*, **65**, 825–832.

Milbrandt, J. A. and M. K. Yau, 2005: A multimoment bulk microphysics parameterization. Part II: A proposed three-moment closure and scheme description. *J. Atmos. Sci.*, **62**, 3065–3081.

Müller, M. D., C. Schmutz, and E. Parlow, 2007: A one-dimensional ensemble forecast and assimilation system for fog prediction, *Pure Appl. Geophys.*, **164**, 1241–1264.

Munn, 1966: *Descriptive Micrometeorology*. Academic Press, New York, San Francisco and London, 245 p.

Muraca, G., D. MacIver, N. Urquizo and H. Auld, 2001: The climatology of fog in Canada. Proceedings of the Second International Conference on Fog and Fog Collection, St. John's, Canada, 513–516.

NOAA [National Oceanic and Atmospheric Administration], 1995: Surface weather observations and reports, Federal Meteorological Handbook No. 1, 94 p. [Available from Department of Commerce, NOAA, Office of the Federal Coordinator for Meteorological Services and Supporting Research, 8455 Colesville Road, Suite 1500, Silver Spring, MD, 20910.

Nav Canada, 2002: Local Area Weather Manual. [Available online at http://navcanada.ca/NavCanada.asp?Language=en&Content=ContentDefinitionFiles\Publications\LAK\default.xml.]

Neumann, J., 1989: Forecasts of fine weather in the literature of classical antiquity. *Bull. Amer. Meteor. Soc.*, **70**, 46–48.

Noonkester, V. R., 1977: Marine fog investigation at San Diego during CEWCOM-1976. Naval Ocean Systems Center Tech. Rep. 172, 77 pp.

Oliver, D. A., W. S. Lewellen, and G. Williamson, 1978: The interaction between turbulent and radiative transport in the development of fog and low-level stratus. *J. Atmos. Sci.*, **35**, 301–316.

Pagowski, M., I. Gultepe and P. King, 2004: Analysis and Modeling of an Extremely Dense Fog Event in southern Ontario. *J. of Appl. Meteor*, **43**, 3–16.

Peak, J. E. and P. Tag, 1989: An expert system approach for prediction of maritime visibility obscuration. *Mon. Wea. Review*, **117**, 2641–2653.

Petterssen, S., 1956: *Weather Analysis and Forecasting.* Vol. 2. McGraw-Hill, 266 p.

Petterssen, S., 1969: *Introduction to Meteorology*. Third Edition, McGraw-Hill Publ. Inc., New York, 333 p.

Phillips, D., 1990: Fog…the thick of it. *The Climates of Canada*, Minister of Supply and Services Canada, pgs. 40–42.

Pilie, R. J., E. Mack, C. Rogers, U. Katz and W. Kocmond, 1979: The formation of marine fog and the development of fog-stratus systems along the California coast. *J. Appl. Meteor.*, **18**, 1275-1286.

Plank, V. G., A. A. Spatola, and J. R. Hicks, 1971: Summary Results of the Lewisburg Fog Clearing Program. *J. Appl. Meteor.*, **10**, 763–779.

Pliny, 1971: *Natural History*, Books XVII-XIX. English translation by H. Rackham, Harvard University Press.

Pruppacher, H. R. and J. D. Klett, 1997: Microphysics of Clouds and Precipitation, 2nd ed., Kluwer Pub. Inc., Boston, 954 p.

Purves, M., 1997: The Ice Fog Events at Whitehorse 3 and 8 January, 1997. Yukon Weather Centre, unpublished Internal Report YWC-97-75. Available online at http://pnrinternal.pnr.ec.gc.ca/paawc/science/library/tech/yukon/75.html.

Rasmussen, R. M., J. Vivekanandan, J. Cole, B. Myers, and C. Masters, 1999: The Estimation of Snowfall Rate Using Visibility. *J. Appl. Meteor.*, **38**, 1542–1563.

Roach, W. T., R. Brown, R. Caughey, S. J. Garland, and C. J. Readings, 1976: The Physics of Radiation Fog: I – A Field Study. *Quart. J. Roy. Meteor. Soc.*, **102**, 313–333.

Roach, W. T., 1994: Back to basics: Fog: Part 1 - Definitions and basic physics. *Weather*, **49**, 411–415.

—, 1995a: Back to basics: Fog: Part 2 - The formation and dissipation of land fog. *Weather*, **50**, 7–11

—, 1995b: Back to basics: Fog: Part 3 - The formation and dissipation of sea fog. *Weather*, **50**, 80–84.

Rogers, C. W., 1988: Program performance specification for North Atlantic fog forecasting. Naval Environmental Prediction Research Facility, Contractor Report CR 88-12, Monterey, CA, 22 p.

Saunders, R., 1997: UK Met Office Forecasters' Reference Book, Chapter 3, Visibility. Meteorological Office College, U.K. Met Office, February 1997.

Schemenauer, R. S. and P. Cereceda, 1994, A proposed standard fog collector for use in high-elevation regions. *J. Applied Meteorology*, **33**, 1313–1322.

Scott, R. H., 1894: Fogs reported with strong winds during the 15 years 1876-90 in the British Isles. *Quart. J. Roy. Meteor. Soc.*, **20**, 253–262.

Scott, R. H. 1896, Notes on some of the difference between fogs, as related to the weather systems which accompany them. Submitted to the fog committee, Quart. J. Roy. Meteor. Soc. XXII, 41–65.

Stoelinga, M. T. and T. T. Warner, 1999: Nonhydrostatic, Mesobeta-Scale Model Simulations of Cloud Ceiling and Visibility for an East Coast Winter Precipitation Event. *J. Appl. Meteor*, **38**, 385–404.

Sundqvist, H., E. Berge, and J. E. Kristjánsson, 1989: Condensation and cloud parameterization studies with a mesoscale numerical weather prediction model. *Mon. Wea. Rev.,* **117**, 1641–1657.

Sutherland, R.A., 1986: Broadband and Spectral Emissivities (2–18 μm) of Some Natural Soils and Vegetation. *J. Atmos. Oceanic Technol.*, **3**, 199–202.

Tardif, R., 2007: The Impact of Vertical Resolution in the Explicit Numerical Forecasting of Radiation Fog: A Case Study. *Pure Appl. Geophys.*, **164**, 1221–1240.

Tardif, R. and Rasmussen, R.M., 2007: Event-based climatology and typology of fog in the New York City region. *J. Appl. Meteor. and Clim.*, **46**, 1141–1168.

Taylor, G.I., 1917: The Formation of Fog and Mist. *Quart. J. Roy. Meteor. Soc.*, **43**, 241–268.

Teixeira, J., 1999: Simulation of fog with the ECMWF prognostic cloud scheme. *Quart. J. Roy. Meteor. Soc.*, **125**, 529–553.

Transport Canada, 2001: Trends in Motor Vehicle Collision Statistics, 1988-1997, prepared by Road Safety and Motor Vehicle Regulation Directorate. February 2001.

Turton, J. D. and R. Brown, 1987: A comparison of a numerical model of radiation fog with detailed observations. *Quart. J. Roy. Meteor. Soc.*, **113**, 37–54.

U.S. Department of Agriculture, 1938: *Atlas of the Climatic Charts of the Oceans*. U.S. Weather Bureau Publication No. 1247, prepared under the supervision of W. F. McDonald, 130 charts.

Villeneuve, P. J., J. Leech, and D. Bourque, 2005: Frequency of emergency room visits for childhood asthma in Ottawa, Canada: the role of weather. *International Journal of Biometeorology*, **50**, 48–56.

Weinstein, A. I. and B. A. Silverman, 1973: A numerical analysis of some practical aspects of airborne urea seeding for warm fog dispersal at airports. *J. Appl. Meteor.*, **12**, 771–780.

Welch, R.M. and B. A. Wielicki, 1986: The Stratocumulus Nature of Fog. *J. Appl. Meteor.*, **25**, 101–111.

Welch, R., S. Sengupta, A. Goroch, P. Rabindra, N. Rangaraj, and M. Navar, 1992: Polar Cloud and Surface Classification Using AVHRR Imagery: An Intercomparison of Methods. *J. Appl. Meteor.*, **31**, 405–420.

Whiffen , B., P. Delannoy , and S. Siok, 2004: Fog: Impact on road transportation and mitigation options. National Highway Visibility Conference, Madison, Wisconsin, 18-19 May 2004.

Willett, H. C., 1928: Fog and haze, their causes, distribution, and forecasting. *Mon. Wea. Rev.*, **56**, 435–468.

Witte, H. J., 1968: Airborne observations of cloud particles and infrared flux density in the Arctic. Ph.D. thesis, University of Washington, 101 p.

WMO, 1966: *International Meteorological Vocabulary*. World Meteorological Organization. Geneva, Switzerland.

Yang, D., H. Ritchie, S. Desjardins, G. Pearson, A. MacAfee, and I. Gultepe, 2009: High Resolution GEM-LAM application in marine fog prediction: Evaluation and diagnosis. *Wea. Forecasting*. In press.